Master's thesis

NTNU
Norwegian University of Science and Technology
Faculty of Information Technology and Electrical Engineering
Department of Electric Power Engineering

Martine Halvorsen Sønju

Comparing Optimization Strategies in Local Electricity Markets Applied to Large Industrial End-users in Norway and Residential Buildings in the UK

Master's thesis in Energy and Environmental Engineering
Supervisor: Kjetil Uhlen
July 2020

NTNU
Norwegian University of Science and Technology

NTNU

Norwegian University of
Science and Technology

Comparing Optimization Strategies in Local Electricity Markets Applied to Large Industrial End-users in Norway and Residential Buildings in the UK

Martine Halvorsen Sønju

Master of Energy and Environmental Engineering

Submission date:	July 2020
Supervisor:	Kjetil Uhlen, IEL
Co-supervisors:	Pedro Crespo del Granado, IØT
	Seyed Naser Hashemipour, IØT
External contact:	Aina R. D. Serigstad, Lyse Elnett AS

Norwegian University of Science and Technology
Department of Electric Power Engineering

Acknowledgments

This thesis concludes my last semester as a M.Sc. student. The five years spent at NTNU have been both educating, fun and challenging. I am very grateful for everything I have experienced during my time in Trondheim.

A big thanks is given to my official supervisor, Kjetil Uhlen. Your availability and guidance is highly appreciated. I would also like to give a big thanks to my co-supervisors Pedro Crespo del Granado, senior researcher at IØT, and Seyed Naser Hashemipour, research assistant at IØT, for always being available and for assisting me through the whole process.

This thesis was in strong collaboration with the European Projects: BEYOND and Positive CityxChange. Thesis inspiration and research discussion with researchers in these projects helped understand better the latest research challenges and frontiers in local markets and P2P trading.

Trondheim, 24.07.20

Martine Halvorsen Sønju

Abstract

The increasing deployment of distributed energy resources (DER), in combination with the growing use of power-demanding devices, arise new challenges for the power system, including supply and flexibility challenges on a local level. To meet these challenges, new local electricity market designs employing local energy and flexibility features should be explored. In this context, peer-to-peer (P2P) energy trade has emerged as a new way of exploiting local energy production and storage to benefit both the local P2P sharing community and the power system on a higher level.

This thesis proposes two different optimization based control system strategies, to be used on a local market level, and investigates the performance of the strategies based on the total cost of electricity during operation for the energy sharing region (ESR), or community, and for each end-user within the ESR. The strategies are also evaluated based on to what degree they can increase the self-consumption of power from DERs within the ESR, and derby decrease the energy consumption from the main grid. The peak demand of such ESRs, or of end-users with high energy demands, are of importance to the distribution system operator (DSO), as the DSO dimensions the local grid according to the highest measured peak power demand. To investigate the relationship between peak power demand and total electricity costs, a multi-objective optimization (MOO) approach based on the ϵ-constraint method is also implemented.

The first optimization strategy introduced is the decentralized control system strategy, which has as objective to minimize the total electricity costs for each end-user within an ESR. The second strategy is the centralized control system strategy, which minimizes the total cost of electricity for the whole ESR. In the decentralized strategy, the end-users can only utilize their own local production and/or storage units and the main power grid to meet their energy demands. The centralized strategy enables P2P energy trade among the end-users within the ESR, meaning that P2P energy can be used in combination with energy from local production and/or storage units and the main grid to meet the energy demand of each end-user within the ESR.

To examine the performance of the two optimization strategies, the strategies were applied to two different cases. The first case concerns a community of 25 residential buildings in London, UK, while the second case concerns three large industrial end-users at Forus, Norway. The two strategies make supply-demand decisions for each of the cases according to their objective function and associated restrictions.

The main results show that the centralized optimization strategy gives the lowest total costs for the ESR with a cost reduction of 1.0-8.0% compared to the decentralized strategy. The centralized strategy does also give the lowest costs for each of the end-users within the ESR, as the P2P energy trade increases the ESR flexibility in addition to reducing the amount of energy consumed from the main grid by 1.4-18.9%. It is observed that the difference in performance between the decentralized and centralized strategies is dependent on the amount of DERs and storage units in the specific case. A high amount of DERs and storage units minimizes the difference in performance between the two strategies. The results from the MOO show that there is a dependency between total electricity costs and peak power demand for the cases studied and that a small increase in cost can reduce the peak power demand by a significant amount.

Sammendrag

Den økende bruken av distribuerte og fornybare energikilder, i kombinasjon med økende bruk av kraftkrevende enheter, skaper nye utfordringer for dagens kraftsystem. Dette inkluderer utfordninger knyttet til forsyning og fleksibilitet på lave nettnivåer. For å kunne møte disse utfordringene bør nye utforminger av lokale elektrisitetsmarkeder som benytter lokal energi og fleksibilitetsfunksjoner utforskes. I denne sammenhengen har peer-to-peer (P2P) energihandel mellom sluttbrukere oppstått som en ny måte å utnytte lokal energiproduksjon og -lagere til fordel for både lokale samfunn samt kraftsystemet på et høyere nettnivå.

Denne hovedoppgaven foreslår to ulike optimeringsbaserte styringssystemstrategier, til å bli benyttet på det lokale markedsnivået, samt vurderer resultatene fra disse basert på total strømkostnad for det lokale samfunnet og for hver sluttbruker innad i dette samfunnet. Strategiene er også evaluert basert på til hvilken grad de kan øke selvforbruket av lokalprodusert energi innad i samfunnet og dermed redusere mengden energi som brukes fra kraftnettet. Effekttopper fra slike lokale samfunn, eller fra sluttbrukere med høyt energiforbruk, er viktig for det lokale nettselskapet, da nettselskapet dimensjonerer strømnettet i henhold til den høyeste effekttoppen. For å utforske forholdet mellom effekttopper og total strømkostnad, har det blitt implementert en optimeringsmetode som kan håndtere flere objektfunksjoner basert på ϵ-restriksjons metoden.

Den første optimeringsstrategien er den desentraliserte kontrollsystem strategien som har som målfunksjon å minimere de totale strømkostnadene for hver sluttbruker innad i et lokalt samfunn. Den andre strategien er en sentralisert kontrollsystemstrategi, som minimimerer de totale strømkostnadene for hele det lokale samfunnet. I den desentraliserte strategien kan sluttbrukere benytte deres egne produksjons- og lagringsenheter, samt strøm fra kraftnettet for å møte deres elektrisitetsbehov. Den sentraliserte strategien muliggjør for P2P strømhandel mellom sluttbrukere innad i det lokale samfunnet. Dette betyr at strøm fra lokale sluttbrukere kan benyttes i kombinasjon med lokal produksjon og energilagere samt kraftnettet for å møte elektrisitetsbehovet til hver sluttbruker innad i det lokale samfunnet.

For å kunne sammenlikne resultatene fra de to optimeringsstrategiene, har strategiene blitt anvendt i to ulike caser. Den første casen er av et lokalt samfunn bestående av 25 bolighus i London i Storbritannia. Den andre casen består av tre industrikunder med høye energibehov lokalisert på Forus i Norge. De to strategiene tar beslutninger om kraftbehov og -tilførsel for hver av casene basert på deres respektive objektfunksjoner og restriksjoner.

Resultatene viser at den sentraliserte optimeringsstrategien gir de laveste totale kostnadene for det lokale samfunnet med en kostnadsreduksjon på 1.0-8.0% sammenliknet med den desentraliserte strategien. Den sentraliserte strategien gir også de laveste totale kostnadene for hver sluttbruker innad i det lokale samfunnet, ettersom P2P strømhandel gir en økt fleksibiliteten i tillegg til å redusere mengden energi som konsumeres fra kraftnettet med 1.4-18.9%. Det er observert at forskjellen i ytelse mellom den desentraliserte og den sentraliserte strategien er avhengig av mengden distribuert fornybar produksjon og lagringsenheter i den spesifikke casen. En høy andel distribuert fornybar produksjon og lagringsenheter minimerer forskjellen mellom de to strategiene. Resultatene fra optimeringsmetoden som håndterer flere objektfunksjoner viser at det er avhengighet mellom de totale strømkostnadene og effekttopper for de studerte casene, samt at en mindre økning i kostnad kan redusere effekttoppen med en betydelig mengde.

Contents

List of Figures

List of Tables

Acronyms

AC	*	Alternating current
BESS	*	Battery energy storage system
CHP	*	Combined heat and power
DC	*	Direct current
DER	*	Distributed energy resource
DSO	*	Distribution system operators
ESR	*	Energy sharing region
EV	*	Electrical vehicle
FIT	*	Feed-in tariff
Li-ion	*	Lithium-ion
LIP	*	Lithium iron phosphate
MOO	*	Multi-objective optimization
PCC	*	Point of common coupling
PS	*	Port of Stavanger
PV	*	Photovoltaic
P2P	*	Peer-to-peer
RES	*	Renewable energy source
RH	*	Risavika Harbor
RPD	*	Reference price data
SOC	*	State of charge
V2G	*	Vehicle to grid
WT	*	Wind turbine

1 | Introduction

1.1 Background and Motivation

The use of electricity as energy carrier, the deployment of distributed energy resources (DERs) and the energy demand of end-users have increased over the last years. To reduce global warming, emphasis has been put on curtailing greenhouse gas emissions by utilizing more environmentally friendly energy carriers and sources. Electricity can be used as a more nature-friendly alternative compared to e.g. oil, gas and coal, provided that the electricity is produced by a renewable energy source (RES), such as hydro, solar and wind.

Electrification of the transportation sector and the increased use of other power-demanding devices have led to a demand increase by the end-users. For instance, several end-users, especially in Norway, have replaced their fossil-fueled car with an electrical vehicle (EV) [22]. Industrial end-users are also starting to join the electric transportation revolution, and are facilitating for charging of larger EVs, electric vessels, etc. The heightened demand can put pressure on the main power grid, as it is dimensioned for the current peak power demand. If the peak demand increases, the local distribution system operator (DSO) must upgrade the grid to meet the new peak. Such power grid upgrades can be very costly, and can in many situations be postponed if the grid is utilized in a better way.

In recent years, several consumers have installed local production units and have thus become prosumers, which can both draw power from and deliver power to the main grid. Some prosumers and consumers have also installed local storage units, where power from production and/or from the grid can be stored. The local production units are mostly photovoltaic (PV) installations and wind turbines (WTs), while the storage units are usually in the form of a battery energy storage system (BESS). Systems with a BESS unit can use different control system strategies in deciding when the battery should be charged and when it should be discharged. The objective of the control strategy varies depending on the choices of the consumer or prosumer. It is often a desire to reduce the electricity and grid-related costs for the consumers and prosumers. A reduction in cost can be achieved in different ways depending on the price model used for energy consumption.

The usage of aforementioned systems with storage units can also possibly lead to grid update deferral, given that they are used in such a way that the peak demand from the main grid is lowered. The EVs can also be aggregated to be used as a storage unit to provide grid flexibility through e.g. a vehicle to grid (V2G) solution. To have a sufficient effect on the peak power demand from the grid, the consumers with production and/or storage units must have high power demands, otherwise, several consumers with lower power demands must cooperate to minimize their peak demand from the grid. With the Norwegian network tariff model, consumers collectively have to pay for grid development, maintenance and operation. This means that a grid update deferral can give lower future grid costs for the consumers and prosumers, as they do not have to pay extra to cover the high investment costs.

In this thesis, two different optimization based control system strategies have been studied and utilized in two different cases from two different countries. The first strategy aims at reducing the

electricity and grid-related costs for each consumer and prosumer within a community separately and is called the decentralized strategy. The second control strategy, called the centralized strategy, looks at the consumers and prosumers as a community and aims at reducing the costs for the whole community. The centralized strategy also grants peer-to-peer (P2P) trading between the consumers and prosumers within the same community, as has been done in e.g. Lüth et al. [19]. P2P trading allows the actors within a community to directly trade power with each other without utilizing the main grid.

The two cases studied in the thesis are different from each other in many aspects. The first case is a community of 25 houses located in London, UK. Some of the houses have installed local production and/or storage units, while other houses have no production nor storage units. The case data is from a project called Low Carbon London[1].

The second case concerns a system of actors with high power demands located at Forus, Norway. The case includes an airport, harbor and industrial area, and is a collaboration project between Avinor, the Port of Stavanger, Forus Industrial Park, the local DSO Lyse Elnett among others, called Elnett21[2]. The airport, harbor and industrial park are planning on installing local production and storage units.

None of the aforementioned control system strategies take into account the peak power demand seen from the grid. To study the relationship between the total cost of electricity and the peak power demand, a multi-objective optimization (MOO) model is studied and utilized on the Elnett21-case and on a simplified version of the 25-houses case with only four houses. The objectives of the MOO is to reduce the electricity and grid-related costs and to reduce the peak demand from the grid.

1.2 Objectives and Problem Description

The thesis aims at assessing the value of different control system strategies utilized in different cases, with the following research questions:

* What will the difference in total electricity costs for each individual consumer or prosumer in a community be, when the objective is to reduce the individual consumer/prosumer costs versus reducing the costs for the whole community?
* What are the advantages and disadvantages with local market optimization?
* Are the control system strategies case dependent, or do they have the same performance independently of the case studied?
* How can multi-objective optimization be utilized to both reduce the peak demand and total cost of electricity?

To answer the research questions, the aforementioned control system strategies will be studied and used in the mentioned cases. The objective of the thesis is to:

* Give a brief review of related literature and a brief introduction to relevant theoretical concepts, like P2P trade and optimization.
* Create the decentralized optimization model with the objective of minimizing the total electricity costs for each individual consumer or prosumer within a community.

[1] More information on the Low Carbon London project can be found on the following webpage: https://data.london.gov.uk/dataset/smartmeter-energy-use-data-in-london-households

[2] See https://www.elnett21.no for further information on the Elnett21-project.

- Make the centralized optimization model with the objective of minimizing the total electricity costs for the whole community, when P2P trade has been enabled.
- Create the MOO model with its two objectives of (i) minimizing the peak demand from the main grid and (ii) minimizing the total electricity costs.
- Simulate the three models on the different cases and analyzing the results based on the research questions.

The different system models have been implemented and solved using multi-period linear programming with a problem-based approach in MATLAB. As all the different objective functions and constraints are linear, MATLAB uses the default solver called *linprog*, which utilizes a dual-simplex algorithm. The needed parameters for the different optimization problems have been imported from Excel to MATLAB. MATLAB was chosen as the programming language to be used in the thesis due to its numerous build in functions, its sophisticated linear programming algorithms, and for its ability to easily generate plots.

1.3 Structure of the Thesis

The thesis starts by presenting the motivation for utilizing different control system strategies for controlling end-user battery systems. Then, a theoretical background of the essential working principles of the control strategies and important terms have been given.

Chapter 2, *Theory and Related Literature*, introduces important terms and concepts of the thesis and presents the different optimization based control system strategies used. The chapter does also give a brief review of related literature.

Chapter 3, *25-houses in London, UK*, introduces the first case of the thesis consisting of several residential buildings located in the UK. Then, the case data and model formulation are given before presenting and analyzing the results from the two optimization approaches.

Chapter 4, *Elnett21, Case in Norway*, introduces the second case of large industrial end-users in Norway. The chapter describes the case data and model formulation before presenting and analyzing the results obtained from utilizing the two optimization approaches in the case.

Chapter 5, *Multi-objective Optimization*, gives a brief introduction to multi-objective optimization and the ϵ-constraint method. Then, the method is applied to one of the end-users in the Elnett21-case based on the decentralized market approach, before applying it to a simplified version of the 25-houses case, i.e. the 4-houses case, based on the centralized market approach.

Chapter 6, *Conclusion*, presents the main findings and conclusions of the thesis and states the main shortcomings and suggestions for further work.

2 | Theory and Related Literature

This chapter gives an introductory overview of some of the important terms and concepts used in the thesis, an overview of the different optimization based control system strategies applied, and a brief literature review of selected articles.

2.1 Peer-to-Peer Trading

Peer-to-peer (P2P) trading is defined as the direct trading of electricity between consumers or prosumers[3], hereby collectively called end-users[4], without the involvement of a third party. By giving end-users the possibility of trading electricity directly, they can gain revenue for their excess power and reduce their electricity expenses by utilizing a low-cost settlement system. P2P trading can also encourage the deployment of distributed energy resources (DERs), as the possible revenue and cost savings of P2P trading can improve the yield on investment in DERs [19].

Figure 2.1 shows the difference between the conventional and a proposed P2P sharing paradigm. Traditionally, consumers buy the necessary amount of power from a chosen retailer at a retail price. Prosumers will buy power at retail price from a retailer when the prosumer demand exceeds the production. When the prosumer production exceeds the demand, the surplus power can be sold to a retailer at an export price. The export price is decided by the local feed-in tariff (FIT) scheme and is usually set lower than the retail price to incentivize self-consumption[5] [42].

In the proposed P2P energy sharing paradigm, the end-users within the same energy sharing region (ESR) can trade P2P power amongst themselves [42]. To not involve a third party, the consumers and prosumers within the same ESR must be electrically connected through a local grid. The end-users within the same ESR are located in the same geographical region, to not get a too large and costly local grid. This means that the ESRs will mostly consist of local communities of prosumers and consumers.

To incentivize P2P energy trading, the price for buying P2P power should be set lower than the price of buying power from the main grid, i.e. the retail price. Usually, the local pricing scheme is set somewhere between the in-feed price of the grid and the electricity price of the main grid. In this way, all consumers and prosumers within a P2P community will benefit from trading energy P2P. After the end-users within the same ESR have traded power, the power deficit or surplus is met through trading with a retailer. To keep track of energy sharing activities and to specify rules for trading, like the implementation process and the core pricing model, an energy sharing coordinator is needed. All power trading between the ESR and the retailer goes through the energy sharing coordinator market operator [42].

[3] A prosumer is a type of consumer that both can consume and produce electricity locally.

[4] In this thesis, the term end-user is used as an umbrella term for consumers and prosumers of the power system.

[5] Self-consumption is the ratio between locally produced power consumed on-site and the overall local production [42].

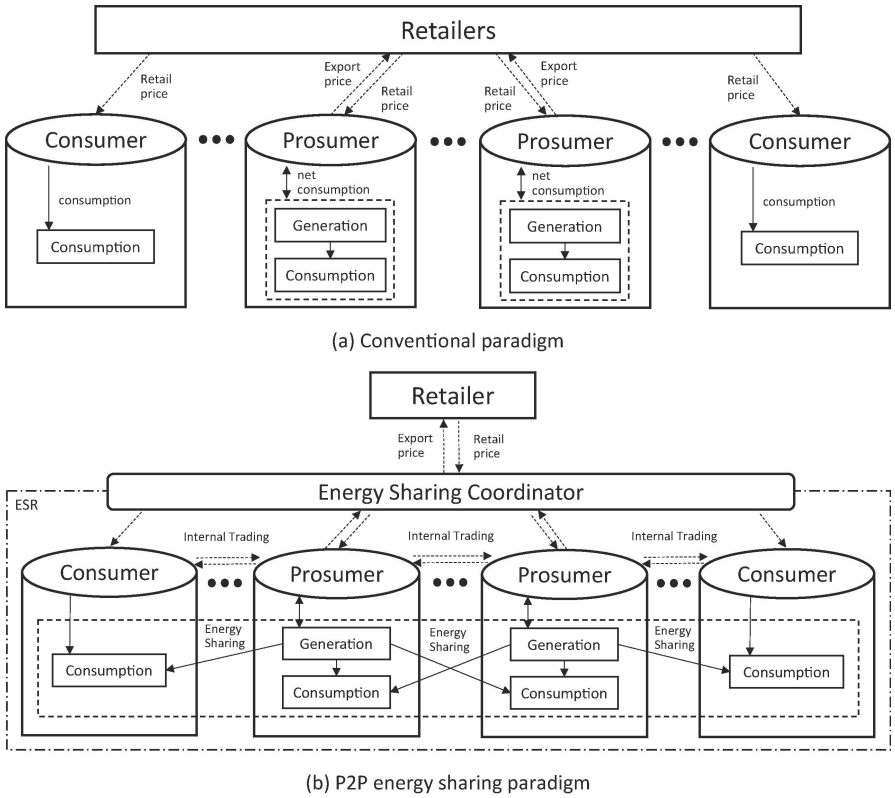

Figure 2.1: Illustrating the difference between the conventional market paradigm (a) and the P2P sharing paradigm (b) [42].

2.2 Optimization Problem

Solving an optimization problem in mathematics means finding all the feasible solutions to the problem and among these choosing the best solution. To be able to solve an optimization problem, the optimization problem type must be identified. There are several types of optimization problems, like continuous or discontinuous problems, problems with or without constraints and deterministic or stochastic problems. There can also be problems with one objective function, several objective functions, or no objective function [23]. The optimization problems studied in this thesis are all continuous, deterministic, with constraints and have either one or two objective functions. The objective functions and constraints are also linear, which makes it possible to use linear programming to solve the different optimization problems.

An optimization problem is solved by utilizing a specific algorithm for finding the optimal solution. There are many different types of solver algorithms, and the chosen algorithm for a specific optimization problem is greatly dependent upon the problem type. The optimization problems studied in this thesis require a solver that can solve an optimization problem with a continuous, differentiable and linear objective function, real numbered optimization variables and linear and equality constraints. Such a problem can be solved by using e.g. a dual-simplex algorithm. The dual-simplex algorithm performs a simplex algorithm on the dual problem instead of on the primal, original, problem. In the dual problem, the right-hand side of the

restrictions in the primal problem is turned into parameters in the objective function, and the parameters in the objective function of the primal problem are turned into the right-hand side of the restrictions in the dual problem. Further, the parameter in front of the first decision variable of the primal problem in the constraint equations that concern this variable, are turned into different parameters on the left-hand side in the first restriction of the dual problem. The second restriction of the dual problem is found by looking at the parameters in front of the second decision variable in the constraint equations of the primal problem, and so on. Due to the structure of the dual versus the primal problem, these problems are mathematically equivalent, but the solving steps of the two problems differ. The different solving steps often make it easier to solve the primal problem by solving the dual problem [21].

2.3 Control System Strategies

This section describes the three different optimization based control system strategies that have been studied in this thesis and lists up the assumptions and simplifications related to the control strategies. More case-specific assumptions and simplifications are given in section 3.3 for the 25-houses case and in section 4.3 for the Elnett21-case.

The last strategy, multi-objective optimization (MOO), has gotten its own dedicated chapter, see chapter 5, and is therefore just briefly described in this section.

2.3.1 Assumptions and Simplifications

There have been made several assumptions and simplifications for all the different optimization strategies and cases, to simplify the problems regarding computational effort and complexity. The assumptions stated in the list below apply to all strategies and cases.

- Only operational costs have been taken into account when making the different objective functions. Meaning it is assumed that all the production and storage units in the different cases have been installed and that the investment, maintenance and other possible costs, related to the production and storage units during the simulation period, have been ignored.
- It is assumed that the needed smart grid technology, like smart meters, have been installed in the ESR communities.
- Full bidirectional information exchange between the technological devices is assumed in each ESR.
- It is assumed that the demand, production and electricity prices are known beforehand and that there are no uncertainties in this data. This implies assuming a perfect forecast model.
- All efficiencies are assumed to be constant for the whole simulation period, including the efficiency factor for P2P energy trading.
- Degradation and possible standby losses of the batteries are neglected.
- Lifetime expansion of the batteries is not considered, which means that e.g. smart charging or discharging of the batteries is not taken into account.
- No limits have been set on the amount of power that can be delivered from, or to, the main or local grid at any time. This means that limits on transmission lines have been ignored

and that an unlimited supply is assumed from the main grid. Possible grid congestion is also ignored.

* Physical power system characteristics like reactive power effects, voltage levels, power flows and balancing of frequency have not been looked at.
* The conversion and distribution losses occurring when selling power from DERs to the main grid are neglected.
* For the strategies that have enabled P2P trading, it is assumed that the end-users within the same ESR have a local grid for trading power with no grid usage costs and that all the end-users put their DER units at disposal. The investment, maintenance and other possible costs related to the local grid have been ignored.

2.3.2 Decentralized Control System Strategy

The decentralized control system strategy looks at each end-user in an ESR, or community, individually. The objective of the strategy is to minimize the operational costs related to the network tariff and electricity costs, i.e. the total cost of electricity, and the optimization is done for each end-user individually. The decentralized strategy is inspired by the decentralized operation strategy of Hidalgo-Rodríquez et al. [16], but it does not utilize binary restrictions like the strategy used in the article.

The decentralized strategy has its pros and cons. An advantage of the strategy is that it does not require information exchange with a third party, as each consumer or prosumer aims to minimize their economic objective function [16]. Using this strategy, each individual end-user will have the lowest total electricity costs possible, but the end-user can only utilize its own production and/or storage units, given that the end-user has any. Another advantage of the strategy is that each end-user is not dependent upon other consumers or prosumers, meaning that possible uncertainties in prosumer production do only affect the prosumer itself.

A disadvantage of the approach can be that as each end-user is looked at separately, the total costs for the whole ESR will be suboptimal. When P2P trading is disabled, the consumers that do not have storage units will have to buy all the necessary power from the main grid. This means that the decentralized control system strategy will give these consumers the same costs as if the strategy was not used at all. Without P2P trading, the consumers without storage will have no flexibility compared to the prosumers with or without storage units and the consumers with storage units, and they will have a higher cost of electricity than they possibly would have had if they could buy P2P power.

Another disadvantage of this control system strategy is that each consumer or prosumer will try to buy power from the grid when the cost of electricity is low. This can lead to high peak power demands of each end-user and of the whole ESR, if there are no cost terms related to the peak demand of the ESR or the individual end-user.

2.3.3 Centralized Control System Strategy

This strategy looks at an ESR of consumers and prosumers as one entity, and the objective is to minimize the total electricity costs during operation for the whole ESR. In the centralized control system strategy, P2P trade has been enabled. The P2P power can only be sold and purchased within the same ESR. As the centralized strategy only considers the total electricity costs of an ESR, and not of the individual end-user within the community, the revenue for selling P2P power and the cost of purchasing P2P power will cancel each other out. The cost of P2P

trade has therefore been left out in the optimization models. To find representable costs for the individual end-users trading power P2P within the ESR, the cost of P2P trade is added after the optimization has been run. To minimize the total electricity costs of an ESR, all the end-users within the same ESR must share their production, storage and demand information with a so-called central unit, such that this unit can make decisions for the whole ESR. The centralized strategy is based on *Flexi User Market* of Lüth et al. [19], and the strategy uses the same market rules as applied in the *Flexi User Market*.

The main advantage of the centralized control system strategy is that the obtained solutions will be optimal for the whole ESR. Meaning that the strategy will give the lowest possible costs for the ESR, and not just the lowest costs of each end-user, like the decentralized control system strategy. The enabling of P2P trade will provide flexibility to consumers without batteries. Now, these consumers can both buy power from other peers and the main grid. The strategy lets the ESR utilize their production and storage units in a way that will benefit the whole ESR and not just the consumers with storage units or the prosumers with or without storage units.

The sharing of information can be a disadvantage of the centralized strategy, as it does not scale well [16]. If there are a lot of end-users in an ESR, the central unit must process and keep track of a lot of information. Even though the costs for the ESR are minimized with the centralized strategy, it is not given that the strategy will give the lowest costs for each prosumer or consumer within the sharing region. The consumers with no storage will get lower total electricity costs, as they can buy P2P power. For prosumers and consumers having batteries, the total electricity costs will depend both on the case, the electricity price, and the P2P trade price. Minimizing the costs for the ESR can also lead to a high peak power demand, seen from the main grid if there are no cost terms in the objective function related to the peak power demand.

2.3.4 Multi-objective Optimization

Multi-objective optimization (MOO) is an optimization approach that involves two or more contradicting objective functions, which should be optimized simultaneously [7]. In this thesis, the MOO is used to study the two objective functions (i) minimizing the total cost of electricity and (ii) minimizing the peak power demand seen from the main grid. These objective functions will be contradicting if minimizing the total electricity costs results in high peak demands, and vice versa if minimizing the peak power demands lead to high total electricity costs. Whether the objectives are contradicting or not will depend on the relationship between the total electricity costs and the peak demand in the specific case that the MOO is applied to. The MOO approach is further explained and used in chapter 5.

Table 2.1 summarizes the features of the three different optimization based control system strategies studied in the thesis.

Table 2.1: An overview of the different control system strategies utilized in the thesis.

Strategy	Decentralized control system strategy	Centralized control system strategy	Multi-objective optimization
Objective	Minimize total electricity costs for each end-user within an ESR	Minimize total electricity costs for the whole ESR	(i) Minimize total electricity costs for each end-user or for the whole ESR (ii) Minimize peak demand, seen from the main grid, of each end-user or of the whole ESR
Power sources	Main grid, DER	Main grid, DER, P2P trade	Main grid, DER, P2P trade
Pros	(i) No information exchange with a third party (ii) Each end-user within an ESR will pay the lowest electricity costs possible using their own DERs (iii) No dependency between end-users	(i) Optimal solution for the ESR (ii) Flexibility options for all consumers and prosumers within the ESR	Investigate the relationship between peak power demand and total electricity costs for an end-user or ESR
Cons	(i) Suboptimal solution for the ESR (ii) No flexibility options for consumers without DERs (iii) Possibly high peak power demands for the ESR	(i) Information exchange with a third party (ii) Possibly high peak power demands for the ESR	With contradicting objectives, the optimal solution cannot be reached by both objectives simultaneously

2.4 Related Literature

In the literature, there have been conducted studies of different optimization based control system strategies and P2P energy trade. Here, just a selection of the existing related articles is studied. This is to give an overview of what has already been achieved in the literature thus far, and to see what possible contributions this thesis can add to the field.

In Hidalgo-Rodríquez et al. [16], a decentralized, centralized and hierarchical-distributed model predictive control was tested on three different home-microgrids with flexible thermal loads. All the home-microgrids have a PV-system, one or two storage types and load. In the article, the used decentralized coordination strategy is similar to the decentralized strategy used in this thesis. Both strategies try to minimize the economic objective function of each separate consumer or prosumer, and both allow for power to be sold to the main grid. The centralized coordination strategy in Hidalgo-Rodríquez et al. [16] has two terms in the objective function, one to minimize total electricity costs of each of the three home-microgrids and one to minimize the power peak at the point of common coupling (PCC) of the microgrids. The reduction of the peak at the PCC is done by minimizing the instantaneous quadratic difference between the power import and export. Compared to the centralized control strategy of this thesis, the centralized coordination strategy of the paper does not allow P2P trading between the end-users. Further, the simulations were only done over seven days and on one case with microgrids on the residential level.

Lüth et al. [19] introduces two different market designs for P2P trading. The *Flexi User Market* and the *Pool Hub Market*, where the market applied rules to a system with individually owned batteries and to a system with one commonly owned battery, respectively. The same market

rules applied to *Flexi User* in Lüth et al. [19] have been applied to the centralized control strategy used in this thesis, as the strategy is inspired by the *Flexi User Market*. Unlike *Flexi User*, the centralized strategy of this thesis does also allow for power to be exported to the main grid. Lüth et al. [19] only tested two market rule types on one community of only four different households of consumers and prosumers, and the peak demand of the community was not considered.

Zepter et al. [41] explores the value of P2P trading by integrating prosumers in the day-ahead and intraday markets and looks at how residential battery storage can arise demand-side flexibility. The article compares the electricity costs of four different cases. The first case is the base case used as a reference case with no battery storage and no P2P trading. The second case has battery storage, but no P2P trading. The third case allows for P2P trading within the community but has no batteries. The last case, case four, has both battery storage and P2P trading. In all of the cases, the objective is to reduce total electricity costs for the community in both the day-ahead and the intraday market stages. Besides that Zepter et al. [41] has an objective function for both market stages, the centralized strategy of this thesis is similar to the model used in the paper on the case with both battery storage and P2P trading. Both strategies allow P2P trading and selling power to the main grid. The model of the paper is only applied to a set of ten households, while the centralized strategy in this thesis is applied to 25 households and to a second case with large end-users.

The last article reviewed is Sæther [31], which has not yet been published. In Sæther [31], the value of P2P trading combined with different flexibility resources and on-site generation is investigated for a Norwegian industrial site. The article uses three different market designs to minimize the total electricity costs for the whole industrial cite. The first design, *Flexible buildings*, does not allow P2P trading or shared flexibility. The second design, *P2P energy trade*, allows both P2P trade between buildings and shared flexibility. While the last design, *P2P energy trade and central community storage*, enables P2P trade and shared flexibility, like the second strategy, in addition to making a shared community storage available. The first market design is similar to the decentralized strategy, while the second design is similar to the centralized strategy of this thesis. The difference between the market designs of Sæther [31] and the control system strategies in the thesis is that Sæther puts a limit on the amount of power that can be sold to the main grid, to not exceed the plus-customer limit[6]. The results from Sæther shows that power is curtailed in the first market design, but not in the second design due to enabling P2P trade. Limiting the amount of power that can be sold to the main grid can give increased operational costs. In addition to putting a limit on the power that can be sold to the main grid, Sæther does only use the market designs on one case.

To summarize, the reviewed articles have either applied different control system strategies, both with and without P2P trading, to a community of residential buildings or to an industrial cite, but not to both end-user types at the same time to compare the performance of the strategies in different cases. The amount of end-users in the different article cases ranges from three to ten. Having two different cases in two different countries, with different end-user types and up to 25 end-users in the same ESR, or community, can give a better foundation for understanding the mechanisms of the control system strategies and P2P trade. In addition, the thesis touches upon the relationship between the total cost of electricity and the peak power demand seen from the grid, which has not been looked at in any of the mentioned articles, through using a MOO approach.

[6] See section 4.2.5 in chapter 4 for further information on the plus-customer limit.

Table 2.2 gives an overview of the mentioned articles with a short explanation of the objective, approach and findings of the different papers.

Table 2.2: Overview of the objective, approach and findings of some relevant articles.

Paper	**Optimal Operation of Interconnected Home-Microgrids with Flexible Thermal Loads: A Comparison of Decentralized, Centralized, and Hierarchical-distributed Model Predictive Control**	**Local electricity market designs for peer-to-peer trading: The role of battery flexibility**	**Prosumer integration in wholesale electricity markets: Synergies of peer-to-peer trade and residential storage**	**Peer-to-Peer electricity trading in an Industrial site: Value of peak load reduction and shared flexibility assets**
Objective	Present and contrast three different model predictive control operations (decentralized, centralized and hierarchical-distributed) for a system of interconnected home-microgrids.	Investigate the role of battery storage and how market design rules affect it.	Find the value of P2P trading when integrating prosumers in the day-ahead and intraday markets and see how battery storage can contribute to demand-side flexibility.	Investigate the value of P2P trading combined with various on-site flexibility resources for an industrial cite.
Approach	Made three different optimization models representing the different coordination strategies for the interconnected home-microgrids, to e.g. compare the resulting power profiles.	Developed an optimization model for P2P trading to evaluate the benefits of end-users using two different market designs; decentralized versus centralized storage.	Utilizes a two-stage stochastic programming approach to integrate a sequenced decision-making in the wholesale system with uncertainty of spot prices and renewable generation.	Uses multi-period linear programming on three different market designs; (i) No P2P or shared flexibility (ii) P2P and shared flexibility (ii) Central storage combined with (ii)
Findings	The centralized strategy can reduce power peaks at the PCC and improve the power balancing among systems.	The combination of flexibility from storage and trade features give up to 31% savings for the end-users.	P2P trade and battery storage raises the self-sufficiency of the community, and can lead to electricity bill savings up to 60%.	Increased self-consumption of the industrial cite, reduced peak power demand and a total electricity cost savings of 6.8-11.0% when comparing (ii) and (iii) with (i), respectively.
Citation	D. I. Hidalgo-Rodríquez et al. [16]	A. Lüth et al. [19]	J. M. Zepter et al. [41]	G. Sæther [31]

3 | 25-houses in London, UK

The 25-houses case is the first of the cases studied in this thesis. This chapter gives an introduction to the case, presents the case data and model formulation before the results are given and analyzed. Both the decentralized and the centralized control system strategies are applied to the 25-houses case.

3.1 Introduction to the Case

The case concerns a system with 25 residential houses located in London, United Kingdom. The system consists of heterogeneous consumers and prosumers with unique load demand patterns. The prosumers produce electricity through a photovoltaic (PV) system and/or through using a wind turbine (WT), and some of the end-users have a battery energy storage system (BESS)[7]. The demand of the end-users is fixed, which means that no load can be shifted nor curtailed[8]. All of the houses are connected to the main power grid and to a local grid that interconnects the 25 houses. Figure 3.1b shows the setup for the case with six of the 25 houses, with symbol explanations given in fig. 3.1a. The system setup figure shows all the different house configurations and the possible power flow directions within the system when P2P energy trading is enabled. The house without production and storage units cannot sell power to the grid nor any peers, as it has no power to sell. All the other house configurations have bidirectional connections to both the local and the main power grid, meaning that they can both purchase and sell power from or to other peers and the main grid.

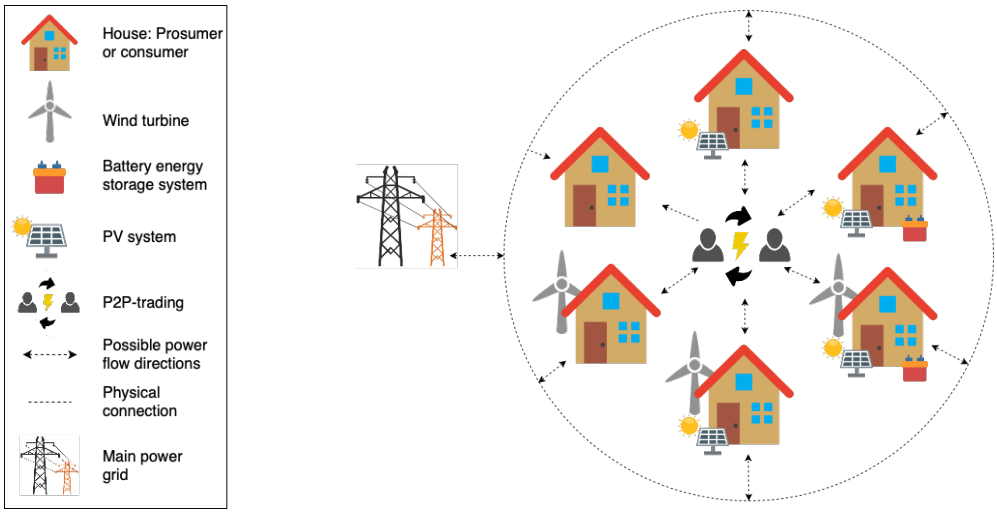

(a) Symbol explanation.

(b) System setup. Only six of the 25 houses are included.

Figure 3.1: The setup for the 25-houses case with P2P trading and explanation of the symbols.

[7] A battery energy storage system (BESS) describes a system that contains a battery and its needed components, like a bidirectional inverter, monitors and controls, to be used in a power system [18].

3.2 Case Data and System

The demand data used in the 25-houses case is historical data from the database of the Low Carbon London project[9]. The project took readings of the energy consumption of 5,567 different households, with and without local production units and BESS, within the Greater London area [15]. For the 25-houses case, the demand of 25 different households, that were subject to a flat rate tariff scheme of 14.23 p/kWh, from the project was used. The chosen households vary in both average electricity demand and in demand pattern. The Low Carbon London project measured the demand for each of the households every 30 minutes from November 2011 to February 2014. The year of analysis for the 25-houses case is set to year 2012, and the analysis period is April to June. A simulation period of three months was chosen instead of a year to not get too long computational times. The demand data for the 25-houses case was taken from April to June 2013 and not from 2012, as the demand data quality was better for year 2013 compared to year 2012. Table 3.1 shows an overview of the average monthly demand for each of the 25 houses when looking at the demand data for the three specified months, and which houses that have production and/or BESS units. The table does also show the nominal capacity of the production units and the usable battery capacity of the storage units. A three-month-long simulation period and a time step of 30 minutes give a total of 4,368 simulation steps.

Table 3.1: An overview of the average monthly demand, local production type and storage for the different households.

House no.	Average monthly demand [kWh/month]	Production type and capacity	Usable battery capacity [kWh]
1	322	-	-
2	483	2 kW_p PV	-
3	833	2.3 kW WT	-
4	267	-	-
5	692	4 kW_p PV	4
6	288	-	-
7	671	2 kW_p PV	-
8	649	2 kW_p PV	-
9	425	2 kW_p PV	-
10	374	-	-
11	459	-	-
12	228	-	-
13	303	-	-
14	265	-	-
15	1,359	4 kW_p PV, 2.3 kW WT	4
16	494	2 kW_p PV	-
17	353	-	-
18	450	-	-
19	264	-	-
20	920	2 kW_p PV, 2.3 kW WT	-
21	462	-	-
22	260	-	-
23	806	4 kW_p PV	4
24	468	2 kW_p PV	-
25	1,097	2 kW_p PV, 2.3 kW WT	-

[8]Shiftable load defines a load that can be time-shifted, but the shifted load must be met within a specific period. Curtailable load represents a load that can be reduced without having to be replaced [26].

[9]More information on the Low Carbon London project can be found on the following webpage: https://data.london.gov.uk/dataset/smartmeter-energy-use-data-in-london-households

Data used for the electricity prices and local production through PVs and WTs in the 25-houses case is taken from Lüth et al. [19]. This is because the article studies a very similar case, but with only four houses instead of 25. Lüth et al. [19] and the 25-houses case have many of the same production and storage units, including 2.3 kW WTs, 4 kW_p PV systems and battery storage units with a usable capacity of 4 kWh. The 25-houses case also includes 2 kW_p PV systems. The PV system production given by Lüth was manipulated to have it fit with the 25-houses case. This section describes what was done in the article to find prices and production data.

The chosen pricing scheme for power consumption[10] from the main grid will have a large impact on the optimization results. For this specific case, the reference price data (RPD) time series is based on the wholesale spot prices given by the former APX Group. The APX Group is now owned by EPEX SPOT, which is the exchange for the power spot markets for several European countries [10]. As the RPD stands for about one-third of the total electricity bill that the UK end-users pay, the RPD time series was up-scaled to be representable for the price at the residential level [19]. Price data from the simulation year 2012 was used for the 25-houses case. Figure 3.2 shows the variation in the electricity prices during the three selected months, while fig. 3.3a and 3.3b show the electricity prices for the first day of April and May 2012, respectively. The figures show that the prices vary from hour to hour without any set pattern for how the prices vary during the day. The figures do show that the prices usually are lower during the night than during the day, which is common.

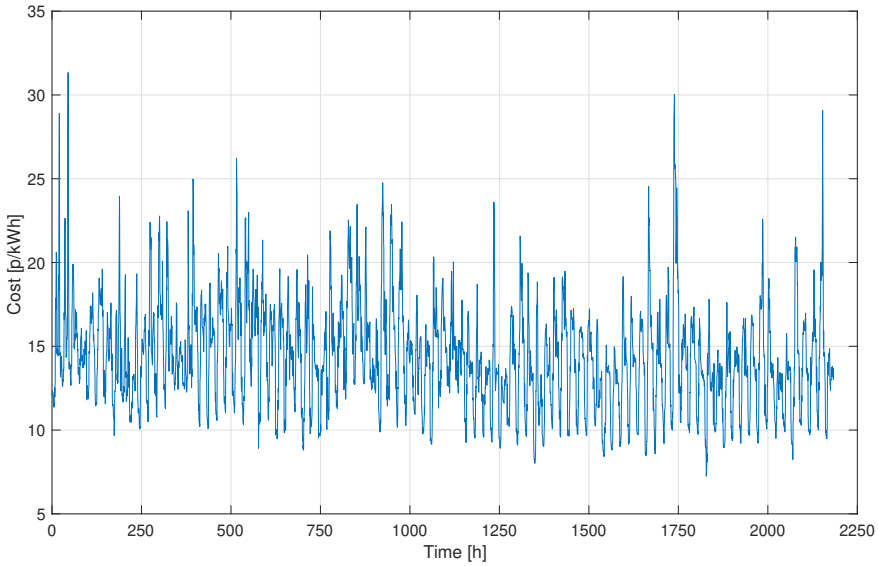

Figure 3.2: Electricity price each hour for the months April to June 2012 for the 25-houses case. The abscissa shows the hours within the three months, with one being the first hour in April and hour 2184 being the last hour in June.

[10]When using the terms power consumption, power demand, power in-feed or similar in chapter 3, the term power refers to the average power over the time step, 30 minutes, and not the actual power per second.

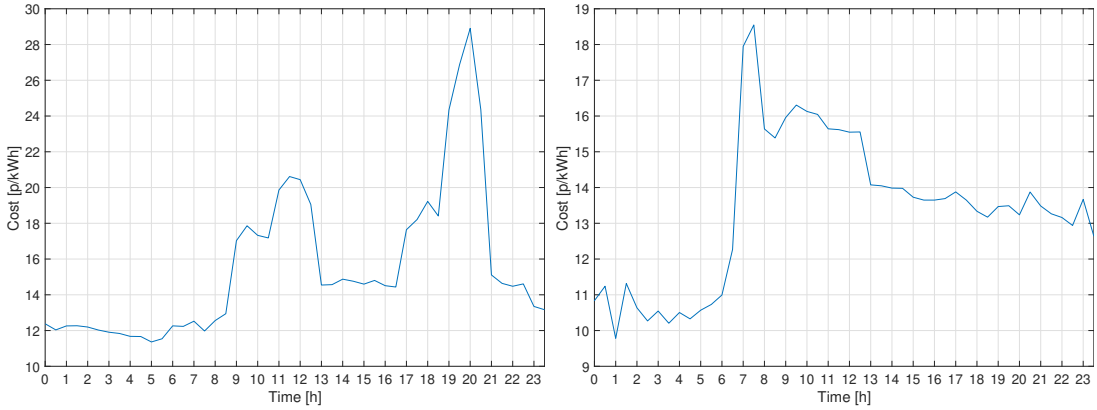

(a) April 1st 2012.

(b) May 1st 2012.

Figure 3.3: Prices for electricity bought from the main grid each hour for different dates.

In the 25-houses case, end-users can either sell power to other peers within the same energy sharing region (ESR), if P2P trading is enabled, or to the main grid. If end-users sell power to the main grid, they must pay a feed-in tariff (FIT) for utilizing the main grid for transporting the sold electricity. From year 2012 to 2020, the FIT rate for the UK was 5.50 p/kWh [25]. When power is sold to the main grid in this case, the seller receives the dynamic wholesale spot price minus the FIT.

When prosumers or consumers buy or sell P2P power, the local grid that interconnects the 25 houses is utilized. When trading P2P there will be conversion and line losses in the local grid, which are assumed to be 7.6% (see [19]). To incentivize P2P trading, the price received when selling P2P must be set higher than the price of selling to the main grid. Further, the price of buying P2P must be lower than the price of buying from the grid. In Lüth et al. [19], the P2P price was set to be 64% of the electricity price, as Lüth assumes that no grid costs occur when using the local grid and that the grid costs account for about one-third of the electricity bill. As the grid in-feed cost is set to be the electricity cost minus a fixed FIT, the P2P price cannot be set to be e.g. 64% of the electricity price. The reason for this is that it then cannot be reassured that the P2P price is between the electricity costs and in-feed costs for all time steps. Thus, it has been assumed that the P2P price is 2.75 p/kWh lower than the electricity cost for the 25-houses case, which is right in the middle of the electricity cost and the in-feed cost.

The local production units, in the 25-houses case, include wind turbines and PV systems. All the WTs in the case are of the same model type, while the PV systems have the same characteristics, but different power ratings. The wind turbine type is a stall regulated turbine with a capacity of 2.3 kW, while the PV system types have a rated power of 2 kW_p or 4 kW_p and efficiency of 21.4%[11]. All the installed PV systems have a tilt of 35°, which is a recommended angle for PV systems installed in the UK. The 2 kW_p PV systems cover an area of 20.8 m^2 [19], while the area covered by the 4 kW_p is assumed to be twice the size, i.e. 41.6 m^2.

[11]The PV system data is based on the panel LG Solar LG370Q1C-V5 NeON R, see https://www.lg.com/us/business/solar-panels/lg-lg370q1c-v5

In the community of the 25 houses, there is a total of four 2.3 kW wind turbines and eleven PV systems. Three of the PV systems have a power rating of 4 kW_p, while the remaining eight PV systems have a 2 kW_p power rating. This gives an aggregated wind turbine capacity of 9.2 kW and an aggregated PV system capacity of 28 kW_p. The total aggregated capacity of renewable production is then 37.2 kW.

The datasheet for the WT only provided discrete values for the power output for some wind speeds. To get the power output from the turbine for all speeds, a polynomial curve was calculated to fit the given data points. The production from the wind turbines was found by combining the polynomial curve with wind speed data from 2012 taken from the UK Meteorological Office, from a station close to London [19]. The total WT production for the simulation period was found to be 6.63 MWh, corresponding to 16.75% of the total community demand in the period. As the data for the wind speed was taken from one measurement station, the WT production is the same for each house that has a WT. Figure 3.4a and 3.4b show the wind turbine production for April and June 1st, respectively, where it can be seen that the WT production is the same for all WTs.

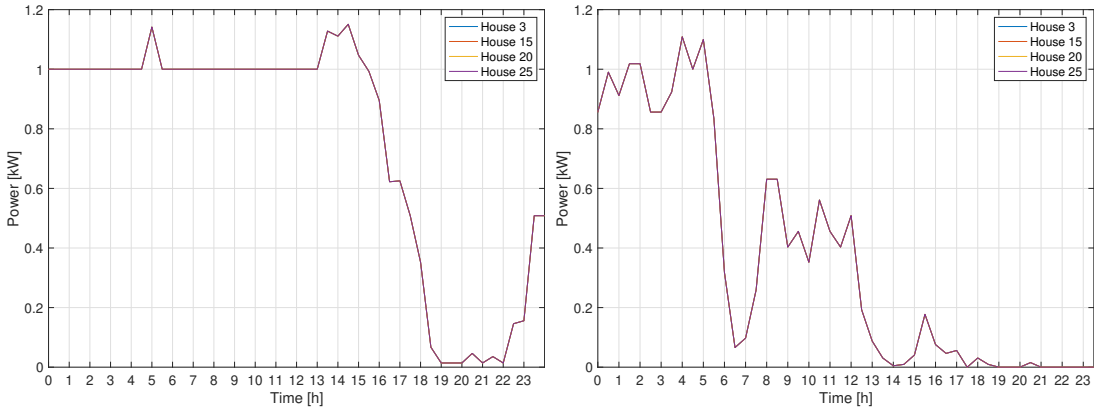

(a) Wind turbine production for April 1st.

(b) Wind turbine production for June 1st.

Figure 3.4: Wind turbine production for April and June 1st 2012 for the different houses[12].

The PV system production every 30 minutes during the simulation period was found through converting global horizontal irradiation data and temperature from HelioClim-3 archives[13] and MERRA-2[14], which gives global reanalysis data, for a pre-specified PV installation. To not get the same PV system output for each house with a PV system, a function was created to manipulate the production from the pre-specified PV installation within some set limits. The used irradiation and temperature data for the case is from year 2006, as it was not possible to obtain data in 30 minutes resolution for the year 2012 [19]. The total PV system production for the simulation period is 12.33 MWh, corresponding to 31.16% of the total demand in the period. The PV system production for April 1st is showed in fig. 3.5a, while the PV production for June 1st is presented in fig. 3.5b.

[12]The production is the same for each household that has installed a wind turbine, due to wind data being taken from the same measurement station.

[13]See http://www.soda-pro.com/nb/web-services/radiation/helioclim-3-archives-for-free for further information.

[14]See https://gmao.gsfc.nasa.gov/reanalysis/MERRA-2/ for further information.

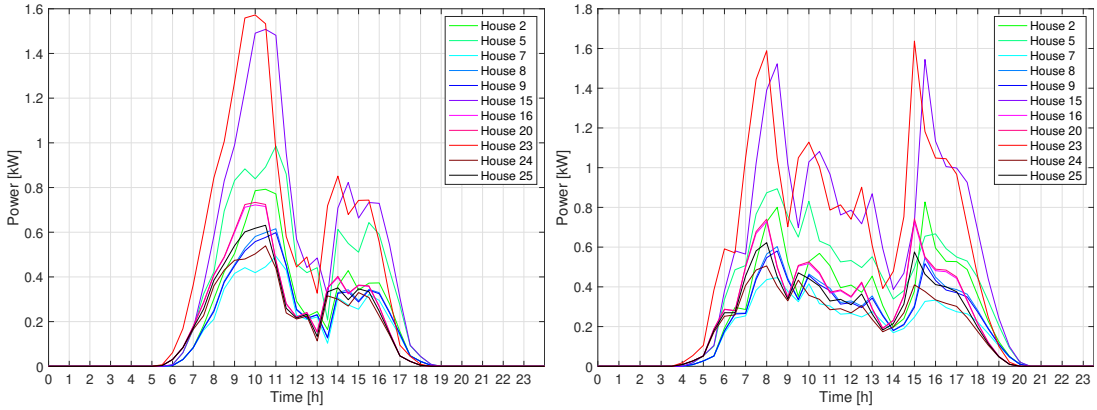

(a) PV system production for April 1st.

(b) PV system production for June 1st.

Figure 3.5: PV system production for April and June 1st 2006[15]for the different houses.

The BESS type used in the 25-houses case is a sonnenBatterie eco 8.0, which is a lithium iron phosphate (LIP) battery that has a usable capacity of 4 kWh and an inverter with a nominal power of 2.5 kW. The battery has a maximum efficiency of 98%, while the inverter has a maximum efficiency of 96% [34]. It is assumed that the charging and discharging efficiencies are constant and equal to the battery efficiency of 98%. The one-way efficiency, i.e. the battery efficiency times the inverter efficiency, of the BESS is 94.08%, which gives a round-trip efficiency of 88.51%. The round trip efficiency denotes the ratio of energy input to the energy retrieved from the BESS. The usable battery capacity and the nominal power of the inverter result in a full charging/discharging time of the battery type of approximately 100 minutes. As there are three sonnenBatteries within the community, the aggregated battery capacity is 12 kWh.

The datasheet for the battery gave the usable capacity of the battery, which is assumed to be the energy that the battery can provide when the nominal capacity is multiplied with the upper and lower SOC limits. This means that the limits on SOC for the battery are already taken into account for the sonnenBatterie eco 8.0.

3.3 Case Assumptions and Simplifications

Some assumptions were made in the 25-houses case to simplify the case. The assumptions listed in section 2.3.1 in chapter 2 do also apply to the case, in addition to the assumptions and simplifications listed below:

* The simulation year is 2012, but the energy demand and PV system production data is from year 2013 and 2006, respectively. This is due to poor demand data quality for year 2012 and that a 30-minute resolution for irradiation and temperature data was not available for the simulation year.
* It is assumed that the limits on SOC have been accounted for in the datasheet of the sonnenBatterie eco 8.0.
* The wind data for the different WTs is from the same measuring station.

[15]The horizontal irradiation and temperature data is from 2006, as it was not possible to obtain data for 2012 in a 30-minute resolution.

3.4 Model Formulation

The optimization approaches used for the 25-houses case must make supply-demand decisions for the different houses when the goal is to reduce the cost of electricity. To do this, a multi-period linear programming model is used for each of the approaches, as the storage level in the battery is dependent on the battery SOC from the previous time step. The multi-period linear programming models make optimized decisions for the system every 30 minutes, time step t, for the optimization horizon T. The two different approaches used for the 25-houses case have different objective functions and restrictions. The first approach aims at reducing the cost of electricity for each house and does not allow P2P energy trading. The second approach aims to reduce the electricity cost of the community of 25-houses when P2P trading is enabled. Both of the approaches have many of the same sets, scalars, parameters and variables in the mathematical model, these are given in table 3.2. It should be noted that there is just one BESS type in the case, which is used in the houses that have battery storage.

Table 3.2: Sets, scalars, parameters and variables used in the mathematical models for the 25-houses case.

Type	Description	Unit
Sets		
$t \in T$	Time, t, within the optimization horizon T	
$h, p \in H$	Houses, h, and peers, p, within the community of houses H	
Scalars		
η_c / η_d	Charging/discharging efficiency of the battery	-
η_{inv}	BESS inverter efficiency	-
P_{inv}	Nominal power of the BESS inverter	kW
E_{bat}	Nominal capacity of the BESS battery	kWh
$\overline{SOC} / \underline{SOC}$	Maximum/minimum limits on the battery state of charge	p.u.
θ_{P2P}	Efficiency factor for converting and transferring P2P power	-
Parameters		
$dem^{(t,h)}$	Demand of house h in time step t	kW
$res^{(t,h)}$	Renewable power production of house h in time step t	kW
$p_G^{(t)}$	Electricity price for power bought from the grid in time step t	p/kWh
$p_{G_{to}}^{(t)}$	In-feed price for power sold to the grid in time step t	p/kWh
Variables		
$G^{(t,h)}$	Power drawn from the grid for house h in time step t	kW
$G_{to}^{(t,h)}$	Power delivered to the grid from house h in time step t	kW
$C^{(t,h)} / D^{(t,h)}$	Battery power charge/discharge of house h in time step t	kW
$S^{(t,h)}$	Battery energy storage level in house h in time step t	kWh
$I^{(t,h)}$	Total P2P power purchase of house h in time step t	kW
$I_p^{(t,h \leftarrow p)}$	P2P power purchase of house h from peer p in time step t	kW
$X^{(t,h)}$	Total P2P power sold from house h in time step t	kW
$X_p^{(t,h \rightarrow p)}$	P2P power sold from house h to peer p in time step t	kW

The objective function in both of the approaches is subject to several constraints. The mathematical constraint-equations are different for the two models, but some of them have the same objective. Both approaches must act by the power balance equation, which ensures that there is a balance between the demand and supply for each node in every time step in the simulation. The power balance equation must be fulfilled at all times to keep a stable system frequency. Next, both approaches update the storage level of the battery by adding the battery charge to, or subtracting the battery discharge from, the battery SOC from the previous time step. The centralized approach has more constraints than the decentralized approach, as there must be set rules for the P2P trade. As pointed out in section 2.3.3 in chapter 2, the P2P costs are not included in the optimization for the centralized approach and have therefore been added after running the optimization.

3.4.1 Approach 1 - Decentralized Strategy

The different houses must get their power demands met with power from local production, local storage or power from the main grid. Only houses that have local production and/or battery storage can utilize these as a power source in approach 1, as there is no P2P trading. Figure 3.6 shows the setup for the decentralized strategy for the 25-houses case.

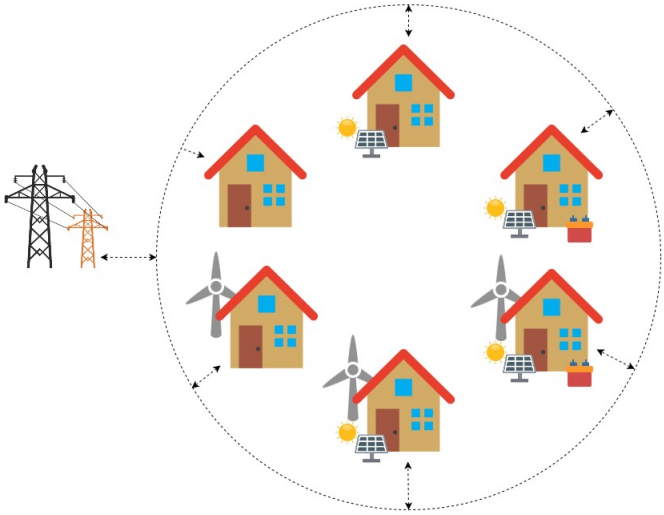

Figure 3.6: Illustration of the setup of the 25-houses case without P2P trading used for approach 1[16]. Only six of the 25 houses are illustrated.

The objective of the approach is to minimize the total cost of electricity for the optimization horizon, T, for each individual house, h. This is done for each day separately within the simulation period. As it would be unlikely to know the exact local production, demand and electricity prices every 30 minutes if the simulation period is long when assuming a perfect forecast model. Equation (3.1) shows the objective function for approach 1 for the 25-houses case. The equation sums up the cost of grid consumption, $G^{(t,h)}$, minus payback for power delivered to the grid, $G_{to}^{(t,h)}$, for each time step within the simulation period. $p_G^{(t)}$ and $p_{G_{to}}^{(t)}$ denote the electricity price and price for power delivered to the grid, respectively. All of the equations in section 3.4.1 hold true for all $h \in H$ and $t \in T$, and all variables are non-negative.

[16]See fig. 3.1a for an explanation of the symbols used in fig. 3.6.

$$\min_{\substack{\forall\ t\in T \\ \forall\ h\in H}} C^{(h)}_{tot,A1} = \sum_{t}^{T} \left(G^{(t,h)} \cdot p^{(t)}_{G} - G^{(t,h)}_{to} \cdot p^{(t)}_{G_{to}} \right) \tag{3.1}$$

The objective function is subject to two constraints, the power balance equation and the equation for the battery storage level. The power balance constraint says that the sum of power drawn from the grid, $G^{(t,h)}$, power produced by renewable units, $res^{(t,h)}$, and battery discharge, $D^{(t,h)}$, must be equal to the sum of the power demand, $dem^{(t,h)}$, power delivered to the grid, $G^{(t,h)}_{to}$, and battery charge, $C^{(t,h)}$, for each time step $t \in T$ and house $h \in H$. Equation (3.2) shows the power balance equation for approach 1.

$$\underbrace{G^{(t,h)} + res^{(t,h)} + D^{(t,h)}}_{\text{Supply}} = \underbrace{dem^{(t,h)} + G^{(t,h)}_{to} + C^{(t,h)}}_{\text{Total demand}} \tag{3.2}$$

The battery storage level constraint says that the battery storage level, $S^{(t,h)}$, is equal to the storage level of the previous time step, $S^{(t-1,h)}$, plus the battery charge, $C^{(t,h)}$, or minus the battery discharge, $D^{(t,h)}$, in the current time step t. The amount of power charged to, or discharged from, the battery is multiplied with the inverter efficiency, η_{inv}, and with the corresponding charging or discharging efficiencies, η_c or η_d. Equation (3.3) shows the battery storage level constraint.

$$S^{(t,h)} = S^{(t-1,h)} + \eta_c \cdot \eta_{inv} \cdot C^{(t,h)} - \frac{1}{\eta_d \cdot \eta_{inv}} \cdot D^{(t,h)} \tag{3.3}$$

A battery has limits on upper and lower storage levels, which are determined by the upper SOC, $\overline{SOC}$, and the lower SOC, $\underline{SOC}$, limits and the nominal capacity of the battery, E_{Bat}. This is showed in eq. (3.4). The battery SOC is a number $\in [0,1]$ [p.u.]. Further, the charging and discharging of a battery is limited by the nominal power of the BESS inverter, P_{inv}, and the inverter efficiency, η_{inv}, as showed in eq. (3.5) and (3.6).

$$E_{bat} \cdot \underline{SOC} \leqslant S^{(t,h)} \leqslant E_{bat} \cdot \overline{SOC} \tag{3.4}$$

$$0 \leqslant C^{(t,h)} \leqslant \eta_{inv} \cdot P_{inv} \tag{3.5}$$

$$0 \leqslant D^{(t,h)} \leqslant P_{inv} \tag{3.6}$$

Power cannot be sold and purchased from the grid in the same time step and a BESS cannot be charged and discharged at the same time. In this model, it will never be optimal to buy and sell power from the main grid in the same time step, as the payback for selling power to the grid always will be lower than the cost of buying power from the grid. Further, the charging or discharging of the BESS are mutually exclusive events, because it will never be optimal to charge and discharge the BESS at the same time due to efficiencies lower than 1 p.u. Based on these facts, restrictions ensuring no simultaneous charging and discharging, or no simultaneous selling and buying grid power, are not needed.

3.4.2 Approach 2 - Centralized Strategy

In the centralized strategy, approach 2, the different houses can get their energy demands met with the same sources as in approach 1, but in addition they can buy power from other houses within the community, called peers, p. Figure 3.1b shows the setup of the 25-houses case using approach 2 with the possible power flow directions.

The objective of the approach is to minimize the total cost of electricity for the whole community within the optimization horizon. This is done separately for each day within the simulation period, due to the aforementioned reasons in section 3.4.1. Equation (3.7) shows the objective function of approach 2 for the 25-houses case. The grid consumption, $G^{(t,h)}$, is summed up for all of the houses and multiplied with the wholesale spot prices, $p_G^{(t)}$. The power sold to the main grid, $G_{to}^{(t,h)}$, is summed for all the houses and multiplied with the in-feed price, $p_{G_{to}}^{(t)}$. All of the equations in section 3.4.2 hold true for all $h, p \in H$ and $t \in T$, and all variables are non-negative.

$$\min_{\substack{\forall\ t\in T \\ \forall\ h\in H}} C_{tot,A2} = \sum_{t}^{T} \left(\left(\sum_{h}^{H} G^{(t,h)} \right) \cdot p_G^{(t)} - \left(\sum_{h}^{H} G_{to}^{(t,h)} \right) \cdot p_{G_{to}}^{(t)} \right) \tag{3.7}$$

The power balance equation used for this method is given in eq. (3.8). The equation is the same as the power balance equation for approach 1, except that total P2P power purchase, $I^{(t,h)}$, has been added as a possible source of power, and that total amount of sold P2P power, $X^{(t,h)}$, has been added as a possible additional demand.

$$\underbrace{G^{(t,h)} + res^{(t,h)} + D^{(t,h)} + I^{(t,h)}}_{\text{Supply}} = \underbrace{dem^{(t,h)} + G_{to}^{(t,h)} + C^{(t,h)} + X^{(t,h)}}_{\text{Total demand}} \tag{3.8}$$

Approach 2 has the same battery constraints as approach 1. This means that eq. (3.3) - (3.6) also have been applied in approach 2. As for the first approach, no constraints are needed for ensuring that power cannot be bought from, or sold to, the main grid in the same time step nor for ensuring that simultaneous charging and discharging of a BESS cannot occur in the second approach. This is because the grid prices and the BESS efficiencies are case dependent, and not approach dependent.

The enabled P2P trading has to follow certain rules, which are added as restrictions to the objective function. The total amount of sold P2P power, $X^{(t,h)}$, from house h in time step t is given by the sum of the electricity flows, $X_p^{(t,h\to p)}$, from the house to the peers $p \in H$, as stated in eq. (3.9).

$$X^{(t,h)} = \sum_{p\neq h} X_p^{(t,h\to p)} \tag{3.9}$$

The purchased power, $I_p^{(t,h\leftarrow p)}$, of house h from peer p is equal to the bought power, $X_p^{(t,h\to p)}$, times the efficiency factor for conversion and transmission of distributed generation to P2P sale, θ_{P2P}, as showed in eq. (3.10).

$$I_p^{(t,h\leftarrow p)} = \theta_{P2P} \cdot X_p^{(t,h\to p)}, \qquad \forall\ p \neq h. \tag{3.10}$$

The total amount of P2P power, $I^{(t,h)}$, bought by house h is given as the sum of all electricity flows, $I_p^{(t,h\leftarrow p)}$, from the different peers $p \in P$ to the specific house h, as showed in eq. (3.11).

$$I^{(t,h)} = \sum_{p \neq h} I_p^{(t,h\leftarrow p)} \tag{3.11}$$

When taking the P2P losses into account and that the P2P power remains within the community, the sum of all the purchased P2P power must be equal to the sum of all the sold P2P power times the P2P efficiency factor, as showed in eq. (3.12).

$$\sum_h I^{(t,h)} = \sum_h \theta_{P2P} \cdot X^{(t,h)}, \qquad \forall t \in T. \tag{3.12}$$

3.5 Case Results and Analysis

The presented linear multi-period models for the decentralized and centralized control system strategies for the 25-houses case are both implemented in MATLAB and solved using the MATLAB-solver *linprog*. The *linprog* solver uses a dual-simplex algorithm, explained in section 2.2 in chapter 2, to find the optimal solution for the objective function with its associated constraints. The system parameters have been read from Excel into MATLAB, and MATLAB was both used to solve the models and to generate plots and graphs presenting the results. Both of the models are implemented and solved on a 64-bit macOS Catalina with Intel Core I5-6360U, 2 GHz CPU and 8 GB RAM.

The performance of the two different control system strategies is measured based on the electricity costs for each house and the total costs for the whole community of houses. The most effective strategy is the one that gives the lowest total electricity costs. The total amount of energy drawn from the main grid and the peak power demand of the community are also noted.

The results and analysis of the two different approaches have been divided into two separate sections. Section 3.5.1 and 3.5.2 show the results and the result analysis for the decentralized (approach 1) and the centralized (approach 2) approaches, respectively. In the last part, section 3.5.3, the results of the different approaches are compared and discussed.

3.5.1 Approach 1 - Results

In the decentralized approach, each house has to make its own supply-demand decisions by using its own local production and storage units, if the house has any, and power from the main grid. The optimization aims at minimizing the electricity costs for each house separately for each day within the 91 days long simulation period. In the 25-houses case, there are some houses with both DERs and BESS, some houses with only DERs, and some houses that have no local production nor storage. The houses with production and/or storage units are optimally scheduled to utilize their resources before covering the possible power deficit with power from the main grid. Possible surplus power from production is sold to the main grid. The houses that do not have any production nor storage units must buy all the necessary power from the main grid.

It took just over 3 minutes to run the optimization model on the 64-bit macOS Catalina for the three stated months in MATLAB, and the optimization comprises 257,712 variables and 122,304 constraints for the simulation period. The total amount of energy drawn from the grid for the

community of houses is 27,864 kWh, which corresponds to a cost of £3,918. The total amount of energy that is fed to the main grid from the community of houses is 7,160 kWh, which gives a total payback of £776. This means that the optimal solution for this method gives a total cost of £3,142 for the community of houses. The optimal solution results in a peak power demand of 5.76 kW for house 25. If the houses are considered as a community, the community would have a peak demand of 21.64 kW.

Figure 3.7 shows the power balance, see eq. (3.2), between supply and total demand for house 15 in week 24, 2013. House 15 has a WT, PV system and a BESS. The upper plot in the figure displays how the average energy demand of the house in each time step, 30 minutes, is met with power from DERs, BESS discharge and with power from the main grid, while the lower plot shows that the total demand consists of the fixed energy demand of the house, power used to charge the battery and power that is being sold to the main grid. The total demand, i.e. the sum of the demand, battery charge and power sold to the grid, of the houses with DERs and/or BESS is not fixed, it is only the actual energy demand of the house that is fixed. For the houses that have both DERs and a BESS, the optimization will decide in which time steps power will be used to charge the battery or sold to the main grid. While the houses that have DERs and no storage, power will be sold to the main grid in time steps when the local production exceeds the fixed demand of the specific house. From fig. 3.7, it can be seen that most of the demand is met with local production. This is because utilizing self-produced energy has no costs in the optimization. The PV production is highest in the middle of the day, as the sun is at its highest at this time, while the production from the WT is more varying during the day and night. Because of the relatively high local production, house 15 does not need to buy that much power from the main grid. This results in low operating costs for the house, as it is the power drawn from the main grid that gives costs in the simulations.

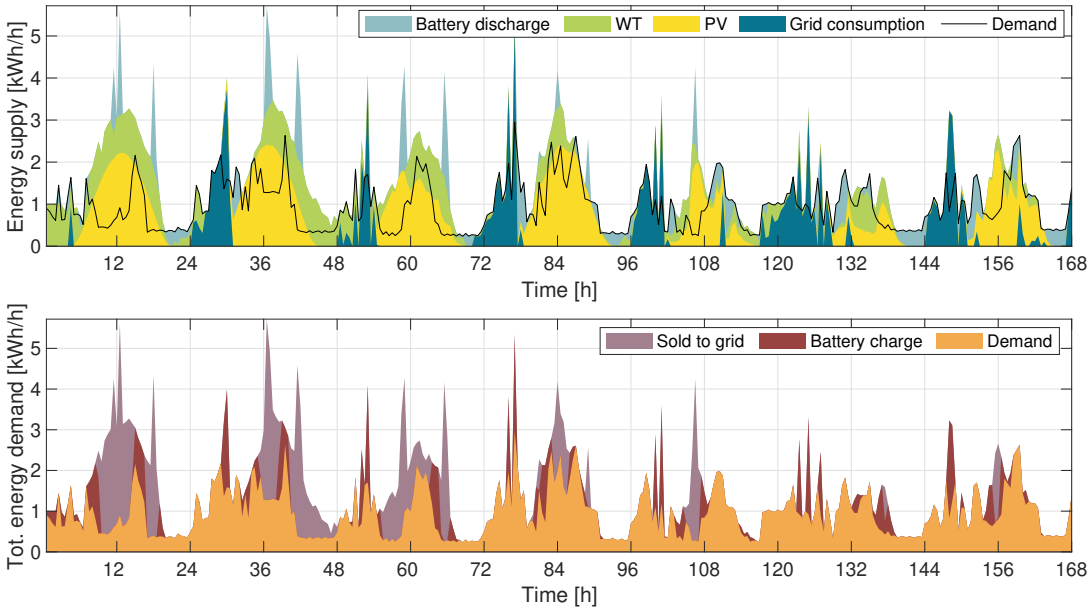

Figure 3.7: The supply-demand decisions made when using approach 1 on house 15 in week 24, 2013.

The optimization of the decentralized approach aims at reducing the electricity costs each day for each house. This means that the houses with local production units try to maximize their self-consumption and minimize grid consumption. If the demand exceeds the local production, the houses with both DERs and BESS units will try to buy power from the main grid when the electricity prices are low. If the local production exceeds the demand, the houses with DERs and BESS units will try to sell power to the main grid when the in-feed costs are high, to get the highest revenue. Figure 3.8 shows the electricity and in-feed costs for week 24. On the first day of that week, the in-feed costs have two peaks, one right around 12 h and one at 18 h. When comparing fig. 3.8 with 3.7, it can be seen that the battery is discharged and that power is sold to the grid in those hours, to get the highest revenue for the sold power.

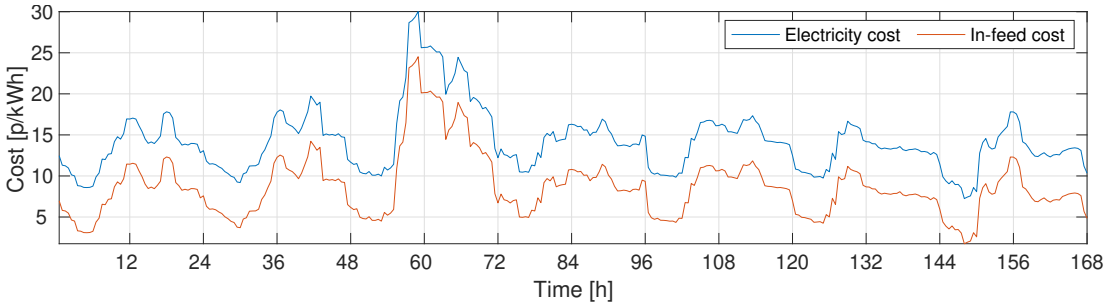

Figure 3.8: The corresponding electricity and in-feed costs for week 24.

Figure 3.9 shows the storage level of the battery of house 15 during week 24. It can be seen from the figure that the battery is fully charged when the local production exceeds the fixed demand and that the battery is discharged when the electricity costs and in-feed costs are high. In periods with low local production, like in the period 71 h to 78 h shown in fig. 3.7, the battery is charged when the electricity cost is low, i.e. at 76 h and 77 h.

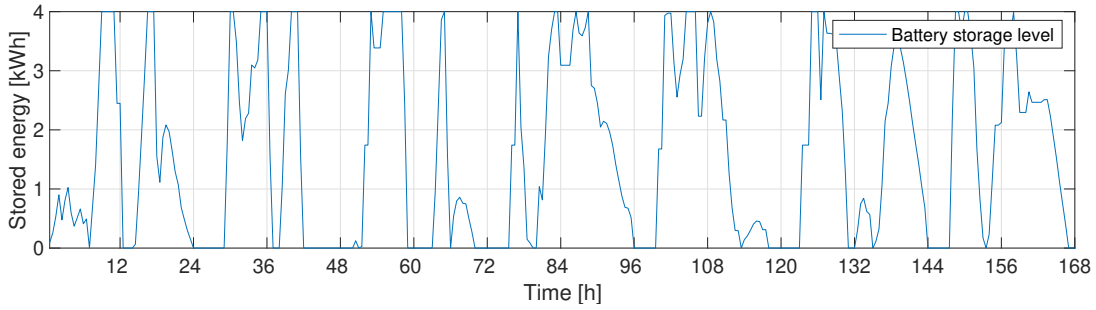

Figure 3.9: Storage level for the battery in house 15 for week 24, 2013.

3.5.2 Approach 2 - Results

Using the centralized approach on the 25-houses case means that the houses are looked at as one community. The objective is to minimize the operational costs each day, i.e. optimization horizon, during the analysis period for the community, and not for each house. In this approach, it has been made possible to use P2P trading. Houses with DERs or BESS units can sell power directly to other peers, and the P2P power can only be traded within the community.

Running the optimization model for the three months took almost 40 minutes on the 64-bit macOS Catalina. The long simulation time is due to that the optimization comprises 5,499,312 variables and 2,747,472 constraints. The total amount of energy drawn from the grid for the community of houses using the second approach is 22,591 kWh, which gives a cost of £3,063. 1,369 kWh is fed to the main grid during the simulation period, giving a payback of £173. This means that the optimal solution gives a total cost for the community of £2,890 for the simulation period. The highest peak demand seen from the grid when looking at the 25 houses as a community is 16.90 kW. If the houses are looked at separately, the highest peak is found to be 5.68 kW for house 25. When it comes to P2P energy trading, a total of 6,697 kWh is sold from peers and 6,188 kWh is bought from peers within the community. This results in a total of 509 kWh of losses during the simulation period.

Figure 3.10 shows how the power balance, see eq. (3.8), between supply and total demand is met with different energy sources for house 3 during week 18, 2013. House 3 has local production through a WT and no battery storage. In time steps when the production exceeds the fixed demand of the house, power is either sold to other peers or to the main grid. From the plots, it can be seen that most of the excess power is sold to other peers. This is because it is economically beneficial for the community to utilize production from DERs locally, rather than selling it to the main grid. The optimization decides that power should be sold to the main grid instead of to other peers in certain time steps, like around 108 h for house 3 in week 18, when e.g. the local production is high compared to the total community demand and there is no need for P2P power.

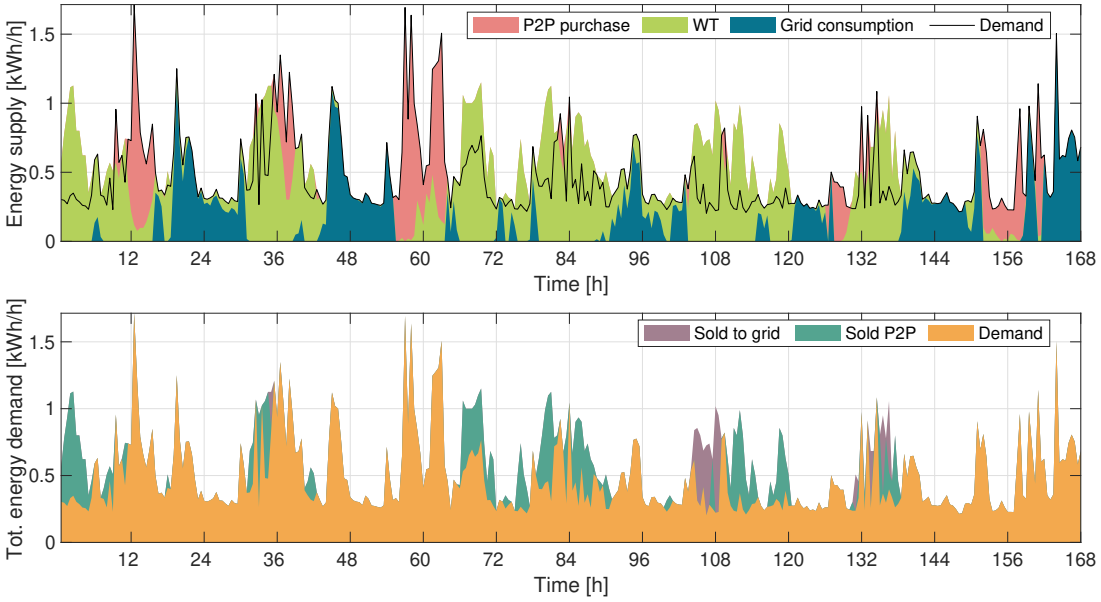

Figure 3.10: Supply-demand decisions made when using approach 2 for house 3 in week 18, 2013.

3.5.3 Comparison of the Results and Discussion

The results for the two different approaches are summarized in table 3.3. In the table, there have also been added results for two reference approaches, which utilize either the decentralized strategy, ref. A1, or the centralized strategy, ref. A2, but with no battery storage. The reference approaches have been added to have a source of comparison for each of the approaches, in addition to comparing them to each other.

Table 3.3: Results from the optimization using the two different control system strategies on the 25-houses case, both with and without storage.

Strategy	Ref. A1 (no storage)	A1: Decentralized Comp. to ref. A1		Ref. A2 (no storage)	A2: Centralized Comp. to: ref. A2		A1
Total costs [£]	3,246	3,142	-3.2%	2,994	2,890	-3.5%	-8.0%
Cost for grid consumption [£]	4,037	3,918	-3.0%	3,202	3,063	-4.3%	-21.8%
Revenues of selling to the grid [£]	791	776	-1.9%	208	173	-17.0%	-77.7%
Grid consumption [kWh]	28,311	27,864	-1.6%	22,921	22,921	-1.4%	-18.9%
Fed to main grid [kWh]	7,702	7,160	-7.0%	1,869	1,869	-26.7%	-80.9%
Maximum community peak [kW]	18.49	21.64	-17.0%	16.90	16.90	0%	-13.5%

The results in table 3.3 show that both the decentralized and centralized control system strategies give lower costs when the battery storage units are present. For the decentralized approach, the costs are reduced by 3.2% when storage is introduced, while the centralized approach gives a cost reduction of 3.5% when storage can be utilized. If the total electricity costs using the two approaches are compared, it can be seen that the centralized approach gives the lowest total operational costs. The total electricity costs for the community are 8% lower when using the centralized compared to the decentralized approach. It was expected that the centralized strategy would give the lowest total costs of the two strategies, as the aim of the strategy is to reduce the operational costs of the community, and not of the individual houses like the decentralized strategy.

The operational costs for the individual houses during the 91 days long simulation period using the different strategies are presented in fig. 3.11. The figure shows that the cost of the individual houses actually is lower when using the centralized strategy for the 25 houses. The reason for this is that the centralized approach allows P2P trading, unlike the decentralized strategy. The P2P trading price is set to be right in between the in-feed cost and the grid electricity cost, to incentivize P2P trading. This means that a higher revenue is gained when selling power to other peers compared to selling to the main grid. The in-feed cost to the grid is set to be 5.5 p/kWh lower than the grid electricity price, which varies in each time step. This means that the P2P trading price can take many different values and still be within the in-feed costs and the electricity costs. It was chosen to set the P2P price to be right in the middle of the in-feed price and the grid price, i.e. 2.75 p/kWh higher than the in-feed costs and thus 2.75 p/kWh lower than the electricity cost. If the P2P price is increased or decreased within the set limits, the costs of the individual houses will either increase or decrease depending on if the house has both DERs and storage units, only DERs units or neither. When the P2P price is increased, it is observed that houses with production from DERs and houses with both battery storage and DER production get lower operational costs, while the houses without DERs and storage get increased operational costs. This is because a higher P2P price gives a higher revenue for the houses that sell P2P power, and thus a higher cost for the houses that buy P2P power.

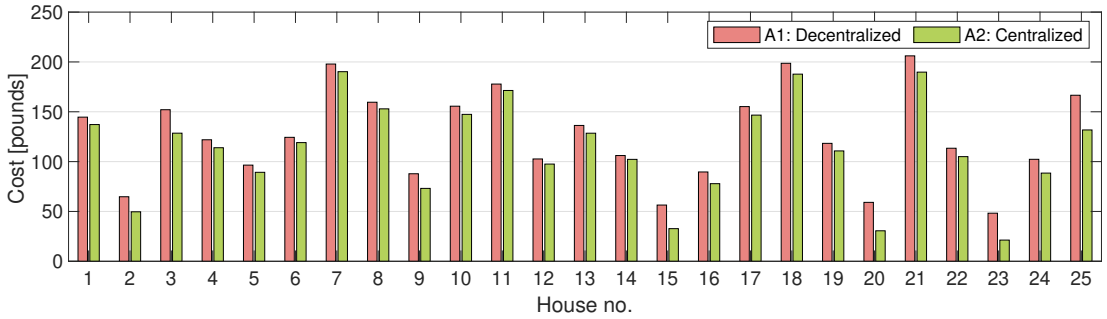

Figure 3.11: Total operational costs for each of the 25 houses using the decentralized and centralized control system strategies.

To observe the influence of the different features of the two approaches, the energy supply and total demand of the 25 houses were aggregated. Figure 3.12 shows the aggregated energy supply for all of the 25 houses using the decentralized and centralized approaches for week 14 in year 2013. The corresponding aggregated total demand for the two approaches is showed in fig. 3.13. The figures show that grid consumption decreases when going from the decentralized to the centralized approach. For the simulation period, the grid consumption is decreased by 18.9%, ref. table 3.3, when comparing the results from the centralized approach with the decentralized approach. Further, it can be seen that less power is sold to the main grid in approach 2, as it is possible to sell power to other peers. The amount of power sold to the grid is decreased by 80.9% compared to approach 1.

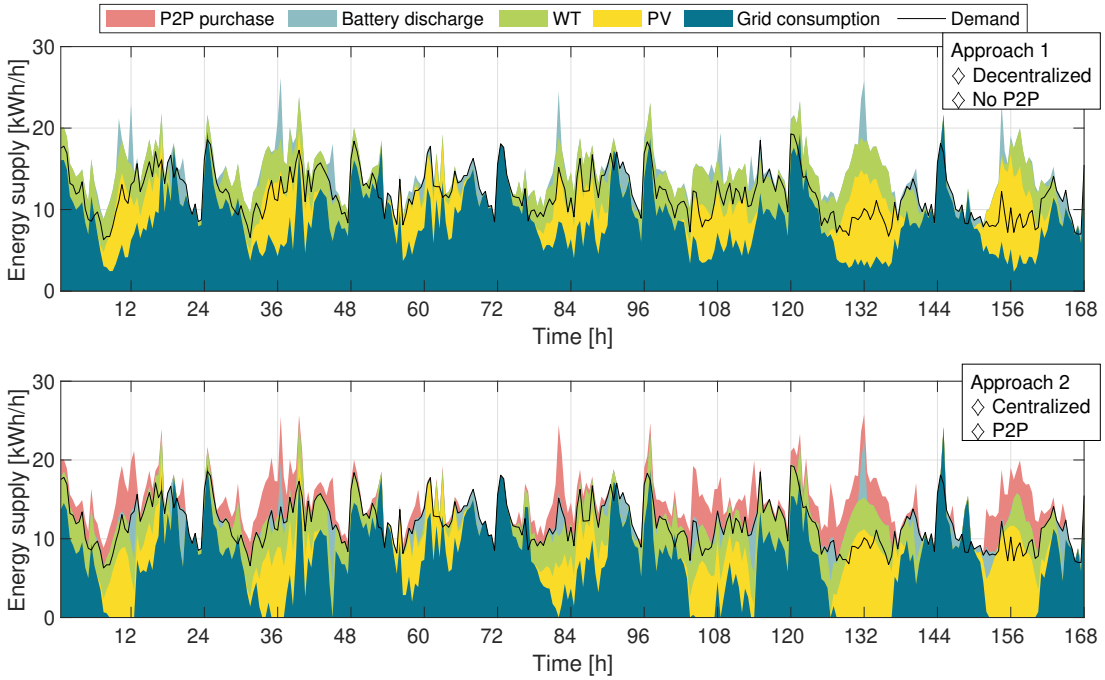

Figure 3.12: The aggregated energy supply for all of the 25 houses using the first and second approach for week 14, 2013.

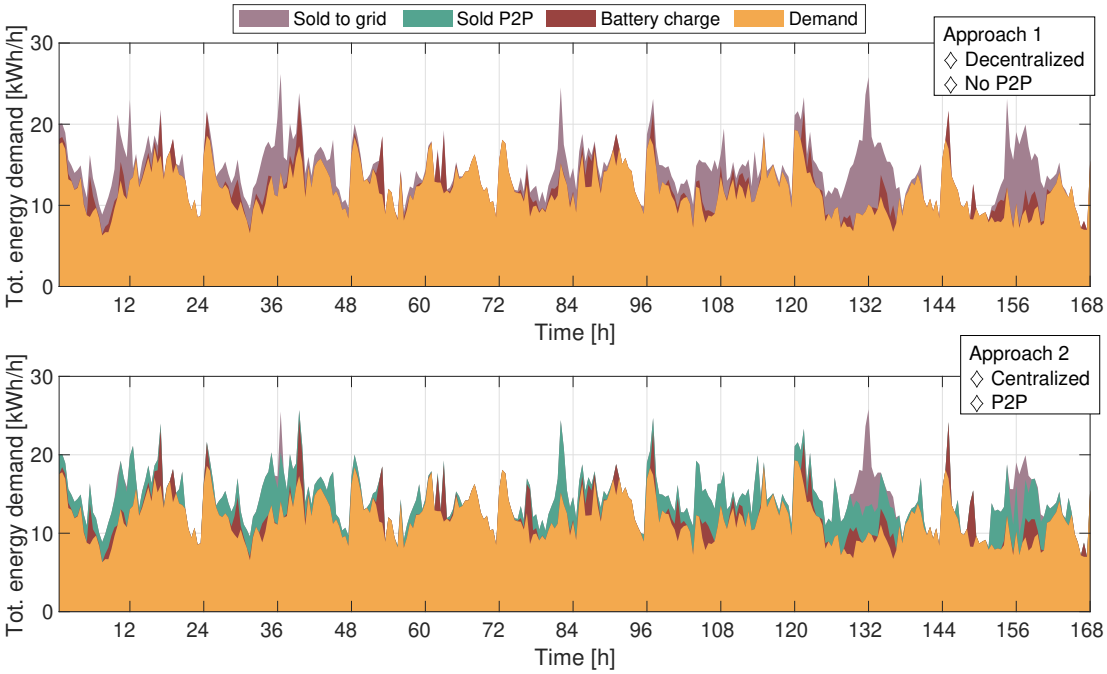

Figure 3.13: The aggregated total energy demand for all of the 25 houses using both approach 1 and approach 2 for week 14, 2013.

The share of the different sources of supply for the two approaches is presented in fig. 3.14, while fig. 3.15 shows the share of the different demand types for the approaches. The aggregated demand and local production of the houses are the same in both approaches. It is the optimization approach that decides when the batteries should be charged or discharged and when power should be bought from or sold to the main grid. For the centralized approach, the optimization also decides how much power should be traded P2P. Figure 3.14 shows that when P2P trading is introduced and a centralized approach is applied, the share of power coming from the grid is reduced by 11.79% from the decentralized approach. While from fig. 3.15, it is seen that the share of power sold to the grid is reduced by 11.86% when comparing the centralized with the decentralized approach. The introduction of P2P trading causes more power to be sold to other peers instead of to the main grid.

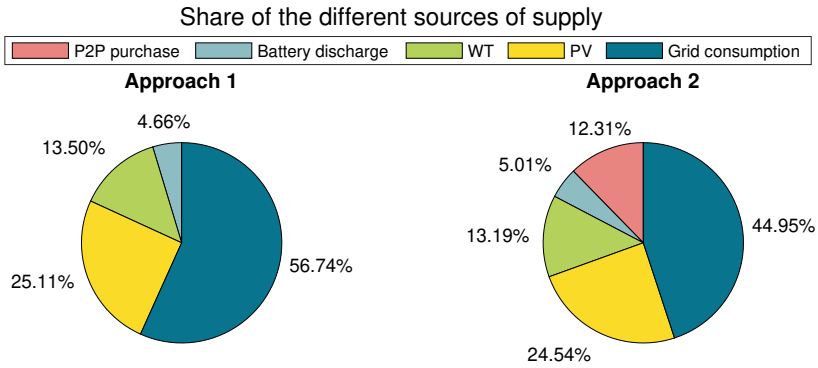

Figure 3.14: The share of different sources of supply for the two approaches for the 25-houses case[17].

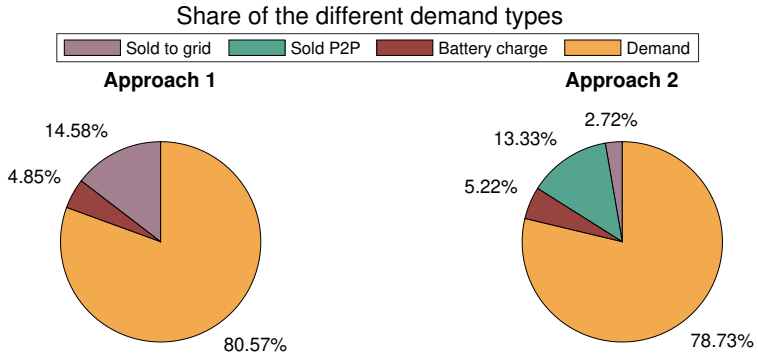

Figure 3.15: The share of different types of demand for the two approaches for the 25-houses case[18].

In both strategies, neither the peak power demand seen from the main grid nor the supply peak, when selling power to the main grid, are considered. This means that the two approaches can give results with high peaks. When looking at the results for both approaches, it is observed that the houses with production and storage units try to buy the necessary power from the main grid in hours when the electricity prices are low, and sell power to the main grid when the in-feed prices are high. This can be seen for both approaches for house 15 during an arbitrary week in the simulation period through looking at fig. 3.7 in section 3.5.1 for the decentralized approach and fig. A.1 in appendix A.1 for the centralized approach. If the figures are compared with the corresponding electricity and in-feed prices for the specific week, see fig. 3.9 in section 3.5.1, it is observed that the spikes in supply and demand seen from the grid are price dependent. As the power demand of the community of 25 residential buildings is relatively low compared to larger grid consumers, like e.g. industrial sites, the peak demand of the community does not have a large overall impact when considering that the DSO has to dimension the grid based on the highest peak demand seen from the main grid. If, on the other hand, the approaches are

[17]The aggregated local production accounts for different shares of the total supply in the two approaches, but the aggregated production is the same in both approaches.

[18]The aggregated demand of the houses accounts for different shares of the total demand in the two approaches, but the aggregated demand is the same for both approaches.

applied to larger communities or to several communities in the same area, the peak demand seen from the grid must be taken into consideration to not trigger possible costly grid updates.

Both control system strategies optimize the supply-demand decisions for each separate day within the 91 days long period. It was chosen to use an optimization period of just one day, due to the assumption of a perfect forecast model. Expanding the optimization period would give more unrealistic results as it is unlikely to know the exact local production, demand and electricity prices for a long period beforehand. The result of this is that the optimization results won't be optimal when looking at a period longer than one day. When observing the utilization of the battery storage, it can be seen from fig. 3.9 in section 3.5.1 that the battery is emptied at the end of each day. The optimization does not take the next day into account when optimizing the use of the storage. To exploit the usage of the battery storage, the optimization approaches could be changed to find the optimal solution for the whole 91-day long period in one go. To get more realistic results, forecasting algorithms could be implemented in both approaches.

The simulation period is set to be three months long, ergo 91 days for the spring months April to June, to reduce computational time. The months April to June were chosen because in this period there is an overall increased production from the PV systems and an overall decrease in the wind turbine production. It was desirable to have a certain amount of renewable production to better see the effect of P2P trading on the results, as more local production implies that the houses within the community will draw less power from the grid and that there will be more flexibility for P2P trade. As the aggregated capacity of the PV system is higher than the aggregated capacity of the wind turbines, the total renewable production will most likely be higher in the spring and summer months compared to the fall and winter months. As the production from the wind turbines is lower in the summer, the spring months were chosen so that also the wind turbine production would be noticeable.

4 | Elnett21, Case in Norway

The first two control system strategies, presented in section 2.3, were applied to a second case with larger industrial end-users to observe how the results would turn out using a different type of case. In this chapter, the Norwegian Elnett21-case is presented as well as the results obtained when using the two strategies.

4.1 Introduction to the Case

The Elnett21-case is from the ongoing Elnett21-project[19] (year 2019-2024), which is a collaboration, research and development project between Avinor, Forus Industrial Park, Lyse Elnett, Smartly and the Port of Stavanger. The partners are all located in the Stavanger region, Norway, where Lyse Elnett is the local DSO. The project aims to find solutions to meet the increasing power demands due to i.e. the electrification of the transportation sector [9].

The Norwegian Elnett21-case of this thesis addresses the three end-users Avinor, Forus Industrial Park and the Port of Stavanger. Avinor operates the airport in Stavanger, Forus Industrial Park concerns an area with a lot of office buildings and industries while the Port of Stavanger Group operates Risavika Harbor, as well as some other harbors in the district. The airport, industrial park and harbor are all planning to install local energy production and storage units as a part of the Elnett21-project. The production units consist of wind turbines (WT) and photovoltaic (PV) systems, while the storage units are battery energy storage systems (BESS) and a vehicle to grid (V2G) solution where electric vehicles (EVs) can be used like a temporary battery storage. The three end-users all have high energy demands, and it is assumed that 10% (see [14]) of the energy demand of all the end-users is shiftable. Shiftable load is a type of flexible[20] load that can be shifted in time, but the total load must still be met within a certain time period [26].

In this thesis, it is assumed that the three end-users are supplied with power from the same transformer station and that there is a local grid connecting the end-users, which makes it possible to trade power between them locally. In reality, the three project participants are not directly connected, and they are not supplied with power from only one transformer station. Between them, there are several transformer- and substations, and there are a lot of transmission cables and overhead lines. The end-users have been placed under the same bus beneath one transformer to simplify the case. Figure 4.1 shows the system configuration of the Elnett21-case with one transformer station which is connected to each of the end-users through a cloud. The cloud can be considered as a "virtual bus", which is used to represent that the end-users are directly connected in the Elnett21-case, but that they are not directly connected in reality. The figure also shows the different types of DERs and storage units installed at the different locations in the case.

[19] For further information on the Elnett21-project see https://www.elnett21.no

[20] A flexible load is a generic term for loads that can be changed in some kind of way. The flexible load can either be shiftable or curtailable. The shiftable loads can be time-shifted, but the total load must be met within a specific time interval. The curtailable loads represent flexible loads that can be reduced, without having to be replaced [26].

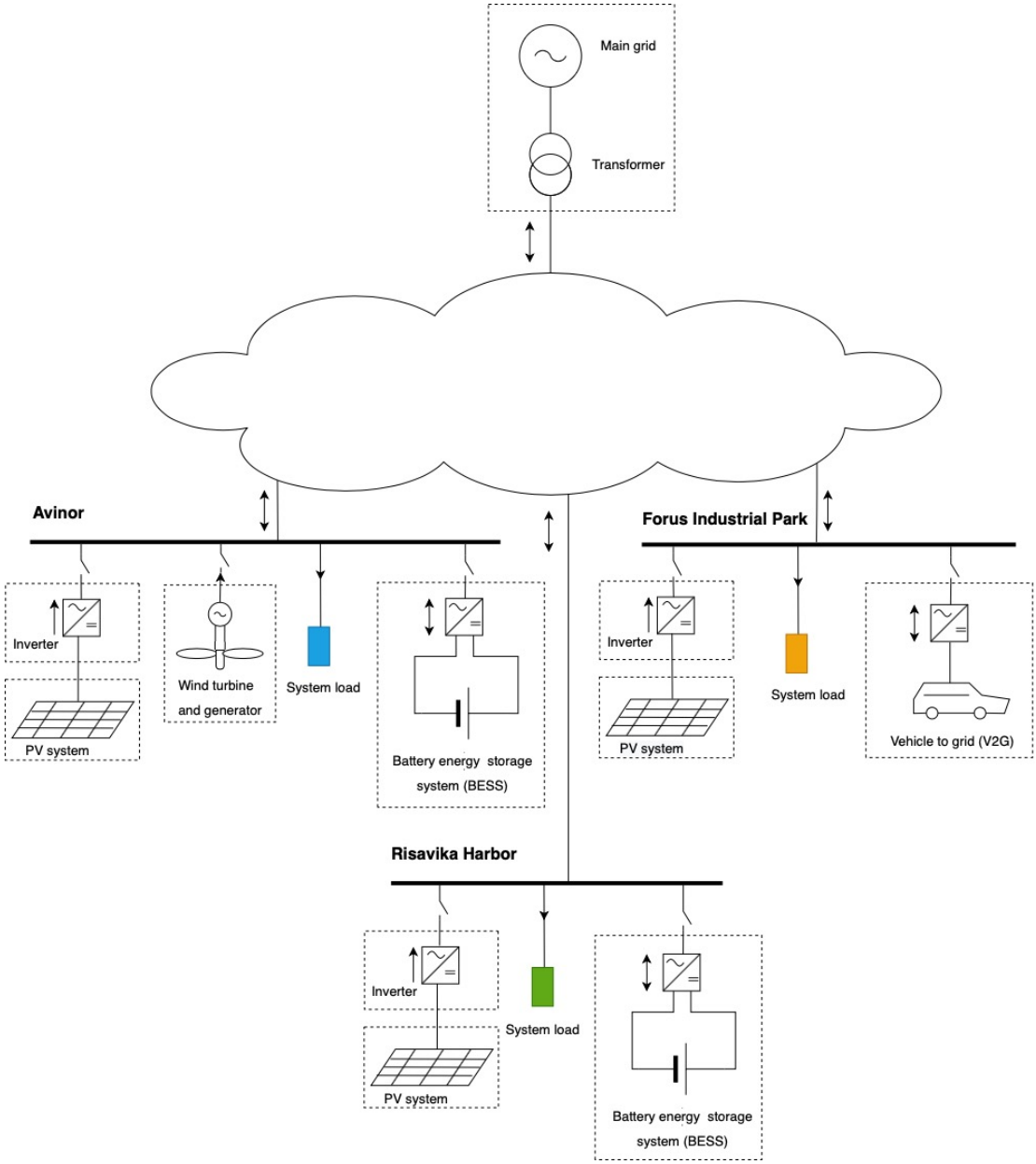

Figure 4.1: The used system configuration for the Elnett21-case. The cloud is used to show that in the case, the end-users are connected through a local grid, but in reality they are not directly connected.

4.2 Case Data and System

The exact demand data for the end-users in the Elnett21-case was not given for any of the project participants. Further, the airport, harbor and industrial area have not yet decided on the type and size of production and storage units to be installed. Based on these facts, the demand data for the end-users had to be generated or put together manually and production and storage units were chosen and sized based on different conceptual studies. This section describes how the demand, production and storage data was found.

Hourly data was used for the period April to June from year 2015. This year was chosen as it was used for finding the demand and production for Stavanger Airport, Avinor, in the specialization project, reference [33]. The simulation period, April to June, with hourly simulation steps results in 2,184 time steps.

4.2.1 Avinor - Stavanger Airport

Avinor is a company that operates most of the airports in Norway. In Stavanger, they operate Stavanger Airport, which takes part in the Elnett21-project. The airport is planning to install production and storage units and has involved the consultant company Norconsult to get an overview of the different possibilities.

The demand of the airport for 2015 was found in the specialization project, [33], using data provided by a report by Norconsult, reference [11]. In 2015, Stavanger Airport had a total demand of 15,713 MWh/yr, while for the simulation period April to June 2015, the demand was 3,653 MWh. As stated in the specialization project, only monthly energy demand data was provided in addition to only one demand curve for a day during the summer. Using the average daily demand for each month, the demand curve was parallel shifted such that the demand each day would be equal to the average daily demand for each month. Using this method, the created demand would have the same monthly demand values as the actual demand curve. Figure 4.2 shows the generated energy demand of Stavanger Airport for the whole simulation period, while fig. 4.3 shows the airport demand during week 15 in 2015. It can be seen from the figures that the demand curve has the same shape each day and that it is exactly the same for the days within the same month.

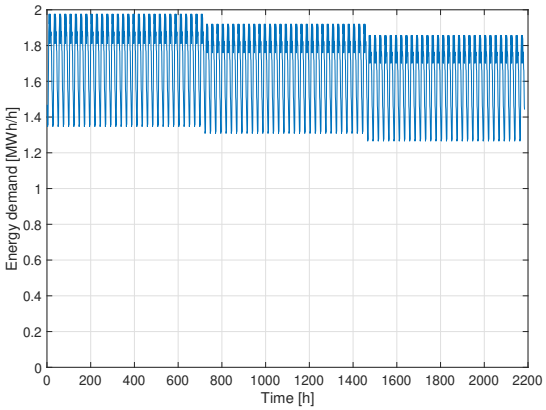

Figure 4.2: The generated demand for Stavanger Airport for the simulation period April to June 2015.

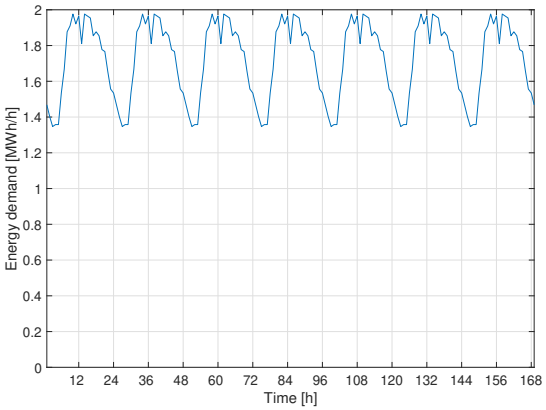

Figure 4.3: The generated demand for Stavanger Airport for week 15 (April) in 2015.

Norconsult proposed that the airport should install PV systems and WTs as production units and a large BESS as a storage unit. Four Wind Technik Nord (WTN) turbines each with a nominal output power of 250 kW, a large PV system with an installed capacity of 4.57 MW_p and a BESS with a capacity of 12 MWh and a power capability of 3 MW was mentioned as an alternative [11]. These units have been chosen for Stavanger Airport in the Elnett21-case.

To find the production from the four WTN250 wind turbines, the power performance curve had to be found using a six-degree polynomial. The fitted power curve for the WTN250 turbines, showed in fig. 4.4, together with wind speed data from a weather station located at the airport, and a scaling factor compensating for insufficient spacing between the turbines, gave a total production of 1,720.37 MWh/yr for 2015. The WT production is equal to 10.95% of the total yearly demand of the airport. For the simulation period April to June 2015, the total WT production was found to be 392.08 MWh, which is equal to 10.73% of the demand in the same period. Figure 4.5 shows the total WT production for an arbitrary week. Further descriptions of how the WT production for Stavanger Airport was found are given in the specialization project (see [33]).

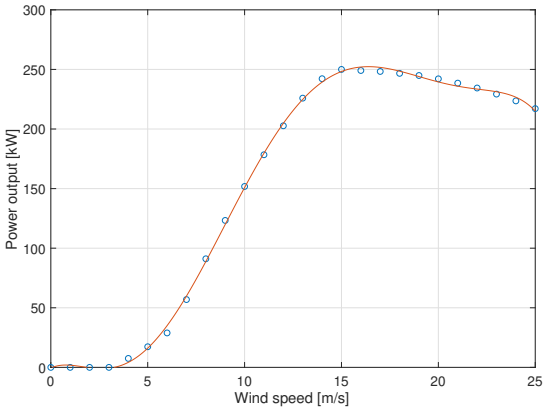

Figure 4.4: Fitted versus discrete power curve for the wind turbine Wind Technik Nord 250 kW (WTN250).

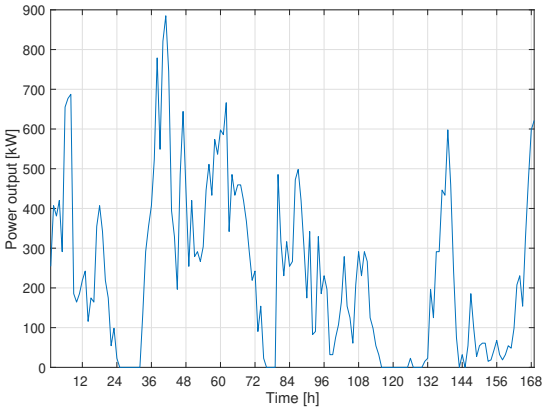

Figure 4.5: Production from the four WTs at Stavanger Airport for week 19, 2015.

The PV production was found using Renewables.ninja, which is a web application that takes input on location (latitude and longitude), PV system capacity, system loss, tilt and azimuth angle of the PV system. The preferred dataset, either the global reanalysis model MERRA-2 or Meteosat-based CM-SAF SARAH, also has to be chosen in addition to choosing if the PV system has tracking or not. When this data is put into the application, it will give hourly production data for the PV system for a specified year. The PV production for Stavanger Airport was found to be 4,593.11 MWh/yr for 2015, which is 29.23% of the yearly demand. For the simulation period, April to June 2015, the PV production was 1,898.57 MWh, which is 51.97% of the demand in the period. The PV production was found using the airport as location, the dataset MERRA-2, a PV system capacity of 4.57 MW_p, no tracking and the default values for system loss, tilt and azimuth angle, of 0.1, 35° and 180°, respectively. Such a PV system will cover around 20,000 m^2 [11]. See the specialization project, [33], for more details.

Figure 4.6a and 4.6b show the production from the PV system at Stavanger Airport for two arbitrary weeks during the simulation period April to June 2015. The first figure shows a week with lower production, while the second figure illustrates a week with higher production.

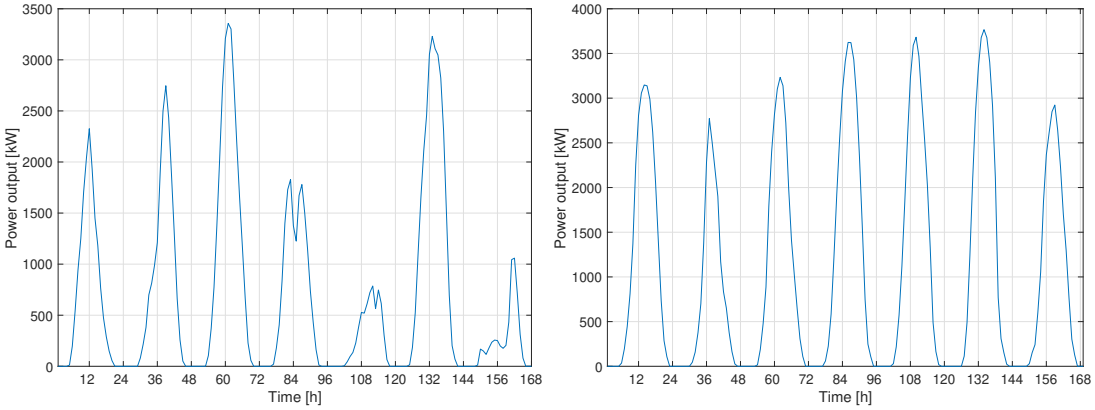

(a) Week 21 (May).

(b) Week 23 (June).

Figure 4.6: The PV system production at Stavanger Airport for two different weeks in 2015.

The BESS was set to have a battery capacity of 12 MWh and an inverter nominal power of 3 MW, as suggested from the Norconsult-report (see [11]), but the battery type was not given. To model the battery characteristics, a lithium-ion (Li-ion) battery was used as it is the most widespread battery of the different technologies. Figure 4.7 shows a typical SOC versus open circuit voltage of a Li-ion battery. The figure shows that the voltage of a Li-ion battery is relatively flat for a SOC between 20-90%, meaning that it is preferable to operate the battery within this region [29]. The recommended limits for SOC were applied to the BESS at the airport.

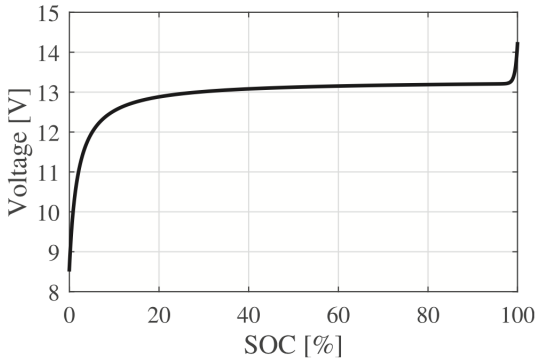

Figure 4.7: Open circuit voltage of a Li-ion battery versus SOC [29].

The BESS has a bi-directional converter, which converts the power from AC to DC when the battery is charging and vice versa when the battery is discharging. Converting power from AC to DC, or inverting power from DC to AC leads to losses. The efficiency of a converter will greatly depend on its topology, but it will often be within the interval of 0.90-0.98 [4]. It is assumed that the BESS at the airport has a converter efficiency of 98%. When it comes to the charging and discharging efficiencies of the battery, these efficiencies are dependent on the battery current. For simplicity, it is assumed that they are constant and equal and they are set to be 0.98 [29, 32]. With the given battery capacity and nominal power of the inverter, it takes around 4 hours to fully charge or discharge the battery in the BESS.

4.2.2 The Port of Stavanger - Risavika Harbor

Risavika Harbor (RH) is a harbor owned by the Port of Stavanger (PS) and is located in Stavanger, Norway [38]. PS is planning on expanding its harbor area at Risavika and has in that context looked at the possibilities of installing local production and storage units. To get an overview of the different possibilities at Risavika, PS involved a consultant company named NIRAS to have them make a conceptual study of RH. The result of this study was several reports where NIRAS has analyzed different opportunities for RH.

NIRAS studied the opportunities of installing different production units like PV systems, wind turbines and combined heat and power (CHP) production. They concluded that PV systems were the most suited production unit that could be installed at RH. The reason for this is that a PV system can be installed on all surfaces on new and existing buildings without taking up space or impose restrictions on utilization of the area in any way. Installing wind turbines will require more space, dependent on the size of the turbine, and an environmental impact assessment. The CHP-technology produces both power and heat but has a much lower electrical efficiency than thermal efficiency. This means that the produced heat must be utilized to increase the overall efficiency [39]. RH has high heating demands according to NIRAS, so CHP could be a good option, but it was not studied further by NIRAS hence it has not been further looked into in this thesis. For the storage, NIRAS explored different technologies like BESS, hydrogen and thermal energy storage. The emphasis was put on the BESS, which therefore was chosen as the storage unit to be used at RH for the Elnett21-case.

Risavika Harbor has industrial buildings, offices and warehouses. The harbor has recently installed three facilities for delivering shore power to offshore vessels. The shore power can be used to e.g. charge batteries on vessels, or to make vessels run on electricity instead of using their fossil-fueled motors while at shore, to reduce emissions.

To find a representative demand profile of Risavika Harbor for the simulation period, 2016 data from the transformer station named Risavika was combined with data from the shore power systems from June 2019 to May 2020, as no data was available for the simulation year 2015. The data from these sources show that the total yearly demand of the harbor is around 49.22 GWh/yr, while the demand for the simulation period April to June 2015 is 12,047.20 MWh.

Risavika transformer station supplies both RH and other close by end-users. It is assumed that RH stands for two-thirds of the total demand of the transformer, as RH is the largest end-user of the nearby consumers [1]. As the simulation period is set to be April 1st to June 30th 2015, and April 1st 2015 was a Wednesday while April 1st 2016 was a Friday, the demand data from Risavika transformer station was shifted two days back to have it start on the same weekday as the other data for the Elnett21 case. This means that the demand data for Risavika transformer station for the period March 30th to June 28th 2016 was used. The reason for doing this is that the demand greatly depends on the day of the week, with lower demands during the weekends.

The demand data from the shore power systems were collected for each hour from June 2019 to May 2020, as the shore power systems were not put into operation before June 2019. In this period, just one cable set was available, meaning that it was only possible to utilize one of the shore power facilities at a time. In reality, all three shore power systems can be utilized at once. This means that the demand from the systems would be higher if the cable sets were available [2]. To get a more representative demand level, it was found reasonable to triple the shore power demand.

The demand data of the shore power systems had various quality throughout the twelve months. In some months, there were days without any data while in other months there where days with

no demand, even though there should always be a base demand to keep the system going. The first three months, June to August 2019, showed low demands compared to the rest of the period, due to i.e. system testing [2]. Thus, to get a representative load demand curve of the shore power systems for the simulations months April to June 2015, the three months with the most consistent data where chosen. Data for April 2020 was used as April 2015 data, data for December 2019 was used as May 2015 data, and data for February 2020 was used as June 2015 data.

Figure 4.8 shows the generated demand for Risavika Harbor for April to June 2015, while fig. 4.9a and 4.9b show the demand of the harbor for two arbitrary weeks within the simulation period.

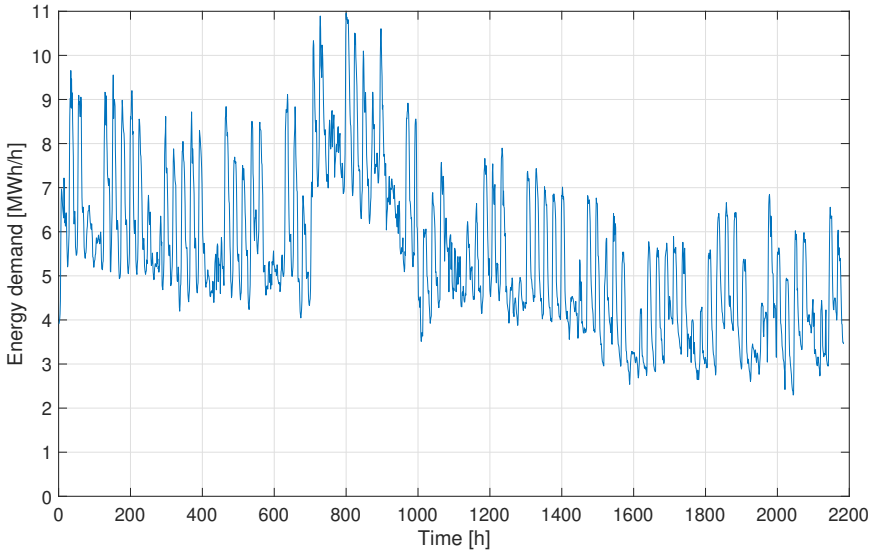

Figure 4.8: Generated demand of Risavika Harbor for the simulation period April to June 2015.

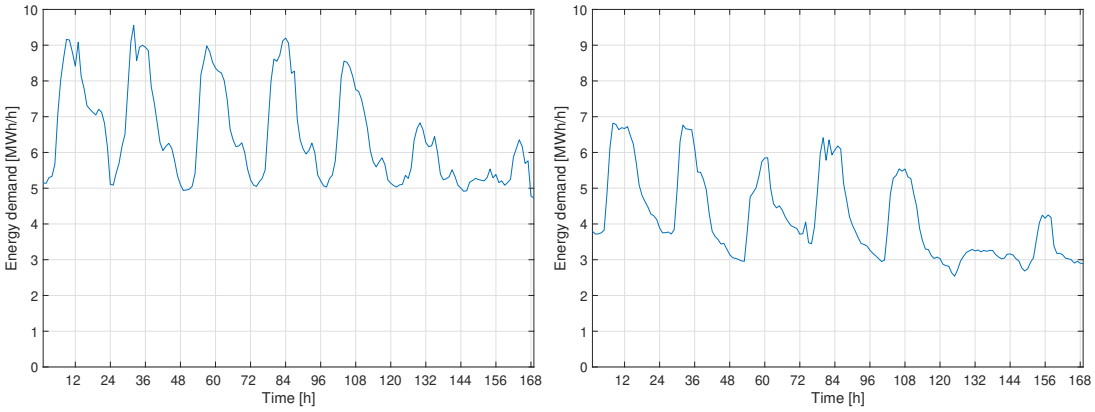

(a) Week 15 (April).

(b) Week 23 (June).

Figure 4.9: The generated demand of Risavika Harbor for two arbitrary weeks in 2015.

It was suggested by NIRAS that Risavika should install a PV system as a local production unit. The consultant company proposed different sizes of the PV system, see [39], but in this thesis it was chosen to use a size of the PV system that would give a yearly production equal to around 30% of the yearly demand. Using Renewables.ninja with Risavika Harbor as location, a capacity of 14.6 MW_p and with the rest of the input being the same as used for the airport, see section 4.2.1, the production for year 2015 was found to be 14,667.15 MWh/yr. This production is equal to 29.8% of the yearly demand. For April to June 2015, the PV production was 6,062.68 MWh, which is 50.32% of the demand of that period. Figure 4.10a and 4.10b show the PV system production for a week in April and a week in June 2015, respectively. If the same relationship between panel size and capacity is used for RH as for Stavanger Airport, the PV system at RH will be around 63,900 m^2, i.e. three times as large as the PV system at the airport.

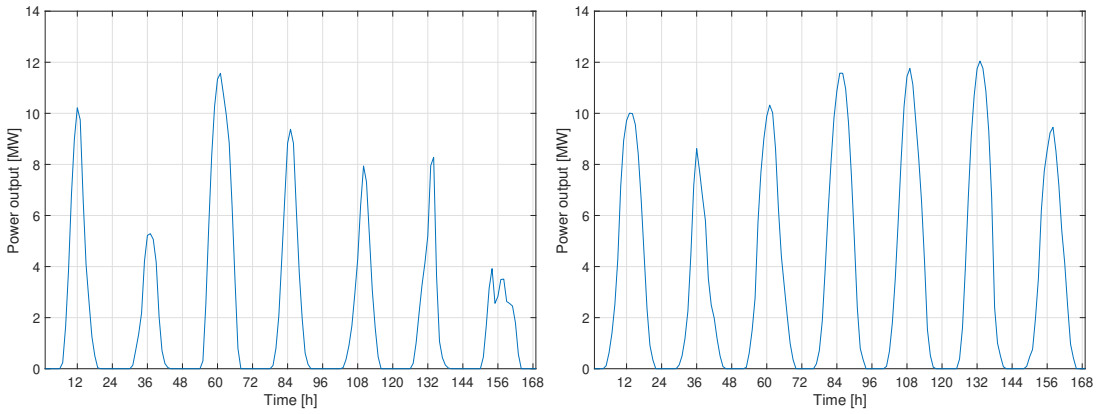

(a) Week 15 (April).

(b) Week 23 (June).

Figure 4.10: The PV system production at Risavika Harbor for two different weeks in 2015.

At Risavika Harbor it was recommended to install a BESS to give the harbor the ability to store power. The size of the BESS is not decided, but a BESS with a capacity of 21.5 MWh and a power capability of 4.8 MW was one suggestion by NIRAS [40]. The battery type and BESS characteristics were not given. Thus, the BESS at RH was modeled in the same way as the BESS at Stavanger Airport, see section 4.2.1, using a Li-ion battery, SOC limits of 20-90%, and a constant converter and charging/discharging efficiency of 98%. It takes approximately 4.5 hours to fully charge or discharge the battery with the given battery capacity and nominal power of the inverter.

4.2.3 Forus Industrial Park - Forus West

Forus Industrial Park (FIP) is a 6,500,000 m^2 large industrial area owned by the municipalities of Stavanger, Sandnes and Sola and is located at Forus, Norway. In FIP there are approximately 2,500 companies and 40,000 employees. The different companies are construction, manufacturing, oil, IT and trade and service companies [13]. Due to the large size of the industrial park, it is divided into areas. It is only the area called Forus West that is involved in the Elnett21-project. Forus West is around 2.780.400 m^2 and has about 30,000 of the total workplaces at Forus. There are approximately 190 buildings at Forus West of various size and age. The composition of the buildings is approximately 54% offices, 14% commercial buildings, 13% warehouses, 10% workshops and 9% other businesses [6, 30].

Forus West has an energy demand of about 128 GWh/yr [1, 6] and a heat demand of about 89 GWh/yr. At Forus, there is a facility for energy recovery of waste, called Forus Energigjenvinning, that delivers approximately 225 GWh/yr heat to the local district heating grid [6]. It is assumed that Forus West gets its heating demand covered by the local heating grid and that the energy demand must be met through local production and/or with power[21] from the main grid.

The actual demand profile for the Forus West area was not provided, thus it had to be generated manually. To find a demand pattern that could be representative for the industrial park, data from Campus Gløshaugen from year 2016 was used in combination with data from a demand generator for buildings.

Campus Gløshaugen is the main campus of NTNU in Trondheim. The demand pattern for campus Gløshaugen can be representable for the demand of various types of office-like buildings. The yearly electricity demand for campus Gløshaugen is approximately 61.60 GWh/yr.

To accompany the demand curve from campus Gløshaugen, and for adding new building types, a demand generator for buildings made by SINTEF was used. The generator takes input on outdoor temperature for each hour throughout the year and the area of different building types. It is possible to choose the following building types: house, apartment, office, shop, hotel, kindergarten, school, nursing home and hospital. To find a somewhat representative demand for Forus West, the temperatures from the closest weather station (Sola) was used for year 2015. As the total area of the buildings at Forus West is unknown, trial and error was conducted to find a total yearly demand which, together with the demand for Campus Gløshaugen, would give a total as close to 128 GWh/yr as possible. The generator did not give the option of choosing all the different building types which are located at Forus West, so it was chosen to use the two categories offices and shops. When selecting a floor area of 241,500 m^2 of offices and 161,000 m^2 of shops, the generator gave a total yearly demand of 66.40 GWh/yr. Combining this demand with the demand for Gløshaug, the total yearly demand of Forus West was found to be approximately 128 GWh/yr. For the simulation period, April to June 2015, the demand was found to be 31,756.50 MWh.

As April to June 2015 is chosen as the simulation period, and the demand data for the industrial park is accumulated from two different sources from different years, the simulation period had to be shifted some days forward or backwards to reassure that the first simulation day was a Wednesday, as April 1st 2015 is a Wednesday. The reason for having the data start on the same weekday instead of starting on the same date, is that the demand profiles are highly dependent on the day of the week. Thus, to get the correct weekly profiles, the data from Gløshaugen and from the demand generator was shifted forward or backwards to start on the closest Wednesday to April 1st in the corresponding data. The data for Gløshaugen is from 2016, where April 1st landed on a Friday. Thus, the data from Gløshaugen was shifted to start on March 30th, as this is the closest Wednesday to April 1st 2016. For the demand generator, the year is not specified. April 1st is on a Sunday for the data from the generator, and the data was thus shifted to start on April 4th, which is the closest Wednesday to April 1st.

Figure 4.11 shows the generated demand for Forus West for the simulation period April to June 2015, while fig. 4.12a and 4.12b show the demand for two arbitrary weeks.

[21] When using the terms power consumption, power demand, power in-feed or similar in chapter 4, the term power refers to the average power over the time step, 1 hour, and not the actual power per second.

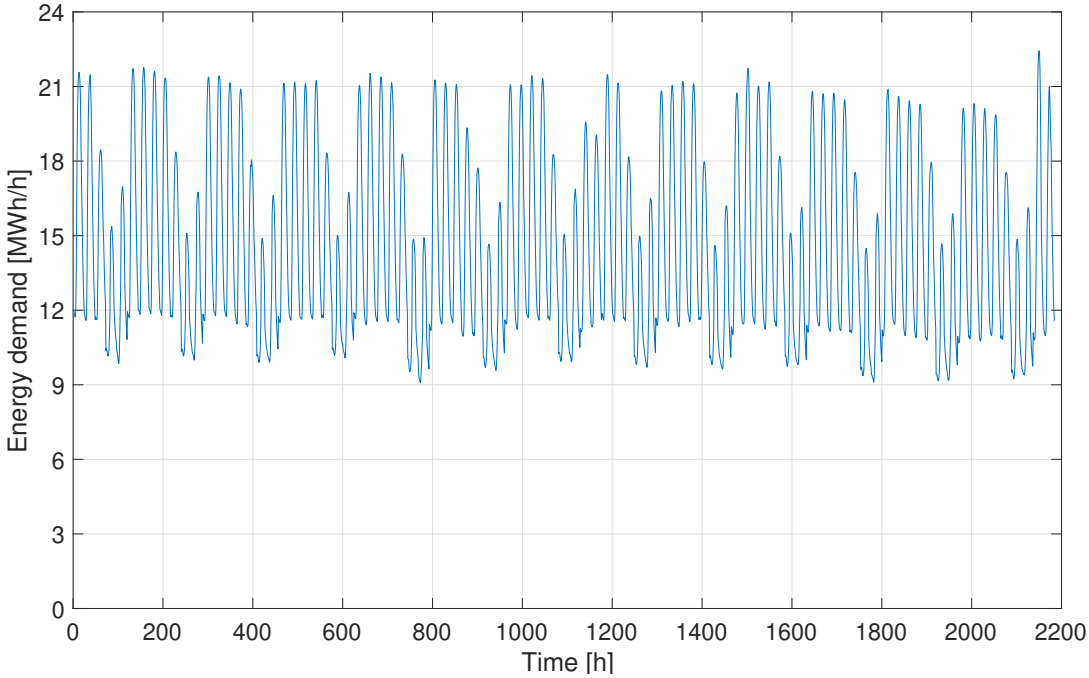

Figure 4.11: The generated demand for Forus West for April to June 2015.

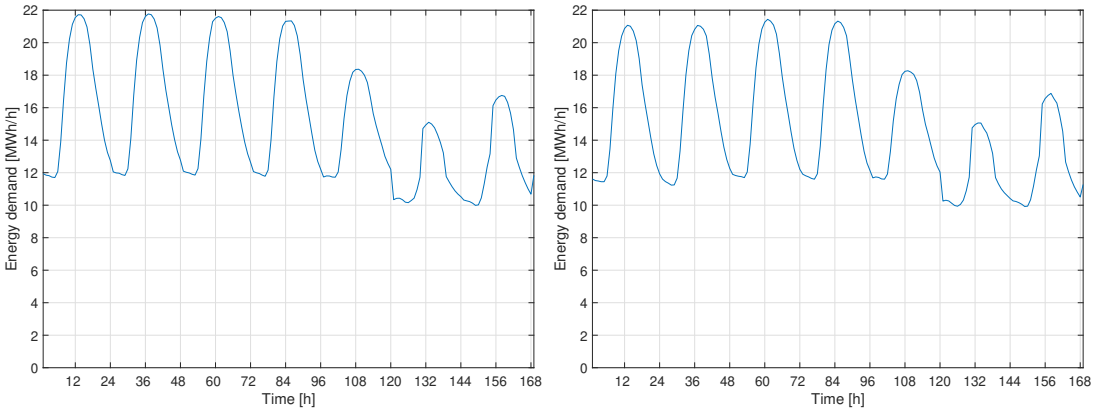

(a) Week 15 (April).

(b) Week 20 (May).

Figure 4.12: The generated demand of Forus West for two arbitrary weeks of the simulation period April to June 2015.

A PV system was suggested to be installed as the local production unit at Forus West [6]. The size of the system is not given and it was therefore chosen to use a capacity of the PV system which would result in a production equal to 30% of the yearly demand of the industrial park, which also was done for the harbor. Using Renewables.ninja, the location of Forus West, a PV system capacity of 40 MW_p and the same parameters as used for both the airport and the harbor, the production for year 2015 was found to be 37,537.95 MWh/yr. This production equals to 29.33% of the yearly demand. During the months April to June 2015, the production

was 15,504.13 MWh which is 48.82% of the demand in that period. Figure 4.13 shows the PV system production for Forus West during an arbitrary week within April to June 2015. The 40 MW_p large PV system will cover an area of around 175,000 m^2, if the same PV system type used for the PV production at Stavanger Airport also is used for Forus West.

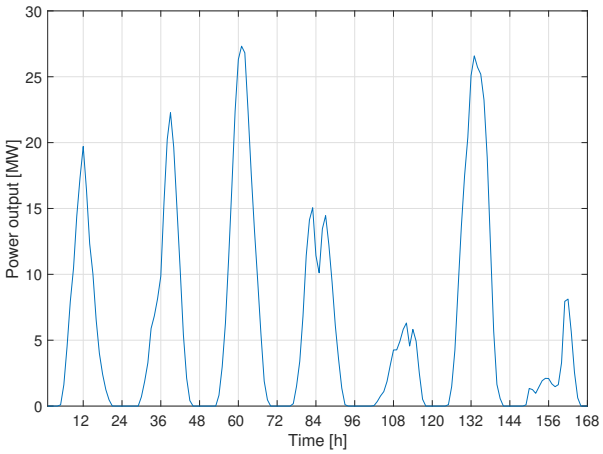

Figure 4.13: The production from the PV system at Forus West for week 21 (May) in 2015.

Industrial sites that hold many employees often have large parking areas where the employees can park their car during working hours. Such parking lots, in combination with the increasing use of electrical vehicles (EVs), make it possible to utilize a vehicle to grid (V2G) technology. V2G allows a bidirectional power flow between the battery of an EV and the power grid, through using power electronic equipment. The V2G technology is said to be able to provide a fast-responding storage which can provide different grid services, like peak shaving, voltage regulation and improvements on the power system stability [37].

For the Elnett21-case it is assumed that Forus West has installed V2G systems at their parking lots. Further, it is assumed that approximately 65% of the employees that work in the Forus West area drive a car to work, as Forus West was constructed to have available parking space for almost all employees [17, 30]. In the beginning of year 2020, about 9.3% of the Norwegian passenger car stock consisted of EVs, according to Statistics Norway (SSB) [35]. With these percentages, it is assumed that there are 1,813 EVs parked at Forus West during working hours, 8 am to 4 pm, during weekdays (Monday to Friday) and that these are available to use with the V2G technology. When the EVs arrive in the morning, it is assumed that the average capacity of the EV batteries is 60% of the nominal capacity. When the EVs leave the parking lot, their batteries are assumed to be charged to 70% of the nominal capacity. The chargers transferring power from or to the EVs are assumed to have a power of 20 kW, and that the chargers can transfer this amount of power each hour [32].

To find the storage capacity of the EVs, an average value of the three most bought EVs in Norway for 2019 was used. The top three EVs of 2019 was Nissan LEAF, Volkswagen e-Golf and Tesla Model S, which all use Li-ion batteries. The different models have been renewed over the years, so their battery capacity ranges from 24-60, 24-36, 60-100 kWh, respectively. Based on the capacity ranges, 50 kWh was used as the nominal capacity for all the EVs [32]. This means that the aggregated capacity of the EVs is 90.65 MWh.

4.2.4 Network Tariff Rates

An end-user that buys power from the main grid has to pay a fee both for utilizing the power grid and for the actual electricity that the end-user consumes. The grid-related costs in Norway are given by the local DSO, which is regulated by The Norwegian Water Resources and Energy Directorate (NVE). Each DSO has an unique network tariff rate, which shall cover grid maintenance, grid upgrades, etc. In the region of the Elnett21-project, Lyse Elnett is the local DSO. This means that all the participants in the project must follow the network tariff given by Lyse Elnett. Table 4.1 shows the network tariff rates for industries at a low voltage level located within Lyse Elnett's license area. The summer months are defined as April to September, while the winter months are defined as October to March. The fees for electricity are given in table 4.2.

Table 4.1: Network tariff rates for industries at a low voltage level with power metered transmission within the license area of Lyse Elnett [20].

Cost type	Amount
Fixed fee	23,500 NOK/yr
Energy price summer	0.245375 NOK/kWh
Energy price winter	0.257875 NOK/kWh
Peak price winter, active power	100 NOK/kW

4.2.5 Electricity Rates and Feed-in Tariff

Prosumers that both consume and produce electricity locally can at times have a larger electricity production than their current load demand. In such situations, the prosumer can store electricity given that the prosumer has storage. If the storage is full or if the prosumer does not have any storage, the prosumer can sell surplus power to the main grid. The feed-in tariff (FIT) in Norway depend on how much power the prosumer feeds into the grid. If the prosumer do not exceed in-feed of 100 kW in any instant, the prosumer will be categorized as a plus-customer. A plus-customer does not have to pay any fees for feeding power into the grid. If the power fed into the grid exceeds the 100 kW-limit, the prosumer must have the necessary licenses (see [27]) to be able to sell power as a power supplier in addition to paying a FIT for utilizing the main grid. This tariff is in Norway set by the transmission grid operator, Statnett. The FIT consists of two parts, a fixed and a variable part. The fixed part is at 0.0116 NOK/kWh for year 2020 and applies for power fed into the grid at any voltage level. The variable FIT part is set based on marginal loss rates, which are calculated for every exchange point in the transmission grid. If a prosumer feeds power into the grid in a point that will contribute to lower grid losses, the prosumer will get paid for the loss reduction that they contribute to. If, on the other hand, the feed-in point of the prosumer does not contribute to lower grid losses, the prosumer will have to pay an energy fee [3, 36].

A prosumer has to make an agreement with a power supplier that will buy the power that the prosumer feeds into the grid. How the prosumer is paid for power fed into the grid is dependent upon the agreement made with the power supplier. In this thesis, Fjordkraft has been chosen as power supplier for all the end-users of the Elnett21-case, as Fjordkraft have both wholesale spot price and prosumer deals. Through Fjordkraft, a prosumer can both buy and sell power at spot price-rates. The market spot prices are set by Nord Pool, which is the operator of the Northern European electricity power exchange market [24]. The end-users in the Elnett21-case

are located in the south-west region of Norway, which means that the day-ahead spot prices for bidding area NO2 (Kristiansand) are used for the simulation period April to June 2015.

The rates for electricity usage and FIT for non-plus-customers are given in table 4.2. The FIT ensures that it will pay off to use own produced energy directly, when this energy is needed, instead of selling the energy to the main grid.

Table 4.2: Rates for electricity usage from power supplier Fjordkraft [12] and feed-in tariff rate [36].

Cost type	Amount
Fixed fee	39 NOK/month
Variable fee, for bought power	0.0549 NOK/kWh
FIT	0.0116 NOK/kWh

4.3 Case Assumptions and Simplifications

In the Elnett21-case, there has been made a lot of assumptions due e.g. missing data and to simplify the case. The assumptions for the optimization strategies, see section 2.3.1 in chapter 2, apply to the Elnett21-case in addition to the assumptions listed below.

* It is assumed that all end-users of the case use Fjordkraft as power supplier and that they all have the necessary licenses to be able to sell power above the plus-costumer limit to the main grid.
* The variable part of the FIT has been disregarded.
* The PV system production is found using Renewables.ninja, and the production is taken from one specific location for each end-user.
* The actual size, in m^2, and placing of the PV systems has not been considered when dimensioning the systems. This means that it might not be possible to install the suggested PV systems with the stated tilt and azimuth angle.
* All the proposed production and storage units for the case have not been installed and it is unknown if they actually will be installed.
* The BESS systems installed are assumed to be charged to the lowest SOC initially.
* 10% of the demand in each time step is assumed to be shiftable for all the end-users. Possible rescheduling costs for load shifting have been neglected.
* The different battery storages are all modeled as lithium-ion batteries.
* The demand for Stavanger Airport is assumed to have the same curve for each day in the simulation period.
* The demand for Risavika Harbor is created by taking two thirds of the transformer station demand from year 2016 and adding the demand from the shore power systems.
* The heat demand of Forus West, 89 GWh/yr, is met through using the district heating grid and is thus not taken into account when looking at the energy demand of Forus West.

* The P2P price, used for calculating the costs of the individual end-users in the second approach, is set to be 0.0058 NOK/kWh lower than the wholesale spot price. This means that the P2P trade price will be right in the middle of the spot price and the in-feed price.

4.4 Model Formulation

The different optimization approaches must make demand-supply decisions based on the electricity prices, flexibility options, the main grid and DER surplus for the Elnett21-case. As for the 25-houses case, multi-period linear programming models were used for the two approaches. The models make optimized decisions for the system according to the objective for the optimization horizon T. The optimization is done for each day separately throughout the 91 days long simulation period.

The two optimization approaches have distinct objective functions, while sharing some of the same restrictions. As the approaches used on the Elnett21-case are the same as those used on the 25-houses case, the optimization models for both cases have similar constraints. Due to different model nomenclature of the cases, the similar constraints are also given in this section. For the Elnett21-case, additional constraints are needed to set rules for the shiftable load and for the usage of V2G. Table 4.3 shows the sets, scalars, parameters and variables of the mathematical models for the Elnett21-case.

4.4.1 Approach 1 - Decentralized Strategy

Using the decentralized strategy, the control system of each of the prosumers in the Elnett21-case aims at reducing the operational costs related to the network tariff and electricity costs. As P2P trading is disabled, each prosumer must cover their power demands using their own production and storage units, and the main grid. Through using flexible loads, the prosumers are able to move some of the demand to hours where the wholesale spot price is lower. Their batteries also make it possible to store locally produced power and/or power bought from the main grid in e.g. low-price hours, such that the stored electricity can be utilized in e.g. expensive hours.

The objective of the decentralized control is to minimize the electricity and grid-related costs in each time step, t, for each individual end-user, e. This optimization is done separately for each end-user each day within the simulation period. The optimization is done daily due to assuming a perfect forecast model, see further explanations in section 3.5.3 in chapter 3.

Equation (4.1) shows the objective function for the decentralized strategy for the Elnett21-case, which sums up the costs of the power drawn from the main grid, $G^{(t,e)}$, and subtracts the payback for power fed back to the main grid, $G^{(t,e)}$, to find the total costs, $C^{(e)}_{tot,A1}$, for end-user e within the optimization horizon T. The costs consist of the wholesale spot price, $p^{(t)}_G$, in time step t and the energy-dependent cost terms of the network tariff, $p_{nt,var}$, and the electricity cost $p_{el,var}$. The fixed part of the network tariff, $p_{nt,fix}$, and electricity cost, $p_{el,fix}$, are not energy-dependent, and they are given in NOK per year and NOK per month, respectively. The corresponding daily costs of these fixed cost terms are found and added to the objective function. The network tariff part that concerns the peak, see table 4.1 in section 4.2.4, is only applied in the winter months, October to March. The simulations done for the Elnett21-case are for three months in the spring, and therefore the cost for the highest peak power has been omitted in the objective function. All equations of section 4.4.1 hold true for all $t \in T$, $t_{EV} \in T_{EV}$ and $e \in E$, unless stated otherwise, and all variables are non-negative.

Table 4.3: Model nomenclature for the Elnett21-case.

Type	Description	Unit
Sets		
$t \in T$	Time, t, within the optimization horizon T	
$t_{EV} \in T_{EV}$	Time, t_{EV}, within 8 am to 16 pm on weekdays of the analysis period T_{EV}	
$e,p \in E$	End-users, e, and peers, p, within the community of end-users E	
Scalars		
η_c/η_d	Charging/discharging efficiency of the BESS battery	-
η_{inv}	BESS inverter efficiency	-
P_{inv}	Nominal power of the BESS inverter	kW
$\underline{E_{bat}}$	Nominal capacity of the BESS battery	kWh
$\overline{SOC}/\underline{SOC}$	Maximum/minimum limits on the battery SOC of the BESS	p.u.
θ_{P2P}	Efficiency factor for conversion and distribution of P2P power	-
$p_{el,fix}$	Fixed cost for electricity	NOK/day
$p_{el,var}$	Variable cost for electricity	NOK/kWh
$p_{nt,fix}$	Fixed cost of network tariff	NOK/day
$p_{nt,var}$	Variable cost of network tariff	NOK/kWh
$\underline{N_{EV}}$	Number of EVs parked and available for V2G	-
$\overline{SOC_{EV}}/\underline{SOC_{EV}}$	Maximum/minimum limits on the battery SOC of the EVs	p.u.
E_{EV}	Nominal capacity of the EV batteries	kWh
$P_{c,EV}$	Nominal power of EV charger	kW
SOC_{start}/SOC_{end}	SOV of the EV storage when arriving/leaving work	p.u.
$\eta_{c,EV}/\eta_{d,EV}$	Charging/discharging efficiency of the EV batteries	-
Parameters		
$dem_{tot}^{(t,e)}$	Total demand, with no shiftable load, of end-user e in time step t	kW
$dem_{shift}^{(t,e)}$	Shiftable load of end-user e in time step t	kW
$dem_{fixed}^{(t,e)}$	Fixed load of end-user e in time step t	kW
$res^{(t,e)}$	Renewable power production of end-user e in time step t	kW
$p_G^{(t)}$	Wholesale spot price for power bought from the grid in time step t	NOK/kWh
$p_{G_{to}}^{(t)}$	In-feed price for power sold to the grid in time step t	NOK/kWh
$p_{P2P}^{(t)}$	P2P price for power bought from or sold to a peer in time step t	kW
Variables		
$G^{(t,e)}$	Power drawn from the grid for end-user e in time step t	kW
$G_{to}^{(t,e)}$	Power delivered to the grid from end-user e in time step t	kW
$C^{(t,e)}/D^{(t,e)}$	Battery power charge/discharge of end-user e in time step t	kW
$S^{(t,e)}$	Battery energy storage level of end-user e in time step t	kWh
$I^{(t,e)}$	P2P power purchase of end-user e in time step t	kW
$I_{P2P}^{(t,e\leftarrow p)}$	P2P power purchase of end-user e from peer p in time step t	kW
$X^{(t,e)}$	P2P power sold from end-user e in time step t	kW
$X_{P2P}^{(t,e\rightarrow p)}$	P2P power sold from end-user e to peer p in time step t	kW
$L^{(t,e)}$	Load demand met in time step t for end-user e	kW
$C_{EV}^{(t,e)}/D_{EV}^{(t,e)}$	Battery power charge/discharge of the EVs of end-user e in time step t	kW
$S_{EV}^{(t,e)}$	EV storage level of end-user e in time step t	kWh

$$\min_{\substack{\forall\ t\in T \\ \forall\ e\in E}} C^{(e)}_{tot,A1} = \sum_{t}^{T} \left(G^{(t,e)} \cdot (p^{(t)}_{G} + p_{nt,var} + p_{el,var}) - G^{(t,e)}_{to} \cdot p^{(t)}_{G_{to}} \right) + \left(p^{(e)}_{nt,fix} + p^{(e)}_{el,fix} \right) \tag{4.1}$$

The objective function is subjected to several constraints, which include constraints on the flexible load, BESS, EV batteries and the power balance. For each prosumer in the Elnett21-case, it is assumed that a certain amount, $\in [0,1]$ [p.u.], of the load in each time step is shiftable, $dem^{(t,e)}_{shift}$. Equation (4.2) shows the shiftable load constraint, which says that the sum of the total demand without shiftable load, $dem^{(t,e)}_{tot}$, minus the met load, $L^{(t,e)}$, within the optimization horizon must be equal to zero. This means that the shiftable load must be met within the optimization horizon, which here is set to 24 hours. The met load demand in a specific time step for a specific end-user must be higher or equal to the fixed demand, $dem^{(t,e)}_{fixed}$, as showed in eq. (4.3). The fixed demand is equal to the total demand without shiftable load minus the shiftable load, see eq. (4.4).

$$\sum_{t}^{T} \left(dem^{(t,e)}_{tot} - L^{(t,e)} \right) = 0 \tag{4.2}$$

$$L^{(t,e)} \geqslant dem^{(t,e)}_{fixed} \tag{4.3}$$

$$dem^{(t,e)}_{fixed} = dem^{(t,e)}_{tot} - dem^{(t,e)}_{shift} \tag{4.4}$$

All the prosumers in the Elnett21-case have some kind of battery storage. When running the optimization for the prosumers with a BESS, there has to be put restrictions on the usage of the BESS. The equations presented for the BESS in the Elnett21-case are the same as those given in section 3.4.1 for the 25-houses case, but they have been repeated here to get the correct nomenclature. Equation (4.5) shows the energy storage level of the BESS. The equation says that the current energy storage level of the battery, $S^{(t,e)}$, of end-user e is equal to the battery storage level of the previous time step t plus the battery charge, $C^{(t,e)}$ or minus the battery discharge, $D^{(t,e)}$, in the current time step. The battery charge or discharge is limited by the corresponding charging or discharging efficiencies, η_c or η_d, and the efficiency of the inverter, η_{inv}.

$$S^{(t,e)} = S^{(t-1,e)} + \eta_c \cdot \eta_{inv} \cdot C^{(t,e)} - \frac{1}{\eta_d \cdot \eta_{inv}} \cdot D^{(t,e)} \tag{4.5}$$

The amount of power that can be sent to the battery of end-user e when charging, or sent away from the battery when discharging, in each time step t is limited by the nominal power of the BESS inverter, P_{inv}, and the inverter efficiency, η_{inv}, as shown in eq. (4.6) and (4.7).

$$0 \leqslant C^{(t,e)} \leqslant \eta_{inv} \cdot P_{inv} \tag{4.6}$$

$$0 \leqslant D^{(t,e)} \leqslant P_{inv} \tag{4.7}$$

The battery storage has an upper and a lower energy storage limit based on the SOC-limits of the battery, $\underline{SOC}$ and $\overline{SOC}$, and the battery nominal capacity, E_{bat}, which is showed in eq. (4.8). There are put limits on the energy storage to avoid damaging the battery by exposing it to overcharging or deep discharging.

$$E_{bat} \cdot \underline{SOC} \leqslant S^{(t,e)} \leqslant E_{bat} \cdot \overline{SOC} \tag{4.8}$$

The storage made up of EVs through V2G has several constraints. Firstly, the EVs are assumed to only be available during working hours from 8 am, $t_{EV,start}$, to 4 pm, $t_{EV,end}$, from Monday to Friday, T_{EV}. Secondly, it is assumed that all the EVs are charged to a specific level when they arrive or leave the parking lot. Thirdly, the charging and discharging power of the EV-batteries is limited by the nominal power of the EV charger and the amount of EVs parked.

The storage level of the EVs is given by eq. (4.9), which is similar to eq. (4.5), when the time is within 9 am and 3 pm and when the simulation day is a weekday, Monday to Friday. The equation says that the current storage level of the EVs, $S_{EV}^{(t_{EV},e)}$, is equal to the storage level of the previous time step, $S_{EV}^{(t_{EV}-1,e)}$, plus the charging, $C_{EV}^{(t_{EV},e)}$, or minus the discharging, $D_{EV}^{(t_{EV},e)}$, of the EV storage in the current time step. Both the charging and the discharging powers are limited by the corresponding charging or discharging efficiencies, $\eta_{c,EV}$ or $\eta_{d,EV}$, respectively.

$$S_{EV}^{(t_{EV},e)} = S_{EV}^{(t_{EV}-1,e)} + \eta_{c,EV} \cdot C_{EV}^{(t_{EV},e)} - \frac{1}{\eta_{d,EV}} \cdot D_{EV}^{(t_{EV},e)}, \qquad \forall\ t_{EV,start} < t_{EV} < t_{EV,end} \tag{4.9}$$

When the EVs arrive the parking lot, it is assumed that the battery SOC of all the EVs is equal to SOC_{start}. The storage level of the EVs at 8 am, $t_{EV,start}$, is given by eq. (4.10). When the EVs leave the parking lot at 4 pm, $t_{EV,end}$, their batteries must be charged to have a state of charge level of SOC_{end}. This is ensured through using eq. (4.11).

$$S_{EV}^{(t_{EV,start},e)} = SOC_{start} \cdot N_{EV} \cdot E_{EV} \tag{4.10}$$

$$S_{EV}^{(t_{EV,end},e)} = SOC_{end} \cdot N_{EV} \cdot E_{EV} \tag{4.11}$$

The storage level of the EV storage unit is limited by the amount of EVs parked, N_{EV}, the nominal capacity of the EV storage, E_{EV}, and the SOC limits on the EV storage batteries, $\underline{SOC}_{EV}$ and $\overline{SOC}_{EV}$, as showed in eq. (4.12).

$$N_{EV} \cdot E_{EV} \cdot \underline{SOC}_{EV} \leqslant S_{EV}^{(t_{EV},e)} \leqslant N_{EV} \cdot E_{EV} \cdot \overline{SOC}_{EV} \tag{4.12}$$

Equation (4.13) shows how the charging, $C_{EV}^{(t_{EV},e)}$, and discharging, $D_{EV}^{(t_{EV},e)}$, of the total EV storage is limited by the nominal power of the EV charger, $P_{c,EV}$, and the amount of parked EVs, N_{EV}.

$$0 \leqslant C_{EV}^{(t,e)}, D_{EV}^{(t,e)} \leqslant P_{c,EV} \cdot N_{EV} \tag{4.13}$$

The balance between supply and total demand for each end-user in each time step must always be restored, to keep a stable system frequency. The power balance equation is dependent upon

the available production and storage units, and will thus not necessarily be the same for each end-user in each time step. The end-users that have a BESS unit will have the power balance equation showed in eq. (4.14a). For the end-user that utilizes EVs with V2G as storage, the power balance is given in eq. (4.14b). In time steps when the EVs aren't available, the charging and discharging variables of the EV storage, $C_{EV}^{(t_{EV},e)}$ and $D_{EV}^{(t_{EV},e)}$, are set to zero.

$$\underbrace{G^{(t,e)} + res^{(t,e)} + D^{(t,e)}}_{\text{Supply}} = \underbrace{L^{(t,e)} + G_{to}^{(t,e)} + C^{(t,e)}}_{\text{Total demand}} \tag{4.14a}$$

$$\underbrace{G^{(t,e)} + res^{(t,e)} + D_{EV}^{(t_{EV},e)}}_{\text{Supply}} = \underbrace{L^{(t,e)} + G_{to}^{(t,e)} + C_{EV}^{(t_{EV},e)}}_{\text{Total demand}} \tag{4.14b}$$

4.4.2 Approach 2 - Centralized Strategy

The centralized control system strategy aims at reducing the operational costs, i.e. the network tariff and the electricity costs, for the whole community of end-users, e, for the optimization horizon, T. In the second approach, P2P trading has been enabled. This means that the end-users can buy and sell power directly to each other without utilizing the main grid. All equations in section 4.4.2 hold true for all $t \in T$, $t_{EV} \in T_{EV}$ and $e, p \in E$ unless stated otherwise, and all variables are non-negative.

The objective function of the second approach for the Elnett21-case is given in eq. (4.15). The equation sums up the cost of grid consumption and subtracts revenue for power sold to the main grid for all time steps within the simulation period for all the end-users. As the objective function sums the costs for all the end-users, the fixed daily grid and electricity costs must be added for each of the end-users.

$$\min_{\substack{\forall\ t\in T \\ \forall\ e\in E}} C_{tot_{A2}} = \sum_{e}^{E}\left(\sum_{t}^{T}\left(G^{(t,e)}\cdot\left(p_G^{(t)} + p_{nt,var} + p_{el,var}\right) - G_{to}^{(t,e)}\cdot p_{G_{to}}^{(t)}\right)\right) + E\cdot\left(p_{nt,fix} + p_{el,fix}\right) \tag{4.15}$$

The objective function is subject to restrictions related to shiftable load, BESS and EV storage, rules for P2P trade and the power balance equation. Some of the constraints applied in the decentralized approach are also applied to the centralized strategy. These include the BESS constraints, eq. (4.5) - (4.8), and the constraints on the EV storage, eq. (4.9) - (4.13). The shiftable load constraint for approach 2 is similar to the one for approach 1, see eq. (4.2), except that it also must be summed for the community of end users, as showed in eq. (4.16), because the flexibility is shared within the community. Equation (4.3) and (4.4) from section 4.4.1 do also apply to the centralized approach for the Elnett21-case.

$$\sum_{e}^{E}\left(\sum_{t}^{T}\left(dem_{tot}^{(t,e)} - L^{(t,e)}\right)\right) = 0 \tag{4.16}$$

Further, the rules for P2P trading must be included. The P2P restrictions of the centralized approach used on the Elnett21-case are similar to those of the centralized approach used on the 25-houses case, see eq. (3.9) - (3.12) in section 3.4.2, but the equations are repeated here with the correct nomenclature.

The sum of sold P2P power, $X^{(t,e)}$, of end-user e in time step t is equal to the total sum of electricity flows, $X_p^{(t,e\rightarrow p)}$, from the specific end-user to the peers $p \in E$. This is showed in eq. (4.17).

$$X^{(t,e)} = \sum_{p \neq e} X_p^{(t,e\rightarrow p)} \tag{4.17}$$

The sum of purchased P2P power, $I_p^{(t,e\leftarrow p)}$, of end-user e from peer p is equal to the P2P power bought, $X_p^{(t,e\rightarrow p)}$, times the P2P efficiency factor, θ_{P2P}, as given in eq. (4.18).

$$I_p^{(t,e\leftarrow p)} = \theta_{P2P} \cdot X_p^{(t,e\rightarrow p)}, \qquad \forall\ p \neq e. \tag{4.18}$$

The overall purchased P2P power, $I^{(t,e)}$, is given as the sum of the purchased P2P power, $I_p^{(t,e\leftarrow p)}$, as presented in eq. (4.19).

$$I^{(t,e)} = \sum_{p \neq e} I_p^{(t,e\leftarrow p)} \tag{4.19}$$

The sum of P2P power sold from the end-users, or peers, within the community must equal the purchases as of eq. (4.20). This is because the P2P power only can be traded within the same energy sharing region.

$$\sum_{h} I^{(t,e)} = \sum_{e} \theta_{P2P} \cdot X^{(t,e)}, \qquad \forall t \in T. \tag{4.20}$$

To ensure that the power balance is obtained, the sum of supply most equal the total demand in each time step. The power balance equation for the end-users with BESS storage is given eq. (4.21a), while eq. (4.21b) is the power balance equation for the end-user using EVs as storage. When the EVs are unavailable, i.e. during the weekend or before 8 am or after 16 pm on weekdays, the charging and discharging variables of the EV storage is set to zero.

$$\underbrace{G^{(t,e)} + res^{(t,e)} + D^{(t,e)} + I^{(t,e)}}_{\text{Supply}} = \underbrace{L^{(t,e)} + G_{to}^{(t,e)} + C^{(t,e)} + X^{(t,e)}}_{\text{Total demand}} \tag{4.21a}$$

$$\underbrace{G^{(t,e)} + res^{(t,e)} + D_{EV}^{(t_{EV},e)} + I^{(t,e)}}_{\text{Supply}} = \underbrace{L^{(t,e)} + G_{to}^{(t,e)} + C_{EV}^{(t_{EV},e)} + X^{(t,e)}}_{\text{Total demand}} \tag{4.21b}$$

4.5 Case Results and Analysis

The multi-period linear programming models presented in section 4.4 are implemented and solved in MATLAB using *linprog* as solver, like for the 25-houses case. System parameters were read from Excel into MATLAB, and MATLAB was used both as solver and to generate plots of the results. The models are run on a 64-bit macOS Catalina with Intel Core I5-6360U, 2 GHz CPU and 8 GB RAM.

As for the 25-houses case, the performance of the control system strategies is measured according to the electricity costs for each end-user and for the ESR. The strategy that gives the lowest total electricity costs for the ESR is the most effective. The total amount of energy drawn from the main grid and the peak power demand are also of interest. As the Elnett21-case consists of large end-users, the peak power demand is important as the local DSO must dimension their grid according to the highest local peak demand.

The results from the decentralized approach are given in section 4.5.1, while the results for the centralized approach are presented in section 4.5.2. The results from the two approaches are compared and discussed in section 4.5.3.

4.5.1 Approach 1 - Results

The decentralized approach makes each end-user minimize their own economic objective function, without allowing P2P trade or shared flexibility. The total electricity costs are minimized each day of the 91 days long analysis period for each separate end-user. The end-users can only utilize their own DERs, energy storage and flexibility, in addition to power from the main grid, when making their demand-supply decisions.

The simulations for the three months took 2 minutes on the mentioned computer using MATLAB. The optimization comprises 18,395 constraints and 34,788 variables for the 91 days long simulation period. The total amount of energy drawn from the main grid for the ESR is 24,265.07 MWh, resulting in a cost of 11,445,765 NOK. During the simulation period, the different end-users deliver a total of 2,306.16 MWh to the main grid. This amount of energy gives revenue of 366,066 NOK, with the electricity and FIT rates given in section 4.2.5. When subtracting the grid in-feed revenues from the grid consumption costs, the total costs for the ESR during the simulation period is found to be 11,079,700 NOK. The optimal solution gives a peak power demand of 71.86 MW for the community, while the highest of the individual end-user peak demands is 50.51 MW for Forus West.

Figure 4.14 shows how the supply-demand decisions are made by the decentralized approach for Stavanger Airport during week 25, 2015. The upper plot shows the different types of energy supply that are available for the airport, while the lower plot shows that the total demand consists of the fixed and flexible demand of the airport, energy sold to the main grid, and energy used to charge the installed BESS. The figure shows that spikes in energy demand from the main grid occur almost every day during the specific week. The first two days have higher renewable production than the last five, resulting in lower demand peaks from the grid. It is seen that when the local production is reduced, the peak demand from the main grid is increased. If the demand-supply decisions for week 25 are compared with the corresponding wholesale spot prices and in-feed prices, presented in fig. 4.15, it is seen that the shiftable load is shifted to time steps when the wholesale spot prices are low, for instance at 52 h, 75 h and 100 h. This is because when the local production is insufficient and power is not drawn from the battery, the costs will be reduced if power is drawn from the main grid in low-cost hours.

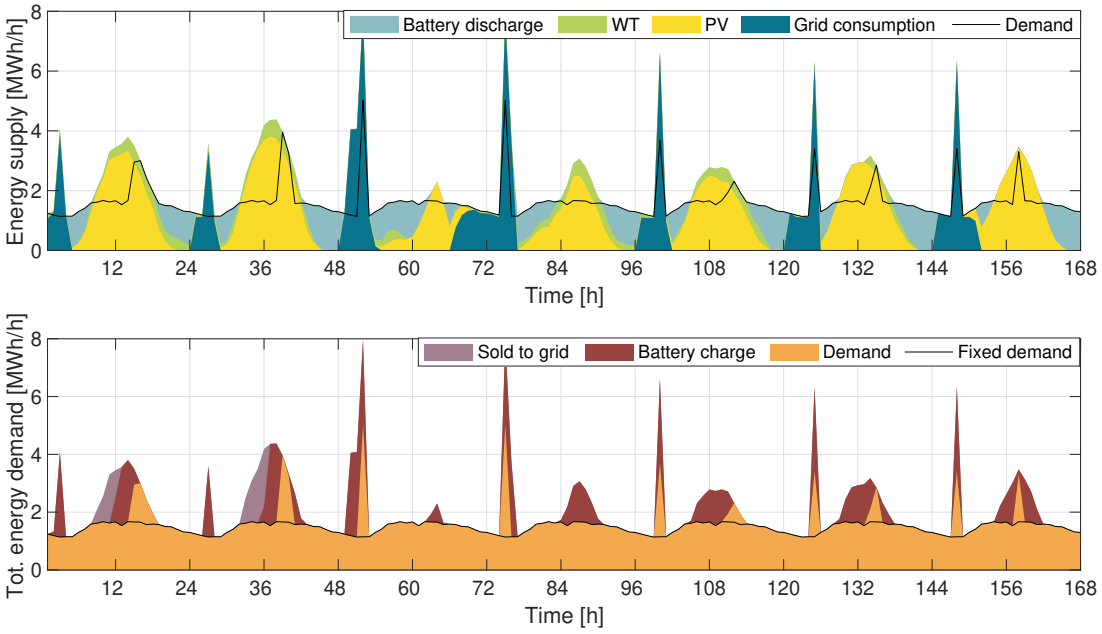

Figure 4.14: Supply-demand decisions made for Stavanger Airport using the decentralized approach during week 25, 2015.

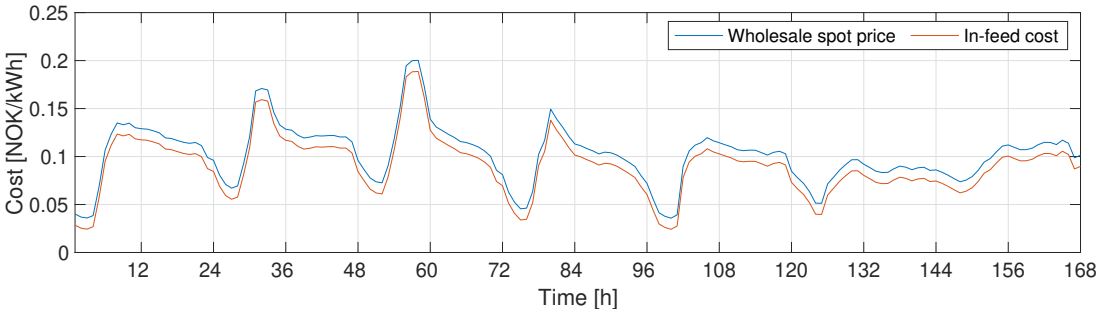

Figure 4.15: Wholesale spot prices and in-feed prices for the Elnett21-case for week 25, 2015.

The optimization results using the decentralized approach show that Stavanger Airport gets a total cost of 664,840 NOK and that the airport consumes 1,471.89 MWh from the grid within the simulation period. Risavika Harbor consumes 6,433.63 MWh from the main grid and the optimization gives a total cost of 3,002,768 NOK for the harbor within the period. Forus West is the largest end-user and has to pay a total of 7,412,093 NOK using the decentralized strategy and draws 16,360 MWh from the main grid in the analysis period.

The supply-demand decisions for Risavika Harbor are shown in fig. 4.16 for week 25 in 2015. Like for Stavanger Airport, the figure shows, when comparing with the corresponding prices shown in fig. 4.15, that power is drawn from the main grid when the prices are low. At 52 h and 75 h, both the harbor and airport have peak demands seen from the main grid. As the harbor and airport both have production and storage units with a certain capacity, it is seen that the behavior of the decentralized optimization is similar for both end-users.

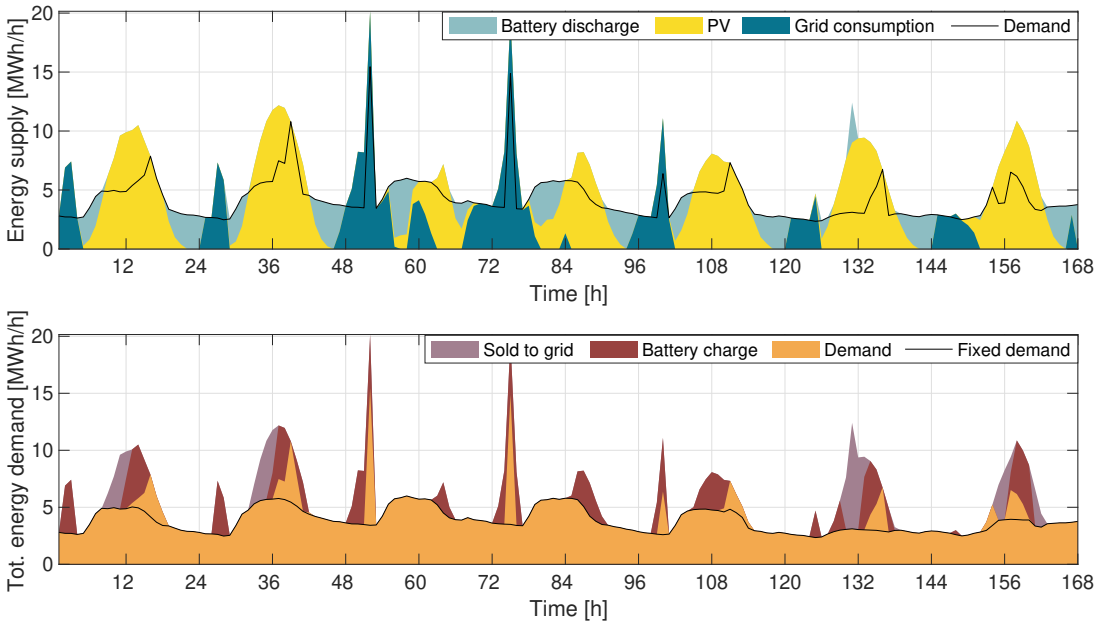

Figure 4.16: Supply-demand decisions made for Risavika Harbor using the decentralized approach for week 25, 2015.

Forus West differs from the harbor and airport in both demand, available DER units and the storage type used. The industrial park has local production through a PV system and uses EVs as temporary storage. Figure 4.17 shows the supply-demand decisions made for Forus West during week 25 in year 2015 when using the decentralized approach. It is seen from the figure that the EVs are discharged and the power is sold to the main grid when the in-feed costs are high, see associated costs in fig. 4.15, at 8 h and 32 h. In fig. 4.18, the storage level of the EVs at Forus West during week 25 is showed. It can be seen from the figure that the stored energy in the EVs is the same for the beginning of each workday and for the end of each workday. It is also seen that the usage of the EV storage varies from one day to the next. This is because the utilization of the EV storage is decided by the optimization. After 112 h, corresponding to a Friday at 16 pm, the industrial park does not have storage for the rest of the week. This means that only production from the PV system and power from the main grid can be used as sources of supply during the weekend for the industrial park.

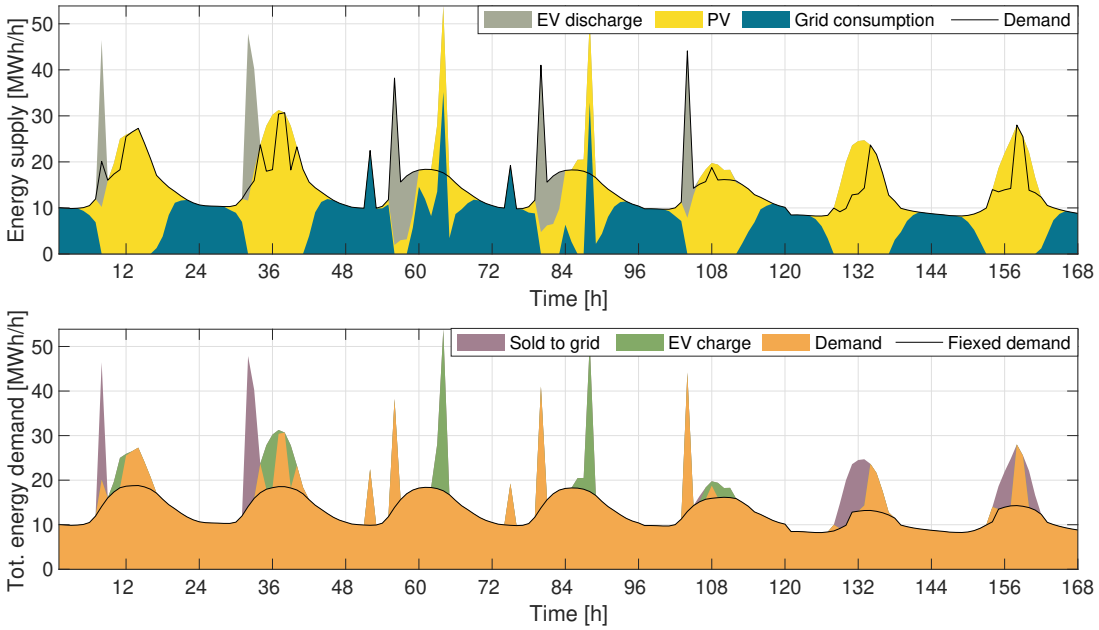

Figure 4.17: Supply-demand decisions using the decentralized approach for Forus for week 25, 2015.

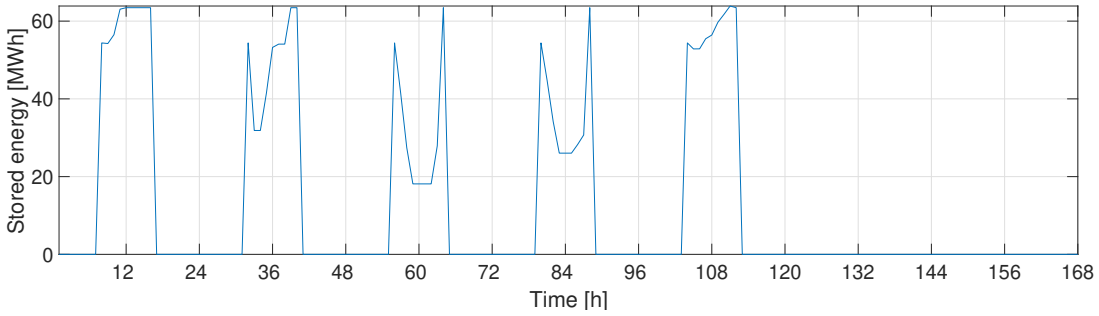

Figure 4.18: The storage level of the EV storage at Forus West when using approach 1 for week 25, 2015.

4.5.2 Approach 2 - Results

When the centralized approach is used on the Elnett21-case, the end-users are considered as a community where power can be traded locally. The aim of the approach is to minimize the total cost of electricity during operation for the whole community for each separate day during the 91 days long simulation period.

It took just over 1.5 minutes to run the MATLAB model with its 27,131 constraints and 60,723 variables for the simulation period on the 64-bit macOS Catalina. The community draws a total of 23,920.86 MWh from the main grid, which has a cost of 11,255,111 NOK. In addition to drawing power from the grid, the community has a grid in-feed of 1,875.59 MWh resulting in a revenue of 290,935 NOK. To get the total costs for the community, the revenue is subtracted

from the cost. This results in a cost of 10,964,176 NOK for the whole community during the simulation period when using the centralized strategy. The peak demand seen from the grid of the community is 60.75 MW, while the largest peak of the end-users is 50.51 MW for Forus West. For the P2P energy trading, a total of 984.67 MWh is sold from peers, while 909.83 MWh is bought from peers within the community. This means that the total P2P loss is 74.83 MWh for the simulation period.

Figure 4.19 shows how supply meets the total demand according to the power balance equation, see eq. (4.21b) in section 4.4.2, for Forus West during week 25 in year 2015. It can be seen from the figure that both the amount of P2P power purchased and sold is not very large. All the end-users in the Elnett21-case have production from PV systems. As the end-users are located fairly close to one another, the solar irradiation will almost be the same for the three locations, giving a PV production profile which is almost identical for each of the end-users. As the PV systems of the different end-users have various capacities, the production profiles will vary in magnitude, but the shape of the production curve will still be similar. The result of this is that power surplus can occur in the community when the PV production is high. When the PV production is low, all of the end-users have to discharge their storage and buy power from the other peers or the main grid to cover their demand. Stavanger Airport also has the opportunity of using power from the WTs, but the power generation from the WTs is very low (10.73% of the airport demand for the simulation period) compared to the demand and compared to the production from the PV system (51.97% of the airport demand during the simulation period). This can result in that P2P power cannot be bought from other peers when required and that P2P power cannot be sold to peers when power surplus occurs, as there is no demand.

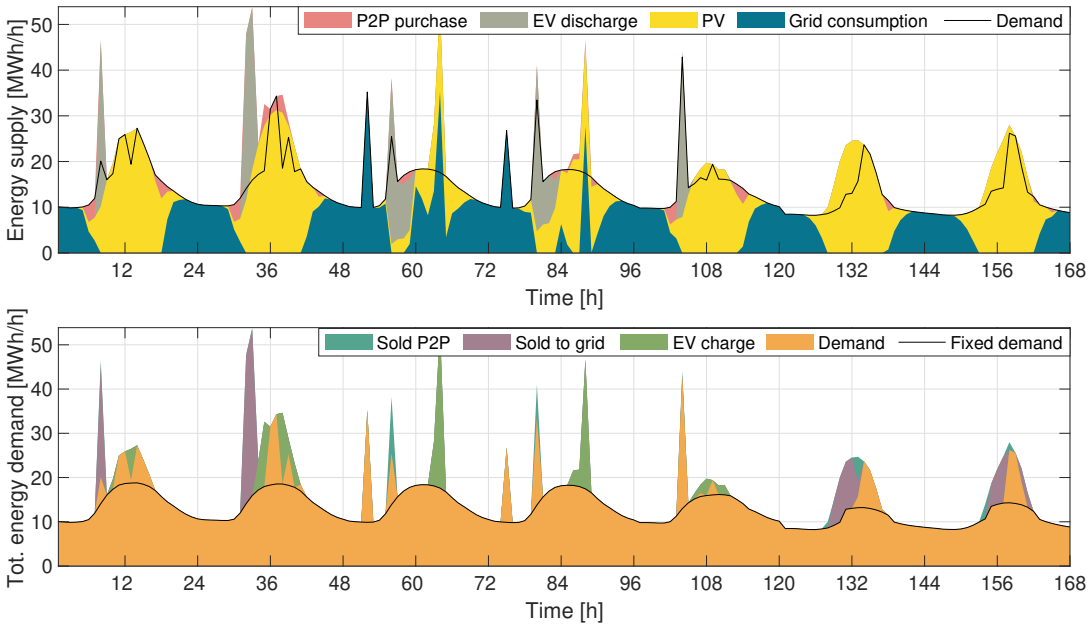

Figure 4.19: How supply meets the total demand of Forus West using approach 2 for week 25, 2015.

4.5.3 Comparison of Results and Discussion

Table 4.4 summarizes the results for the two different approaches for the Elnett21-case. Like for the 25-houses case, the approaches where run on the Elnett21-case both with and without storage. The reason for doing this is to have a source of comparison for each of the approaches, in addition to comparing them with each other.

Table 4.4: Results from using the two control system approaches on the Elnett21-case, both with and without storage.

Strategy	Ref. A1 (no storage)	A1: Decentralized Comp. to ref. A1		Ref. A2 (no storage)	A2: Centralized Comp. to: ref. A2		A1
Total costs [NOK]	12,075,903	11,079,700	-8.3%	12,026,645	10,964,176	-8.8%	-1.0%
Cost for grid consumption [NOK]	12,478,043	11,445,765	-8.3%	12,397,100	11,255,111	-9.2%	-1.7%
Revenues of selling to the grid [NOK]	402,140	366,066	-10.0%	370,455	290,935	-21.5%	-20.5%
Grid consumption [MWh]	26,274.80	24,265.07	-7.6%	26,099.39	23,920.86	-8.3%	-1.4%
Fed to main grid [MWh]	2,675.56	2,306.16	-13.8%	2,481.18	1,875.59	-24.4%	-18.7%
Maximum community peak [MW]	81.41	71.86	-11.7%	79.84	60.75	-23.9%	-15.5%

From table 4.4, it is seen that the total costs of the community during the simulation period are decreased by 8.3% for the decentralized strategy when storage is included. For the centralized approach, including a storage reduces the costs by 8.8%. The difference in total costs using the decentralized versus the centralized approach is not very big. The centralized approach only reduces the total costs by 1.0% of the costs found when using the decentralized approach. Concerning the peak demand of the community, it is seen from the table that the centralized strategy reduces the peak power demand found by using the decentralized strategy by 15.5%. As the end-users of the Elnett21-case have large demands, a reduction of 15.5% of the peak demand is high.

The total electricity costs for each end-user in the Elnett21-case using the two different control system strategies are presented in fig. 4.20. From the figure, it can be seen that the operational costs are almost the same regardless of the strategy being used. The main reason for this is that each end-user has both production and storage units, meaning that all end-users have flexibility in both approaches. For Stavanger Airport, the cost of using the decentralized approach is 2.39% lower than the cost given by the centralized approach. The centralized approach gives a cost which is 3% lower than the costs given by the decentralized approach for Risavika Harbor. For Forus West, there is just a cost difference of 0.74% between approach 1 and 2, where the centralized approach gives the lowest costs. Thus, the centralized approach gives the lowest individual end-user costs for two of the three end-users in the case. The costs of the individual end-users using the centralized approach are dependent upon the P2P trade price. Changing the P2P price, as long as the price is in between the grid in-feed cost and the wholesale spot price, will thus affect the costs of the individual end-users in the second approach.

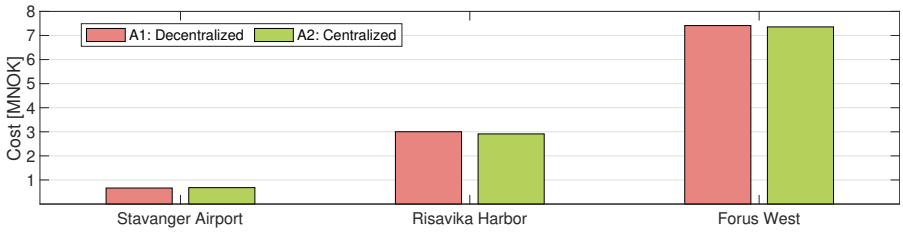

Figure 4.20: Total operational costs for each end-user in the Elnett21-case using the decentralized and centralized control system strategies.

In the Elnett21-case, 10% of the total load in each time step is assumed to be shiftable for each of the end-users. The only constraints of the objective functions of the decentralized and centralized strategies related to the shiftable load are that the shiftable load must be met within the optimization horizon, i.e. within 24 hours, and that the load met in each time step must be greater or equal to the fixed demand of that time step. This means that load can be shifted to any hour within the specific day and that there will not be any economic consequences in doing so, as possible rescheduling costs have been ignored. The optimization approaches are free to move the shiftable loads as desired within the set limits. This means that load can be shifted to every hour of the day, both during the day and night. As the wholesale spot prices normally are lower during the night, see fig. 4.15 in section 4.5.1, much of the shiftable load will be moved to these hours to reduce the electricity costs. The optimization approaches do not take into consideration if the load actually can be shifted to these hours in real life. For large end-users, shiftable loads can consist of power to e.g. heating, cooling and logistics. Shifting these demand types in time can affect comfort, operational costs of the individual end-users, production plans, etc.

For Stavanger Airport, shiftable loads can be e.g. power to heating, cooling, ventilation and logistics[5]. The airport does not have typical opening hours, as planes can arrive and depart the airport practically any time during the day. This gives room for shiftable load, as heating and cooling processes are necessary also during the night. Forus West on the other hand, has more rigid hours of operation. During the night, the activity of the industrial park is substantially lower than during the day. Also, it must be noted that Forus West is assumed to get its heat demand covered through a district heating grid, meaning that power to heat cannot be a shiftable load for the industrial park, as electricity is not used to meet the heat demand. Thus, shiftable loads for the industrial park can be power to e.g. cooling, ventilation and logistics. Risavika Harbor does also have more rigid operating hours, with lower activity during the night. For the harbor, shiftable loads can be power to heating, ventilation, cooling and logistics. The harbor can, for example, charge vessels during the day and night while staying at the quayside.

The aggregated energy supply for the Elnett21-case using the decentralized and the centralized approaches for week 19 in 2015 are displayed in fig. 4.21, while fig. 4.22 shows the corresponding aggregated total energy demand. The figures show relatively small differences in how the available supply sources meet the total demand for each of the approaches. Going from the first to the second approach gives a reduction in grid consumption of 1.4% and a reduction of the amount of power sold to the main grid by 18.7%, see table 4.4, as power both can be sold to peers within the community and to the main grid in the second approach. When comparing fig. 4.21 with the corresponding wholesale spot prices and in-feed costs, see fig. A.2 in appendix A.1, it can be seen that P2P purchase within the community occur when the wholesale spot price has its price peak each separate day. The spikes in grid consumption for both approaches occur in time steps when the grid price is low e.g. at 51 h and 75 h, see fig. A.2. It can be seen that these spikes are higher for the second approach meaning that more power is purchased from the main grid when the wholesale spot prices are low, which results in decreased total electricity costs.

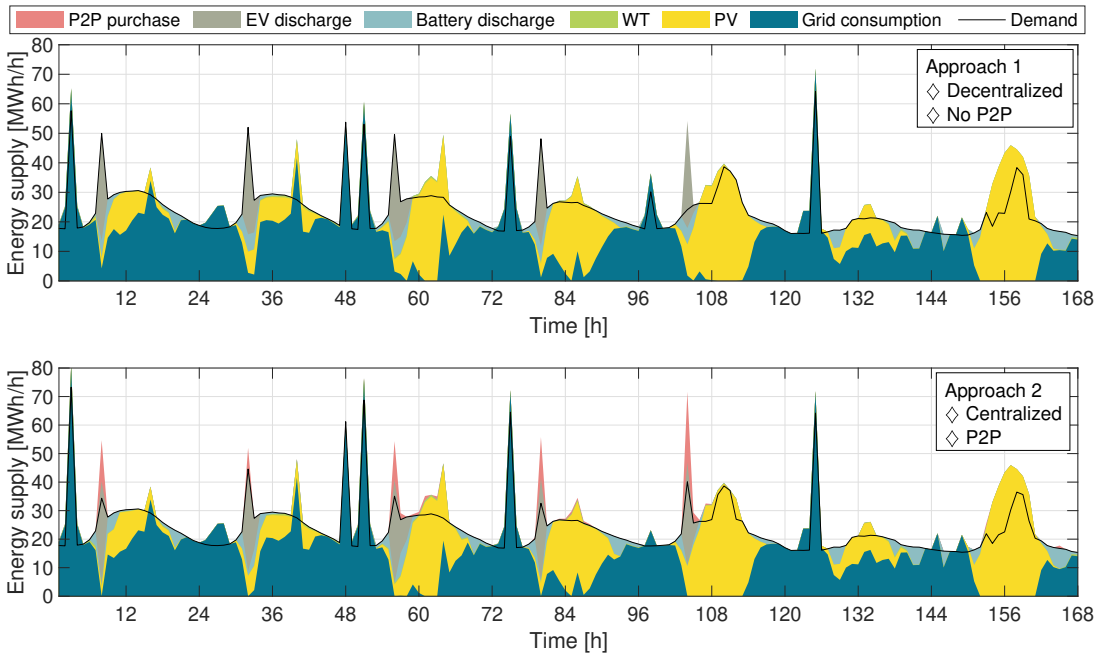

Figure 4.21: Aggregated energy supply for all the three end-users using approach 1 and 2 for week 19, 2015.

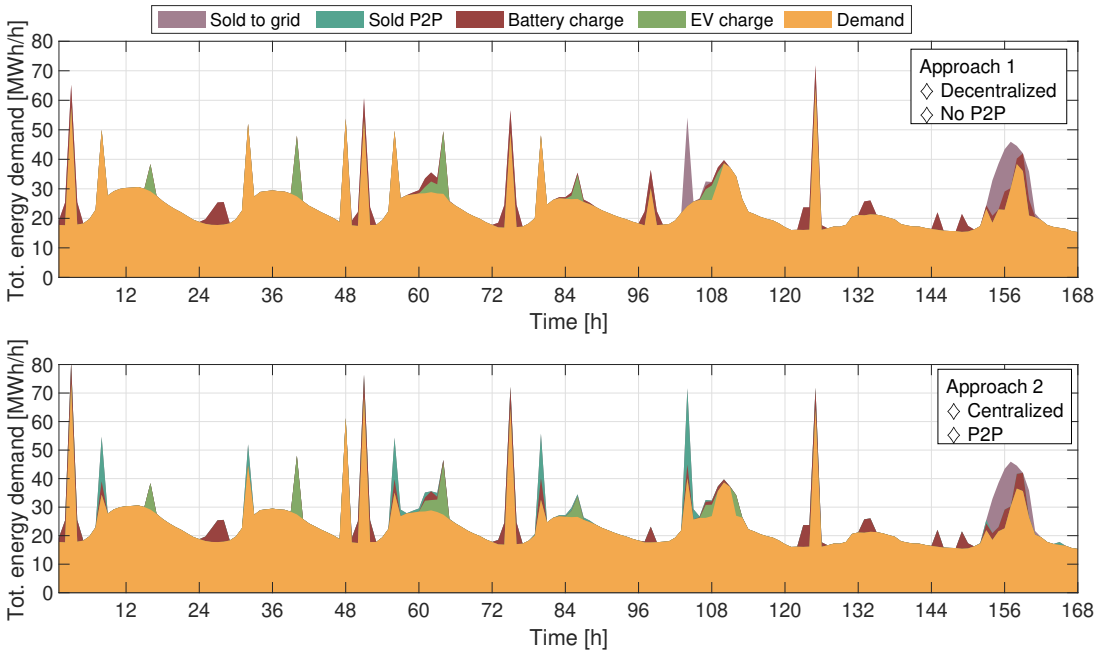

Figure 4.22: Aggregated total energy demand for all the three end-users using approach 1 and 2 for week 19, 2015.

The share of the different supply sources and the different demand types for the two approaches are presented in fig. 4.23 and 4.24, respectively. The first figure shows that the difference in sources of supply using the two different control system strategies is relatively small, as P2P purchase only accounts for 1.68% of the different supply sources in the centralized approach. The second figure shows that sold P2P power only accounts for 1.83% in the centralized approach, which results in that the share of the different demand types is almost the same when using the decentralized and centralized approaches on the Elnett21-case.

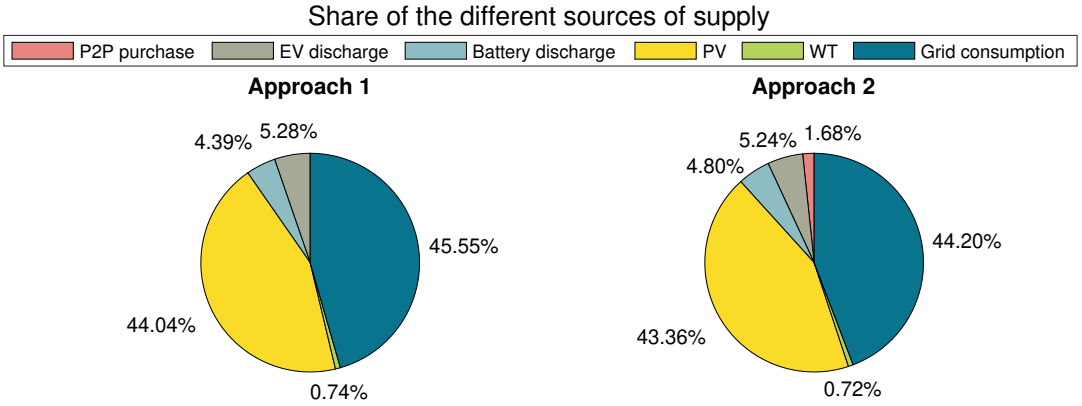

Figure 4.23: The share of the various sources of supply for the two approaches for the Elnett21-case[22].

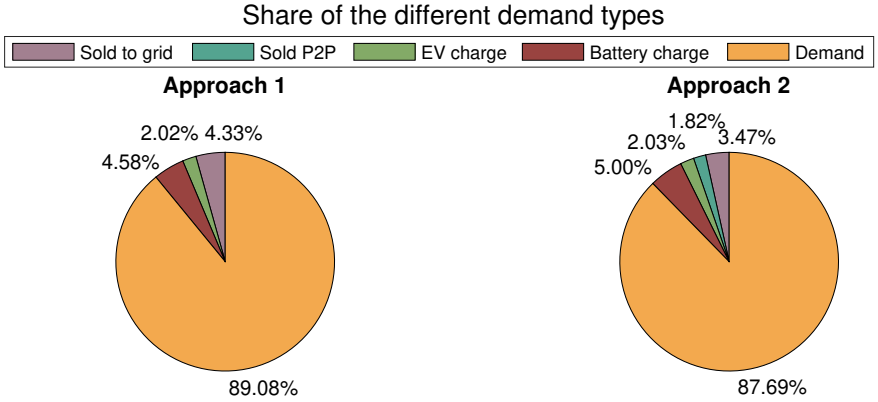

Figure 4.24: The share of the various demand types for the two approaches for the Elnett21-case[23].

[22]The aggregated production from DERs accounts for different shares of the total supply in the two approaches, but aggregated DER prduction is the same in both strategies.

[23]The aggregated demand of the end-users accounts for different shares of the total demand in the two approaches, but the aggregated demand is still the same in both approaches.

5 | Multi-objective Optimization

The multi-objective (MOO) optimization approach tries to optimize two or more objective functions simultaneously. In MOO problems, objective functions show contradicting behavior, like reducing the total costs of a product while maintaining a high quality, which can make the decision-making challenging. In many practical engineering applications, decisions must be made between such conflicting objectives. In this situation, the concept of one optimal solution will be replaced by the Pareto set, which is made up of a set of optimal solutions. Then, the decision-maker should select the most preferred solution in this set based on the trade-offs between the different objective functions [7].

MOO problems are mainly solved by using analytical or numerical methods. The analytical methods comprise strict mathematical proofs and derivation to reach an exact solution, while the numerical methods use appropriate iteration formulas to reach an approximate solution. The numerical methods include both classical numerical methods and intelligent numerical methods based on heuristic search algorithms. Among the classical methods there are the a priori methods including, but not limited to, the weighted sum method and the ϵ-constraint method. In the weighted sum method, multiple objectives are transferred into a single objective by multiplying each objective with a corresponding weighting coefficient. The weighting coefficients are set based on the relative importance of the different objectives. The advantage of the weighted sum method is that it is simple and easy to apply, but it can be a challenge to set the weight vectors such that a Pareto-optimal solution in the desired region can be obtained. The ϵ-constraint method, on the other hand, keeps one of the objective functions while the others are turned into constraints. Using the ϵ-constraint method, both convex and non-convex problems can be solved [8, 28].

In this thesis, the ϵ-constraint method was chosen as the solving procedure for the different MOO problems, as the solving procedure can give the Pareto set.

5.1 ϵ-constraint Method

The ϵ-constraint method reformulates the multi-objective problem into a single objective one. As mentioned above, a multi-objective problem aims to find the Pareto set instead of one optimal point. Therefore, it focuses on optimizing one objective and models the other objectives as constraints. Figure 5.1 demonstrates the concept of the epsilon-constraint for a two-objective (f_1 and f_2) problem with contradicting behaviors. The blue lines show the borders of the feasible region. In this case, f_2 is the main objective and f_1 is converted to a constraint. In the left figure, f_1 is divided into ten equal intervals. This means that the problem must be solved ten times aiming to minimize f_2 subject to the problem constraints as well as the constraint related to f_1. In each iteration, f_1 is limited by an upper bound which is illustrated as the dashed lines in the left figure. The circles in the figure illustrate the optimal solution of the described problem in each iteration. The Pareto set is formed of these circles. A more smooth Pareto set can be achieved by increasing the number of iterations which can be seen in the figure to the right.

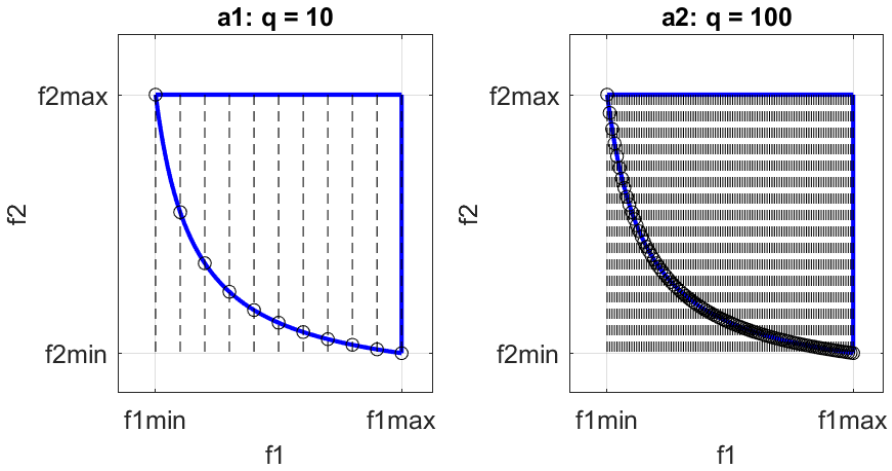

Figure 5.1: The ϵ-constraint approach in MOO.

Equation (5.1) - (5.3) illustrate the extension of the ϵ-constraint method for problems with K amount of objective functions. The calculation is performed in the feasible region of the problem, which means that the other constraints related to the structure of the problem must be taken into account. In all equations in this chapter, n is the iteration number and q is the total amount of iterations.

$$\min f_1(\bar{X}) \qquad s.t. \quad f_2(\bar{X}) \leqslant e_2, ..., f_K(\bar{X}) \leqslant e_K \tag{5.1}$$

$$e_2 = f_{2_{min}} + (\frac{f_{2_{max}} - f_{2_{min}}}{q}) \cdot n \qquad n = 0, 1, ..., q \tag{5.2}$$

$$e_K = f_{K_{min}} + (\frac{f_{K_{max}} - f_{K_{min}}}{q}) \cdot n \qquad n = 0, 1, ..., q \tag{5.3}$$

5.2 Controlling the Peak

As cost reduction is the main priority of the end-users, they try to employ various flexibility sources to reduce the RES curtailment and consume low price energy. This might lead to spikes in grid imports during low price periods of the day. This has been seen for both the decentralized and the centralized control system strategies when applied to the 25-houses case and the Elnett21-case. Therefore, it seems necessary to consider the peak demand in the scheduling of assets. Two-objective approaches for controlling the peak and costs are analyzed in the following. It is worth noting that the described formulations in the previous chapters are considered in the following subsections, and that MOO is used to analyze a specific day.

In the multi-objective method, the operational costs are considered as one of the objectives and are defined depending on the type of the market structure, which is described in previous chapters. This objective is further referred to as f_1. The other objective, called f_2, is the highest amount of energy imported from the grid during the day. Equation (5.4) shows the peak in the linear programming of the market model.

$$f_2 \geqslant \sum_{i=1}^{N} G(t,i) \qquad \forall\ t \in T \tag{5.4}$$

If eq. (5.4) is considered along with all the P2P, energy storage, shiftable load, power balance and EV constraints of section 4.4.1 in chapter 3, as the feasible region of the problem, the multi-objective problem is shown in eq. (5.5) and (5.6).

$$\min_{feasible\ region} f_2 \tag{5.5}$$

$$f_1 \leqslant f_{1_{min}} + (\frac{f_{1_{max}} - f_{1_{min}}}{q}) \cdot n \qquad n = 0, 1, ..., q \tag{5.6}$$

5.3 MOO in Practice

This section shows the results of using the MOO approach on the Elnett21-case and on a new case of four houses, hereby called the 4-houses case[24], located in London, UK. For the Elnett21-case, MOO is applied to the decentralized market approach for Stavanger Airport. While for the 4-houses case, MOO is applied to the centralized market approach for the community of houses.

5.3.1 MOO Used on the Elnett21-case

The MOO was used on the Elnett21-case, described in chapter 4, using a decentralized approach. The first objective function of the MOO was to reduce the peak demand seen from the main grid of each end-user, while the second objective function was to reduce the total cost of electricity for each end-user. The reason for choosing the decentralized approach for this case is that the end-users have high energy demands, which means that peak control for each end-user is important. Also, as the market model has been evaluated in previous chapters, the main focus is on the analysis of MOO for Stavanger Airport, see section 4.2.1 in chapter 4 for further information on the specific end-user.

Figure 5.2 shows the Pareto set for Stavanger Airport in the target day consisting of 20 scenarios (q=20). As can be seen from the figure, a peak reduction leads to a very low cost increase for the specific end-user. When the peak is reduced from the highest value to the lowest value, corresponding to a decrease in peak by 18.02%, i.e. 257 kW, the costs are only increased by 0.12%, i.e 10 NOK. This means that the peak demand in this specific case can be reduced without triggering a high cost. It should, however, be noted that the cost increase of 10 NOK is just for the specific day, and that the extra cost will be aggregated when looking at the yearly costs. For other days than the one studied here, the cost of decreasing the peak demand seen from the grid can be higher or lower than what has been shown in fig. 5.2. In such days, it is up to the decision maker to select the most preferred operating point, which usually is the midpoint of the Pareto set.

[24]The 4-houses case is described in appendix A.2.

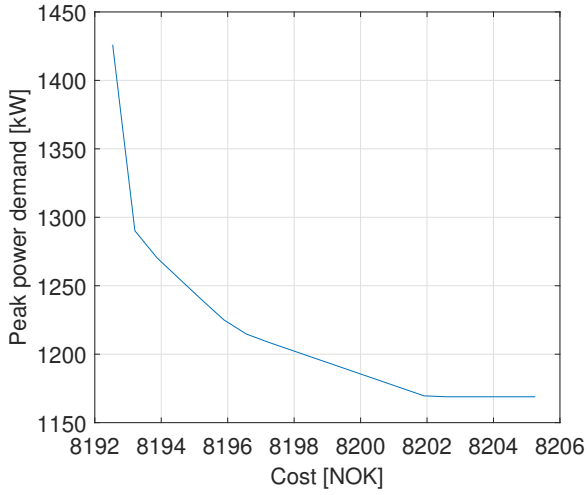

Figure 5.2: Pareto set for Stavanger Airport for day 1 in week 15, 2015.

A better comparison between various scenarios can be done based on fig. 5.3. As mentioned earlier, the problem must be run several times and each time the upper bound of the cost increases. This means that the first and last iterations correspond to pure peak minimization and pure cost minimization, respectively. Figure 5.3 (a) shows the grid consumption for these two extreme scenarios. In the cost minimization scenario, the end-users import power from the main grid as much as they can when the price is low. While in the peak mitigation scenario, the grid import is lower within the low price periods. The other scenarios are somewhere between these two scenarios, as shown by the blue lines in fig. 5.3 (b).

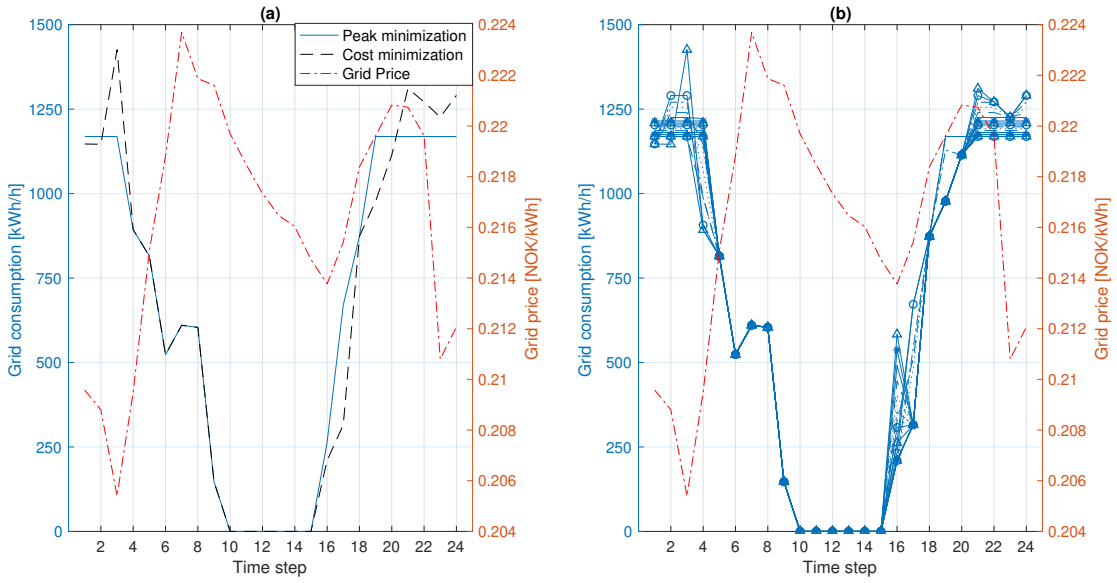

Figure 5.3: Grid consumption of Stavanger Airport for day 1 in week 15, 2015. (a) Extreme scenarios (b) All scenarios.

5.3.2 MOO Used on the 4-houses Case

The 4-houses case concerns a case of four houses located in London, UK, and is described in appendix A.2. In the 4-houses case, the MOO is applied to the centralized market approach for one specific day, as the demand of residential buildings is much smaller compared to the demand of an airport, industrial park or harbor. Figure 5.4 compares the cost and peak demand in the MOO problem with the cost and peak in extreme scenarios, i.e. SO cost and SO peak. The figure shows that minimizing each objective leads to an increase in the other, as the two objectives are contradicting. In this case, scenarios 1 to 7 are dominated by the 8th scenario. In the 8th scenario, the community has a lower cost than the previous scenarios with the same peak.

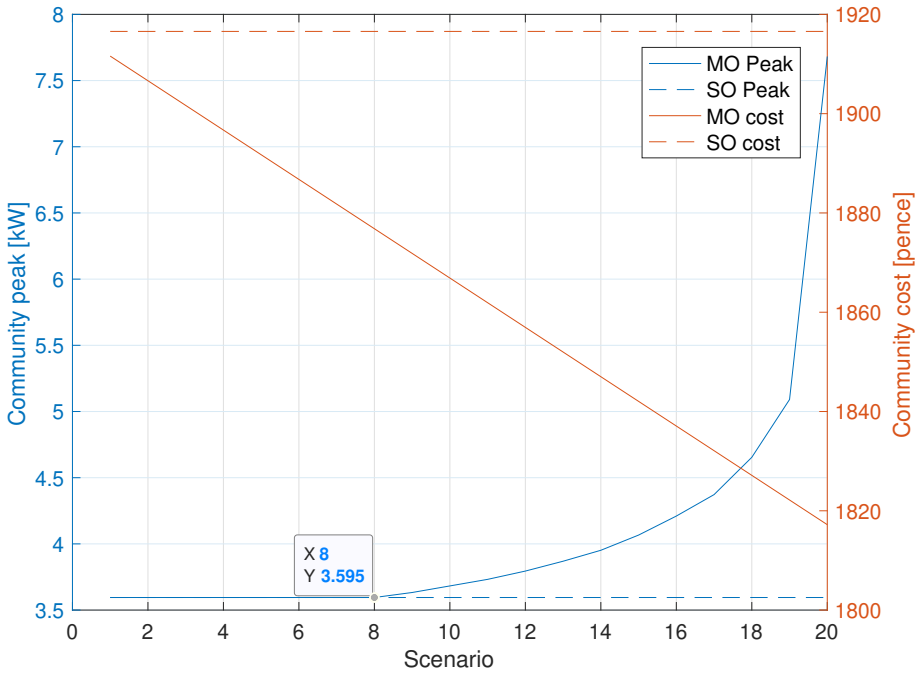

Figure 5.4: Comparison of total costs and peak demand for the community of houses.

In fig. 5.5, the Pareto set of the whole community of houses is illustrated. The figure shows that a peak reduction of 53.2%, i.e. 4.09 kW, will result in a cost increase for the community of 3.2%, i.e. 60 pence, for the specific day. Compared to the Pareto set for Stavanger Airport, the cost of decreasing the peak is higher, but in return the peak demand is reduced by a percentage almost three times as high. Based on the Pareto front for the 4-houses case, the community can select the most preferred point. Based on the selected point, the schedule of the various houses can be set. At the same time, the community can consider the costs of each individual house before making a decision. Along with the costs, the amount of traded energy, shown in fig. 5.6, can also be a measure in the decision making process. P2P trading plays an important role in peak shaving, as there is a high amount of traded energy in the first scenario. It can also reduce the grid dependency, and hence the costs. As the P2P trading give losses, the amount of trade in the cost minimization scenario is lower than the first scenario, which focuses on peak reduction. The priority of the middle scenarios is to use RES locally, than have trading among various peers.

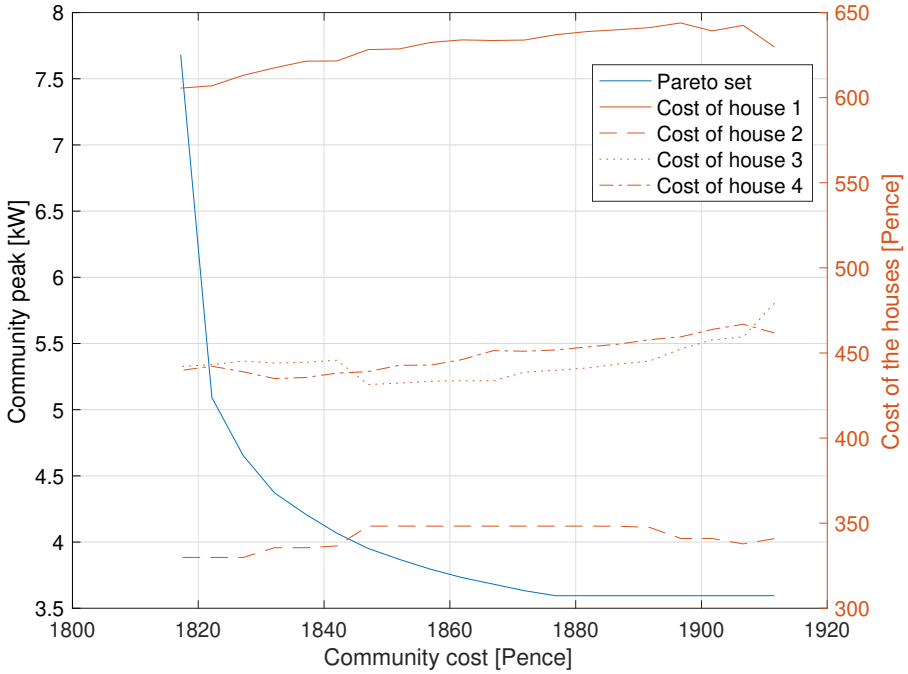

Figure 5.5: Pareto set for the 4-houses case for one specific day.

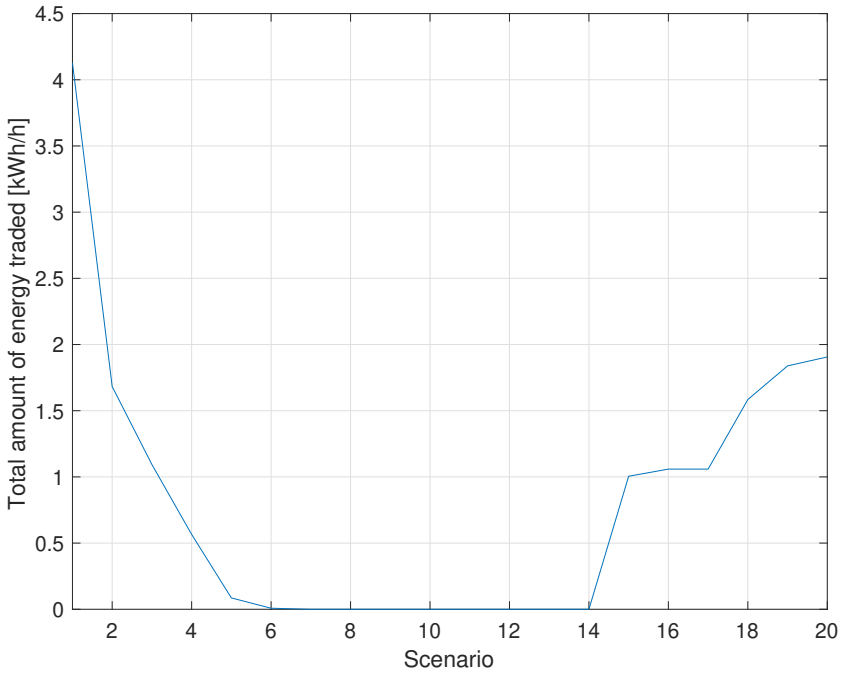

Figure 5.6: The total amount of traded P2P energy in various scenarios for the 4-houses case.

Figure 5.7 shows the aggregated battery storage level for the three batteries in the 4-houses case. The plot to the left, (a), shows the aggregated storage level for the community peak minimization scenario. The middle plot, (b), shows the aggregated storage level for scenario 10, while the plot to the right, (c), shows the aggregated storage level in the community cost minimization scenario.

According to fig. 5.7 (a), it is obvious that in the peak minimization scenario, the batteries are employed to reduce the grid import in peak hours. While, as the concentration on the cost minimization increases, the community tends to use the batteries throughout the day, as shown in fig. 5.7 (b) and (c). In the community cost minimization problem, the batteries are forced to be charged and discharge twice during the day.

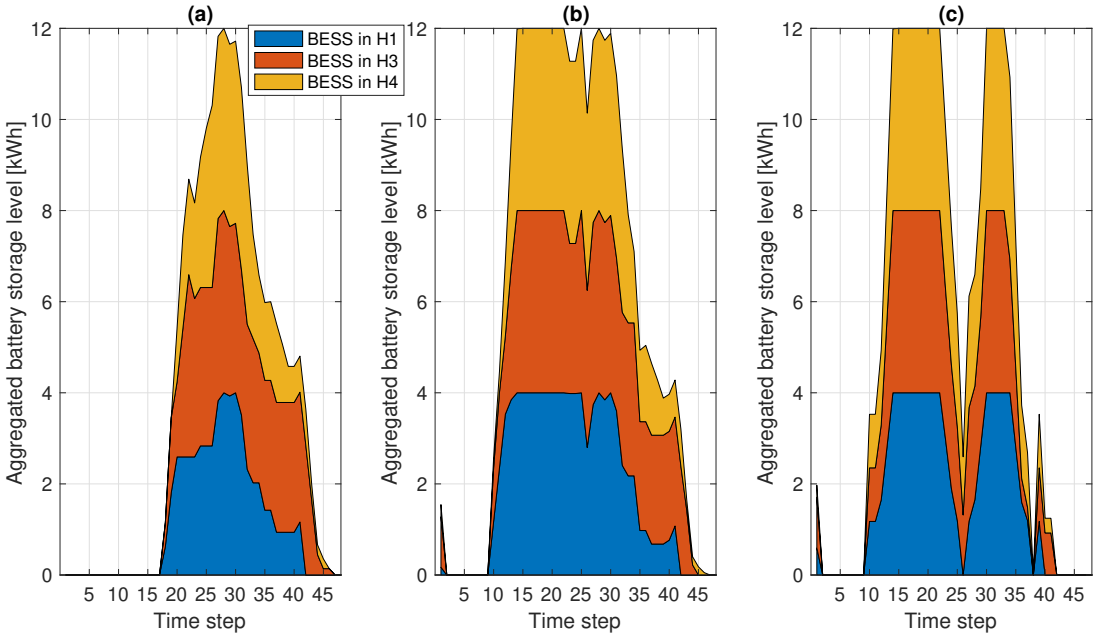

Figure 5.7: The aggregated battery storage level each time step, 30 minutes, for a specific day for different scenarios for the 4-houses case. (a) Scenario 1 (Peak minimization), (b) Scenario 10, (c) Scenario 20 (Cost minimization).

6 | Conclusion

This thesis studies the performance of two different optimization strategies in local electricity markets applied to two unique cases. The first strategy is the decentralized strategy, which has as objective to minimize the total cost of electricity of the individual end-users within a community. The second strategy is the centralized strategy, where the objective is to minimize the total electricity costs for the whole community when enabling P2P energy trading. The thesis has also briefly studied the relationship between total electricity costs and peak power demand for two different cases through utilizing a multi-objective optimization (MOO) approach based on the ϵ-constraint method.

All of the optimization approaches used are based on multi-period linear programming. The approaches have been implemented and simulated using MATLAB with a simulation period of 3 months, April to June, and with a simulation period of one day for the MOO approach. The cases studied include a case of 25 residential buildings in the UK (25-houses case), a case of three large industrial end-users in Norway (Elnett21-case), and a simplified case of four residential buildings in the UK (4-houses case). The decentralized and centralized approaches have been applied to both the 25-houses case and the Elnett21-case, while the MOO approach has been applied to the Elnett21-case and the 4-houses case. This chapter presents the main findings of this thesis, in addition to giving the main conclusions which can be drawn from the results and discussion presented in previous chapters.

The comparison of the decentralized versus the centralized control system strategies shows that the centralized strategy gives the lowest total electricity costs of both the community and for each end-user within the community for both cases studied. For the 25-houses case, the centralized approach gives a cost reduction for the ESR which is 8.0% better compared to the decentralized approach, giving a cost difference of £252. While for the Elnett21-case, the total electricity costs for the ESR when using the centralized approach are 1.0% lower than the costs found when using the decentralized approach. This percentage results in a cost difference of 115,524 NOK. The centralized strategy does also give the lowest amount of energy consumed from the main grid for the different communities, in addition to giving the lowest community peak power demand seen from the grid for both the 25-houses case and the Elnett21-case. The total energy demand is reduced by 18.9% and 1.4% compared to the decentralized strategy for the 25-houses case and the Elnett21-case, respectively. Concerning the peak power demand, the centralized strategy reduces the peak power demand for the community by 13.5% and 15.5% for the respective cases compared to the decentralized strategy. It has also been seen that the centralized approach reduces the amount of power fed to the main grid with 80.9% from the decentralized strategy for the 25-houses case, which results in an increased self-consumption for the community. With these results, it can be concluded that the centralized strategy has proven to be the most preferred strategy of the centralized and the decentralized strategies, when the aim is to reduce the total cost of electricity.

The results from studying the two control system strategies on the two distinct cases show that the difference in performance between the two strategies depends on the case, but that the centralized strategy has the best performance regardless of the cases studied in this thesis. The 25-houses case shows a larger difference in performance between the strategies compared

to the Elnett21-case. The reason for this is that each end-user in the Elnett21-case has both local production and storage units, which decreases the benefits of P2P energy trading. The Elnett21-case does also have some flexible load, which also decreases the benefits of P2P energy trade. In the 25-houses case, each end-user does not have local production and/or storage units. When enabling for P2P trade in the centralized strategy, the end-users without production and/or storage gets increased flexibility as they now also have the opportunity of buying power from other peers. Thus, giving a better performance of the centralized strategy compared to the decentralized strategy for the 25-houses case.

The MOO approach was used on Stavanger Airport, from the Elnett21-case, based on the decentralized market approach, and the 4-houses case using the centralized market approach. Both cases were studied for one day to get an idea of the relationship between the peak power demand seen from the main grid and the total electricity costs. The results from the MOO show that a small increase in cost can reduce the peak power demand by a substantial amount for both of the cases studied, for the specific day. When choosing a control system strategy for an ESR, both the peak power demand seen from the main grid and the total electricity costs should be taken into consideration. This is because the peak power demand is of interest to the local DSO, while the cost minimization is of interest to the community of end-users. The local DSO dimensions their grid according to the current peak power demand. If this peak is increased, the DSO will often face costly power grid updates. To postpone such costly upgrades, the peak power demand of the community could be decreased by utilizing an appropriate control system strategy. Through utilizing MOO, it is possible to find a solution that will benefit both the local DSO and the local community by selecting a point of the Pareto set. Choosing the midpoint on the Pareto set will often be a good compromise for both the DSO and the local community.

6.1 Shortcomings and Further Work

The main shortcomings of the study in this thesis and some suggestions for further work are given below:

* Forecasting algorithms can be implemented in the different control system strategies presented to predict the future demand, production and prices for electricity, instead of assuming a perfect forecasting model to get more realistic results. The optimization horizon can also be increased without giving too optimistic results.
* The different optimization approaches can be run for a longer time period to see how the different approaches compare with each other when increasing the analysis period to e.g. one year. As only the months April to June were used in the simulations, it is not know how the different approaches perform in relation to each other during the fall and winter.
* Only the dual-simplex algorithm was used when solving the optimization problems. Other solvers can be exploited to possibly decrease the computational time.
* The value of battery storage when using the different approaches can be studied.
* P2P energy trade can be implemented in the decentralized approach through using e.g. different decomposition methods. In this way, the results of a decentralized approach with P2P trading can be compared with the results of the centralized approach with P2P trading.
* The MOO approach can be studied further to see how the relationship between peak power demand and total electricity is when having a longer analysis period.

Bibliography

[1] "E-mail correspondence with Aleksander Klungland, Lyse Elnett employee, in June 2020."

[2] "E-mail correspondence with Åsta Vaaland Veen, Port of Stavanger employee, in June 2020."

[3] "E-mail correspondence with Åshild Helland, Lyse Elnett employee, in February 2020."

[4] H. Abu-Rub, M. Malinowski, and K. Al-Haddad. *Power Electronics for Renewable Energy Systems, Transportation and Industrial Applications*. John Wiley & Sons, 2014.

[5] F. Angizeh et al. "Flexibility Scheduling for Large Customers". In: *IEEE Transactions on Smart Grid* 10.1 (2019), pp. 371–379.

[6] Balcoo. *Forus Næringspark AS - Energinøytralt Forus - Konseptutredning for innovative energi- og klimaløsninger i bygg, områder og energisystem - Sluttrapport*. 2019.

[7] K.-H. Chang. *e-Design*. Academic Press, 2015. Chap. 19 - Multiobjective Optimization and Advanced Topics, pp. 1105–1173.

[8] Y. Cui et al. "Review: Multi-objective optimization methods and application in energy saving". In: *Elsevier, Energy* 125 (2017), pp. 681–704.

[9] Elnett21. *About Elnett21*. URL: `https://www.elnett21.no/about-elnett21` (visited on 04/12/2020).

[10] EPEX SPOT. *About EPEX SPOT*. URL: `https://www.epexspot.com/en/about` (visited on 03/10/2020).

[11] F. S. Fadnes et al. *Avinor AS - Stavanger lufthavn - Sola, Konseptutredninger - innovative energiløsninger*. Norconsult, 2018.

[12] Fjordkraft. *Solstrøm*. URL: `https://www.fjordkraft.no/strom/stromavtale/solkraft/` (visited on 03/19/2020).

[13] Forus Næringspark. *Om Forus*. URL: `https://www.forusnaeringspark.no/forus-naeringspark/` (visited on 01/30/2020).

[14] H. C. Gils. "Assessment of the theoretical demand response potential in Europe". In: *Elsevier, Energy* 67 (2014), pp. 1–18.

[15] Greater London Authority. *SmartMeter Energy Consumption Data in London Households*. 2015. URL: `https://data.london.gov.uk/dataset/smartmeter-energy-use-data-in-london-households` (visited on 02/28/2020).

[16] D. Hidalgo Rodriguez and J. Myrzik. "Optimal Operation of Interconnected Home-Microgrids with Flexible Thermal Loads: A Comparison of Decentralized, Centralized, and Hierarchical-Distributed Model Predictive Control". In: (June 2018).

[17] Institute of Transport Economics (TØI). *Reisevaneundersøkelsen 2013/14 - Arbeidsreiser*. URL: `https://www.toi.no/getfile.php/1340019-1427184806/mmarkiv/Bilder/7020-TOI_faktaark_arbeidsreiser-6k.pdf` (visited on 06/23/2020).

[18] R. Kempener and E. Borden. *Battery Storage for Renewables: Market Status and Technology Outlook*. International Renewable Energy Agency (IRENA), 2015.

[19] A. Lüth et al. "Local electricity market designs for peer-to-peer trading: The role of battery flexibility". In: *Applied Energy* 229 (Aug. 2018), pp. 1233–1243.

[20] Lyse Elnett. *Priser og vilkår bedrift*. URL: `https://www.lysenett.no/nettleie/priser-og-vilkar-bedrift/` (visited on 03/20/2020).

[21] MathWorks. *Linear Programming Algorithms*. URL: `https://se.mathworks.com/help/optim/ug/linear-programming-algorithms.html#budwan6` (visited on 06/22/2020).

[22] Ministry of Transport. *Norway is electric*. URL: https://www.regjeringen.no/en/topics/transport-and-communications/veg/faktaartikler-vei-og-ts/norway-is-electric/id2677481/ (visited on 06/25/2020).
[23] NEOS. *Types of Optimization Problems*. URL: https://neos-guide.org/optimization-tree (visited on 05/07/2020).
[24] Nord Pool AS. *The power market*. URL: https://www.nordpoolgroup.com/the-power-market/ (visited on 04/24/2020).
[25] Office of Gas and Electricity Markets (Ofgem). *Feed-In Tariff (FIT) rates*. URL: https://www.ofgem.gov.uk/environmental-programmes/fit/fit-tariff-rates (visited on 04/17/2020).
[26] S. O. Ottesen and A. Tomasgard. "A stochastic model for scheduling energy flexibility in buildings". In: *Energy* 88 (Aug. 2015), pp. 364–376.
[27] M. A. Pedersen. "Teknisk-økonomisk planlegging av mikronett". MA thesis. NTNU, 2018.
[28] Purdue University. *Lecture 9: Multi-Objective Optimization*. URL: https://engineering.purdue.edu/~sudhoff/ee630/Lecture09.pdf (visited on 06/06/2020).
[29] I. Ranaweera and O.-M. Midtgård. "Optimization of operational cost for a grid-supporting PV system with battery storage". In: *Renewable Energy* 88 (2016), pp. 262–272.
[30] Rogaland Revisjon IKS. *Forvaltningsrevisjon av samfunnsplanlegging - Stavanger, Sandnes og Sola kommune*. 2016.
[31] G. Sæther. "Peer-to-Peer electricity trading in an Industrial site: Value of peak load reduction and shared flexibility assets". Unpublished work. 2019.
[32] G. Sæther. "Peer-to-Peer Energy Trading in Combination with Local Flexibility Resources in a Norwegian Industrial Site". MA thesis. NTNU, 2019.
[33] M. H. Sønju. "Control system strategies, local production and local storage: A case study for a Norwegian airport". Unpublished work. Jan. 2020.
[34] Sonnen. *Technical Data sonnenBatterie eco 8.0*. 2018. URL: https://sonnenbatterie.de/sites/default/files/datenblatt_sonnenbatterie_eco_8.0_row.pdf (visited on 03/10/2020).
[35] Statistics Norway (SSB). *Bilparken*. URL: https://www.ssb.no/bilreg (visited on 06/26/2020).
[36] Statnett. *Tariffer for transmisjonsnettet 2020*. 2020. URL: https://www.statnett.no/globalassets/for-aktorer-i-kraftsystemet/tariff/tariffhefte-2020.pdf (visited on 03/19/2020).
[37] K. M. Tan, V. K. Ramachandaramurthy, and J. Y. Yong. "Bidirectional battery charger for electric vehicle". In: *2014 IEEE Innovative Smart Grid Technologies - Asia (ISGT ASIA)*. 2014, pp. 406–411.
[38] The Port of Stavanger. *About the Port of Stavanger*. URL: https://www.stavangerhavn.no/en/about/ (visited on 05/11/2020).
[39] Å. V. Veen, P. Bårdsen, and J. Rosengren-Kolstø. *Risavika Havn AS - Konseptutredning for innovative energiløsninger - Mulighetsstudie nr. 3 - Energiproduksjon*. NIRAS, 2018.
[40] Å. V. Veen, P. Bårdsen, and J. Rosengren-Kolstø. *Risavika Havn AS - Konseptutredning for innovative energiløsninger - Mulighetsstudie nr. 4 - Lagringsteknologi*. NIRAS, 2018.
[41] J. M. Zepter et al. "Prosumer integration in wholesale electricity markets: Synergies of peer-to-peer trade and residential storage". In: *Energy and Buildings* 184 (2019), pp. 163–176.
[42] Y. Zhou, J. Wu, and C. Long. "Evaluation of peer-to-peer energy sharing mechanisms based on a multiagent simulation framework". In: *Springer Comput Manag Sci 13* 222 (2018), pp. 993–1022.

A | Appendix

The appendix provides some additional plots for both the 25-houses case and for the Elnett21-case, in addition to giving a brief explanation of a third case of four houses in London, UK used in chapter 5.

A.1 Additional Plots for Both Cases

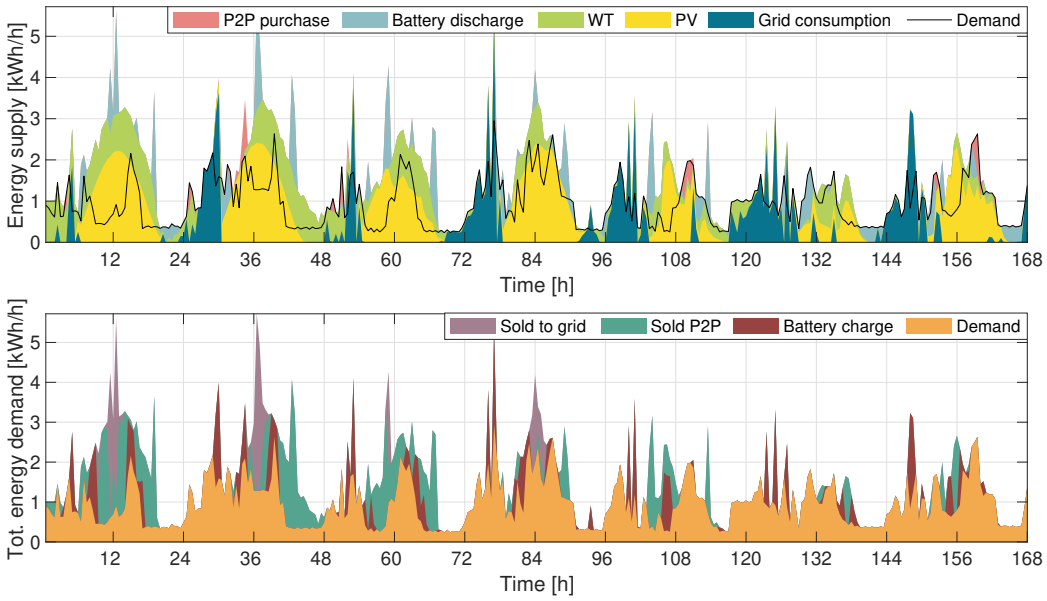

Figure A.1: Supply-demand decisions when using the centralized control system strategy on house 15 in the 25-houses case in week 24, 2013.

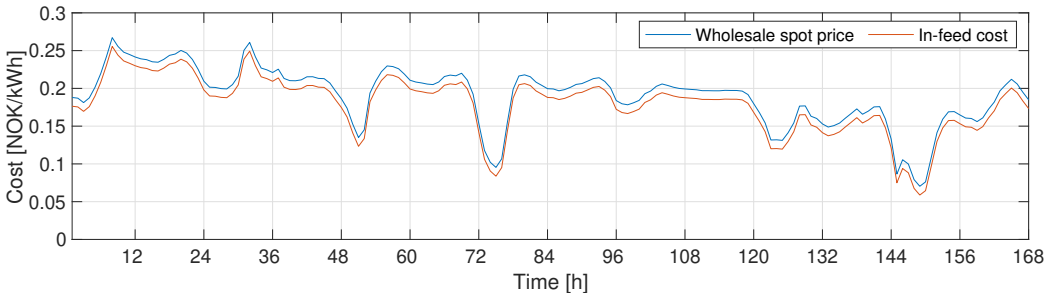

Figure A.2: Wholesale spot prices and in-feed cost for the Elnett21-case during week 19 in 2015.

A.2 4-houses in London, UK

This section introduces an additional case with four houses located in the UK, and the case considers the same four houses used in Lüth et al. [19]. The 4-houses case can be considered as a simplified version of the 25-houses case and it has been added to be used with the MOO approach, as the results from MOO are harder to interpret when there are many end-users within the ESR.

The 4-houses case, with fewer end-users, is added to have a simpler case to be studied by the MOO approach. simplify the MOO optimization, making it easier to present in this thesis because a simpler case with less end-users was needed for the MOO optimization, as the results from the optimization are harder to interpret when there are many end-users within the ESR.

A.2.1 Introduction to the Case

The 4-houses case consists of four households located in London, UK. Each of the households have their own unique load demand pattern. The load is fixed for all of the houses, which means that no load is shiftable nor curtailable. The households are of the same type as the households in the 25-houses case, as they can have local production units in the form of wind turbines and PV systems, and local storage in form of a BESS. The four houses are connected to the main power grid and to a local grid interconnecting the houses, as in the 25-houses case. Figure A.3 shows the setup for the 4-houses case with enabled P2P trading. The houses are numbered from 1 to 4 and the average monthly demand, for the simulation period, is given for each of the houses.

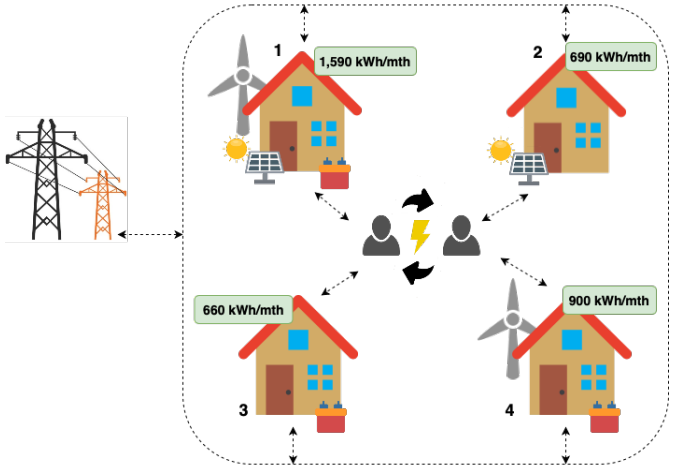

Figure A.3: Setup for the 4-houses case with P2P trading[25]. Each of the houses are numbered, 1-4, and the average demand during the simulation period is given for each house. The various production and storage units at the different houses are also shown.

[25]See fig. 3.1a in chapter 3 for an explanation of the symbols used in fig. A.3.

A.2.2 Case Data and System

The demand data for the four households in this case is taken from the Low Carbon London project[26], which is the same project that the data for the 25-houses case is taken. The 4-houses case uses demand data for year 2012, while the 25-houses case uses data from 2013. The simulation period for the 4-houses case is set to just one day, i.e. April 1st 2012. The time step is put to 30 minutes, which gives a total of 48 simulation steps. Note that the four households in the 4-houses case are not any of the same households as the ones chosen for the 25-houses case. The different houses in the community have the following characteristics:

* House 1 has the largest monthly energy demand of the four houses with its demand of 1,590 kWh/month. The household has installed both a 2.3 kW WT, a 4 kW_p PV system and a 4 kWh BESS.
* House 2 has installed a 4 kW_p PV system and has a monthly energy demand of 690 kWh/month.
* House 3 has the lowest demand of the four houses with an energy demand of 660 kWh/month. The house has no production units, but it has a 4 kWh BESS.
* House 4 has installed a 2.3 kW WT and a 4 kWh BESS. The average demand of the house is 900 kWh/month.

The exact same electricity prices and pricing scheme that was used for the 25-houses case, see section 3.2 in chapter 3, are also used for the 4-houses case. The production and storage units of the 4-houses case are the same as those used in the 25-houses case. Meaning that the WT has a capacity of 2.3 kW and is stall regulated, the PV systems are rated at 4 kW_p with an efficiency of 21.4% and that the BESS is a LIP sonnenBatterie eco 8.0 with a usable capacity of 4 kWh and with a 2.5 kW inverter. The production from the PV systems is the same for both houses that have installed a PV panel, as the production is taken from the pre-specified PV installation. See section 3.2 in chapter 3 for more information on the production and storage units.

The model formulation for the 4-houses case is the same as the models used for the 25-houses case, see section 3.4 in chapter 3.

[26] More information on the Low Carbon London project can be found on the following webpage: https://data.london.gov.uk/dataset/smartmeter-energy-use-data-in-london-households

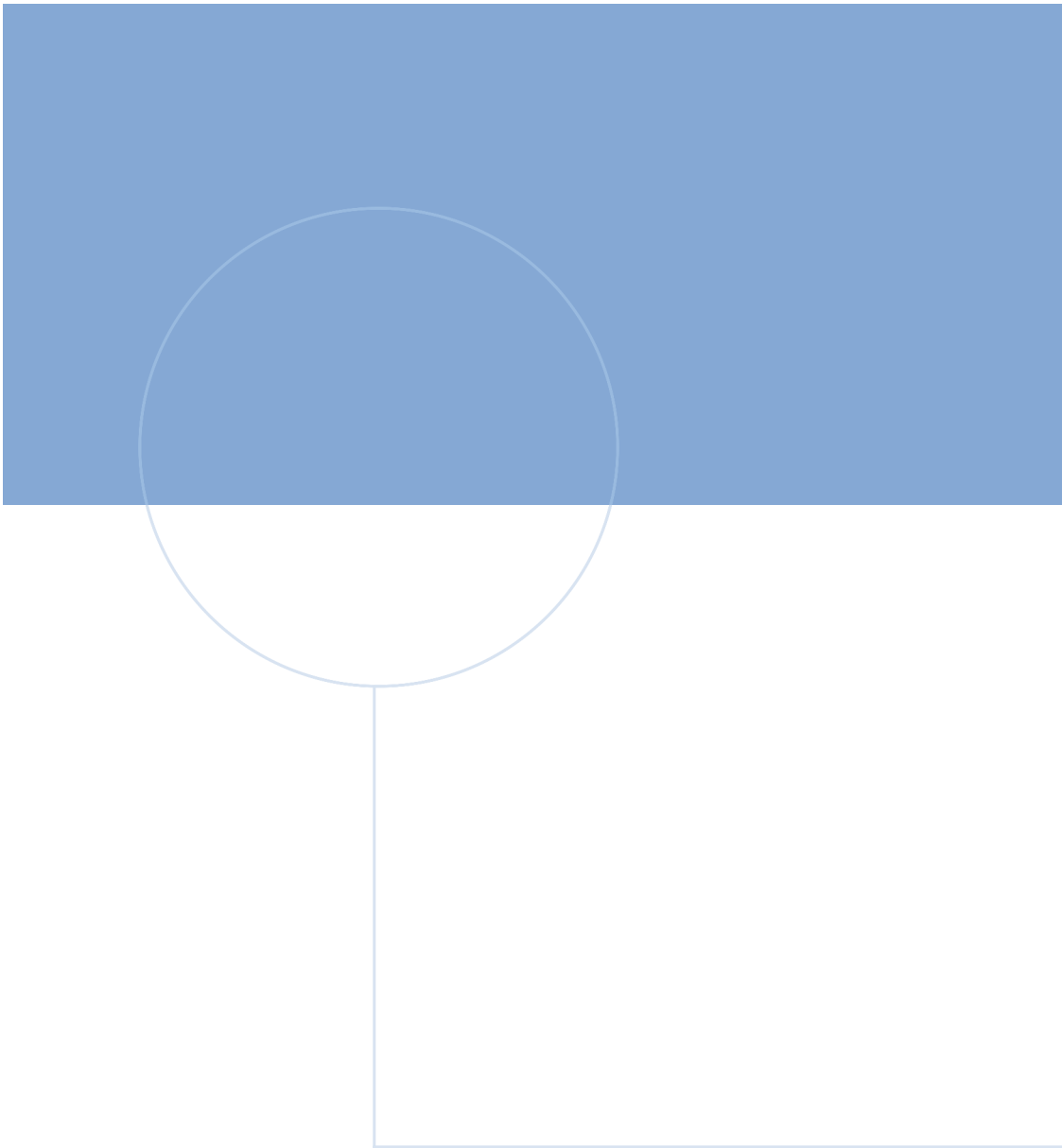

NTNU

Norwegian University of
Science and Technology